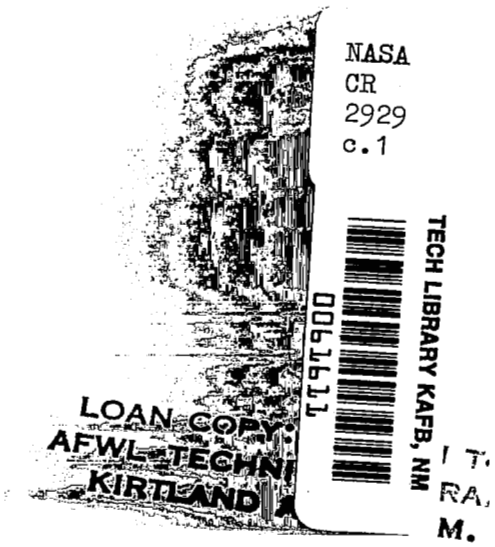

NASA Contractor Report 2929

Interaction of Hydrogen Chloride With Alumina

R. R. Bailey and James P. Wightman

GRANT NSG-1195
FEBRUARY 1978

NASA

TECH LIBRARY KAFB, NM

0061611

NASA Contractor Report 2929

Interaction of Hydrogen Chloride With Alumina

R. R. Bailey and James P. Wightman
Virginia Polytechnic Institute & State University
Blacksburg, Virginia

Prepared for
Langley Research Center
under Grant NSG-1195

National Aeronautics
and Space Administration

**Scientific and Technical
Information Office**

1978

FOREWORD

The Principal Investigator was on Research-Study Leave from Virginia Polytechnic Institute and State University at the University of Bristol (U.K.) during the period 1 September 1975 to 15 June 1976. During that time, calorimetric studies were done by the Principal Investigator in the Physical Chemistry Department at the University of Bristol as a part of the Grant. A detailed summary of the calorimetric work is given in Appendix 12.

The help of Mr. Frank Mitsianis in taking the SEM photomicrographs is recognized. Mr. W. R. Cofer, III of the NASA - Langley Research Center is acknowledged for obtaining some of the X-ray powder diffraction patterns. Thanks to Andy Mollick and Mr. Frans van Damme of the University Glassblowing Shop for the construction and repair of the vacuum system. A special recognition is given to Professor D. H. Everett, Leverhulme Professor of Physical Chemistry at the University of Bristol (U.K.) for the opportunity to conduct studies on the Calvet microcalorimeter.

TABLE OF CONTENTS

LIST OF TABLES

LIST OF FIGURES

Figure Page

I. INTRODUCTION

The quality of the environment is the subject of increasing concern. Hydrogen chloride is generally not regarded as a major air pollutant. However there are specific instances in which its environmental impact is of interest. Hydrogen chloride, HCl, is naturally present in the environment as a product of volcanic activity. It is found in solution in some rivers, such as the Vinago River in the Andes, which originate from volcanoes.[1] Hydrogen chloride was first recognized as an air pollutant in the 19th century when it was produced as a byproduct in the Lablanc process for manufacturing washing soda.[2] In recent years, the incineration of chlorinated hydrocarbons and the manufacture of products which release hydrogen chloride into the environment as a byproduct[3] have caused a greater environmental concern for this dangerous gas.

Solid rocket propellants[4] which have been developed for use in the NASA Space Shuttle Program produce hydrogen chloride, aluminum oxide (alumina), carbon monoxide and water vapor during combustion. A system consisting of several gases and solid particles, such as a rocket exhaust, can undergo many different interactions. Interaction of the exhaust components could lead to chemical reactions, aeresol formation, catalysis, absorption and adsorption. The problem is complicated by the fact that electron diffraction studies[5] have shown that the aluminum oxide produced in the exhaust is of two crystalline phases. The larger particles are alpha alumina and the smaller particles are gamma alumina.

The main objective of this research was to initiate a fundamental study of the interaction of HCl and alumina. The results of such a study form a basis on which to assess the adsorption process in the exhaust cloud as a possible sink mechanism for the potentially dangerous hydrogen chloride.

When two immiscible phases (gas/solid) are brought into contact, usually there is a greater concentration of one phase at the interface than in the bulk. This concentration gradient is caused by forces of attraction between the two phases and leads to the concept of adsorption. Adsorption is usually classified as either physical or chemical depending on the forces responsible for the adsorption. If the adsorption is due to van der Waals interaction, the process is called physical adsorption (physisorption). Chemical adsorption (chemisorption) occurs when a chemical bond is formed between the solid (adsorbent) and the gas molecule (adsorbate).

Alumina and silica-alumina have been used industrially for many years as adsorbents, heterogeneous catalysts and catalyst supports. Treatment of alumina catalysts with hydrogen halides has resulted in increased activity towards isomerization, alkylation, polymerization and other acid catalyzed reactions.[6] Spectroscopic studies by Peri,[7,8] Tanaka and Ohasawara[9] and others[10] have attempted to explain this enhanced activity.

While infrared spectroscopic studies have been made of hydrogen chloride treated gamma alumina and gamma alumina of different degrees of surface hydration, no systematic quantitative study of hydrogen chloride adsorption on gamma alumina has been reported, further, no

study of hydrogen chloride adsorption on alpha alumina has been reported.

A study of the fate and interaction of HCl, H_2O and Al_2O_3 is necessary to partially asses the impact of these exhaust products on the environment. This report presents a quantitative study of the adsorption of hydrogen chloride and water on alpha and gamma alumina. Studies of the influence of temperature, pressure and pretreatment conditions were made. The effect of pre-adsorbed water on hydrogen chloride adsorption was studied and may give insight into the poisoning of catalysts by water. Differences in the adsorption properties of alpha and gamma alumina were considered and give added emphasis to the role which bulk and surface structures play in adsorption and catalysis. Thermodynamic analysis of gas adsorption and solution adsorption gave insight into differences of gas phase and liquid phase adsorption, the condition of oxide surfaces in the presence of water and the mechanism of hydrogen chloride adsorption on these surfaces.

Certain commercial materials and/or names of manufactures are identified in this paper in order to specify adequately which materials were involved in the research effort. In no case does such identification imply recommendation or endorsement of the materials by NASA.

II. HISTORICAL

A. Introduction

A review of the literature pertinent to the adsorption of hydrogen chloride on alumina is presented in this section. No attempt is made to review all the literature on adsorption. Standard references on adsorption include, Young and Crowell,[11] Ross and Oliver,[12] Flood[13] and Hayward and Trapnell.[14]

B. Solid Propellant Exhaust Studies

Solid rocket propellants proposed for use in the NASA Space Shuttle Program may pose an environmental problem.[4] The propellant[15] is composed of an ammonium perchlorate oxidizer dispersed in a synthetic rubber binder fuel containing aluminum and various other additives. Predictions of the exhaust product concentrations from such a solid rocket motor are available.[16] Typical exhaust composition is 30.2% Al_2O_3, 20.9% HCl, 9.4% H_2O, 24.2% CO, 3.4% CO_2, 2.5% H_2, 8.7% N_2 and 0.6% $FeCl_3$. NASA has an ongoing experimental program to measure the effluent concentrations[15,17,18] and to study the interaction of the effluents.[19,20] The data obtained in these studies will be used in the verification of atmospheric models, such as the NASA multilayer dispersion model.[21] This model will be used to define those weather conditions during a launch which would produce unacceptable effluent concentrations and hence present a launch constraint.

C. Alumina System

Aluminum oxide exists in several different crystalline forms

which can be interconverted, usually by heating. Early studies with the alumina system dealt with preparation of various forms of alumina based on temperature-pressure relationships. The bulk crystal structure was investigated as well as the physical and chemical properties of the various forms. Extensive reviews of the X-ray patterns, structure, nomenclature, thermal transistions and physical and chemical properties of the aluminum oxides are given by Rooksby[22] and by Werfers and Bell.[23]

The surface chemistry of aluminum oxide has not been as widely researched as the bulk structure and properties. Bielanski and Sedzimir[24] investigated the thermal preparation, chemical properties and some adsorptive properties of several aluminas. Three sequences of phase transformations were reported:

Series I: Mixture of bayerite, hydragillite and a small amount of boehmite $\longrightarrow \gamma \longrightarrow \theta \longrightarrow \chi \longrightarrow \alpha\text{-}Al_2O_3$

Series II: Boehmite $\longrightarrow \gamma \longrightarrow \delta \longrightarrow \theta \longrightarrow \chi \longrightarrow \alpha\text{-}Al_2O_3$

Series III: Bayerite $\longrightarrow \gamma \longrightarrow \theta \longrightarrow \chi \longrightarrow \alpha\text{-}Al_2O_3$

The rate of dissolution of the different forms of alumina in HCl and in NaOH decreased with increasing temperature of calcination. This was attributed to a decrease in the surface area during the transition from the low temperature gamma (γ) or delta (δ) forms to the high temperature alpha (α) form. BET surface areas measured using CO_2 adsorption at $-79^{\circ}C$ confirmed this decrease in surface area. The specific density of the alumina was proportional to the temperature of calcination. Adsorption of water vapor on the different aluminas exhibited a dependence on the temperature of the calcination, but

only a slight dependence on the time of the calcination was observed. From the amount of water adsorbed over a given time period and the change in the rate of adsorption, Bielanski and Sedzimer concluded that increasing calcination temperature decreased the number of micropores in the γ-alumina and thus decreased the rate of the slow adsorption step. Negligible adsorption of water occurred on alpha alumina.

D. Surface Studies of Alumina

Studies of the adsorption and surface properties of aluminum oxide have been directed mostly at gamma alumina because of its important use in catalysis. Few studies have been concerned with the alpha alumina surface. Hair[25] reviews the adsorption and surface properties of alumina prior to 1967.

Hightower[6] discussed the nature of active sites on γ-alumina for several different reactions, including ortho-para hydrogen conversion, H_2 - D_2 exchange, olefin isomerization, polymerization and alcohol dehydration. Using two test reactions (D_2 exchange and olefin isomerization) as well as infrared spectroscopy, Hightower found four types of surface sites on γ-alumina.

Another review of the chemisorption sites on γ-alumina which stresses its catalytic importance was given by Cvetanovic and Amenomiya.[26] The review considers the sites for ethylene adsorption, hydrogen exchange and changes in active sites during activation of alumina.

Recent studies have used many adsorbates on alumina including H_2S,[27,28] amines,[29] CO_2,[30] CO,[31] HF,[32] acetylenes,[33] alcohols,[34]

SO_2,[35] and pyridine.[36] These studies have employed a variety of techniques such as infrared spectroscopy, Raman spectroscopy, kinetic measurements and electron paramagnetic resonance.

E. Adsorption of Water on Alumina

The most extensive study of the alumina surface was an infrared spectroscopic study reported in a series of papers by Peri.[37-42] Using transparent aerogel plates of γ-alumina, Peri and Hannan[37] investigated the hydration and dehydration of alumina up to 1000°C.

Undried alumina aerogel plates showed broad absorption bands at 3300 and 1650 cm^{-1} corresponding to stretching and bending frequencies found in liquid water. These two bands disappeared after outgassing the sample under vacuum at 400°C indicating that a liquid film of water had been removed. Infrared spectra taken after outgassing the alumina at 650 - 700°C showed absorption bands characteristic of isolated surface hydroxyl groups. Even after evacuation at 900°C, the spectra still revealed the presence of isolated hydroxyl groups on the surface of alumina, although the intensity of the bands was decreased. Rehydration experiments showed that adsorption of water vapor on alumina dried at 800°C did not produce hydroxyl groups at room temperature but rehydration to form hydroxyl groups could occur at elevated adsorption temperatures. Infrared spectra taken after adsorption of other gases such as NH_3, D_2, and CCl_4 showed the importance of the isolated hydroxyl groups in the adsorption process.

A quantitative study by Peri[38] on the rehydration of dried alumina showed that the extent of surface hydration is primarily controlled by drying temperature. Dry alumina could "chemisorb"

one molecule of water per 11-16 $\AA^2$ of surface at 100°C depending on the drying procedure.

A statistical model for the surface of γ-alumina has been proposed by Peri[41] to explain the results of his dehydration-rehydration experiments. The model is based on the preferred exposure of a single crystal plane (100) of spinel at the surface of gamma alumina. The ideal dry surface is assummed to contain only oxide ions, with one oxide ion occupying an area of 8 $\AA^2$ as shown in Figure 1. Each aluminum ion is surrounded by 4 oxide ions. During hydration the entire surface is converted to hydroxyl ions. The dehydration process was simulated by allowing adjacent OH groups to combine and form water molecules which are desorbed. By randomly removing two adjacent hydroxyl groups at a time from the surface one eventually obtains a surface containing five different types of OH groups as shown in Figure 2.

The result of this statistical analysis reinforces the results of Peri and Hannan's[37] infrared work, where three distinct peaks were found in the spectrum. The model predicts that the alumina surface will be quite complex unless mobility of the OH groups is possible. Only at extremely high temperatures would mobility of the hydroxly groups be possible, thus the surface properties of alumina will be determined by the nature of the hydroxyl groups. Peri[38] showed that hydroxyl groups are still present at 900°C and therefore significant mobility is not likely. Mobility causing OH removal may be possible during transformation to different crystal forms, for example the change to alpha alumina at 1200°C.

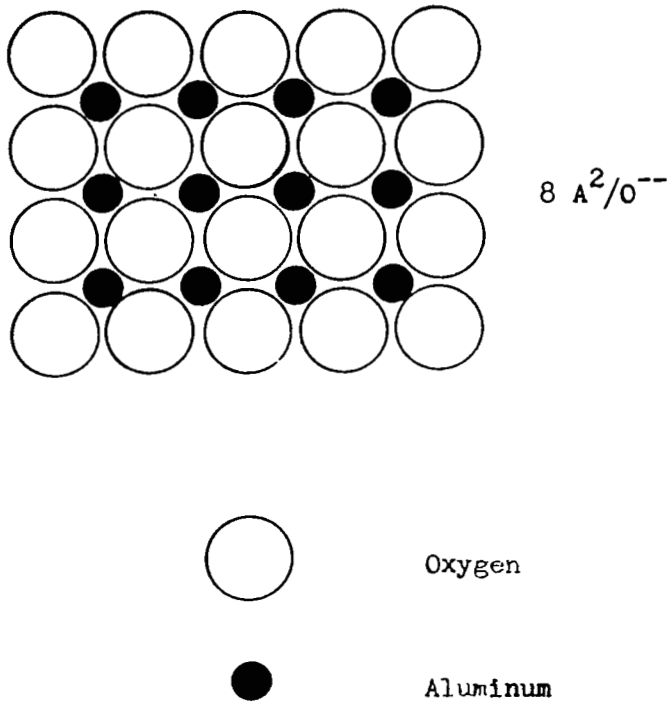

Figure 1. Ideal Gamma Alumina Surface (41)

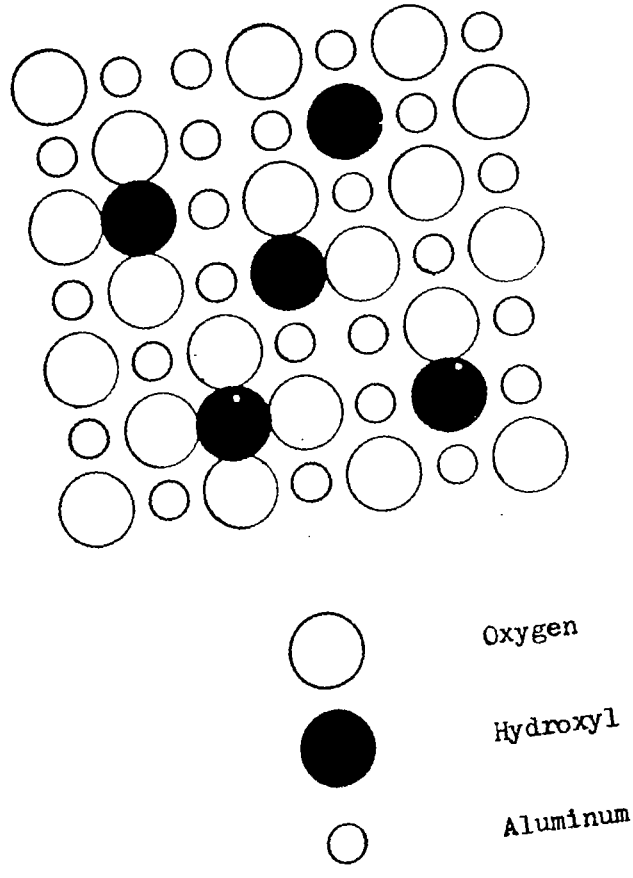

Figure 2. Gamma Alumina Surface After Dehydration (41)

De Boer, et al.[43] studied the adsorption of water on four different aluminas (gibbsite, χ-γ mixture, χ-γ-K mixture and boehmite) dried at 1200°C. Loss of weight at 1200°C after saturation with water vapor was directly related to the amount of adsorbed water. The amount of the adsorbed water physisorbed and chemisorbed was found by determining weight loss of the alumina at 120°C (physisorbed) and further loss after ignition at 1200°C (chemisorbed). Chemisorbed water amounted to 24.8 mg $H_2O/100m^2$ and 33mg $H_2O/100m^2$ of physisorbed water. The amount of chemisorbed water found on the four aluminas was essentially the same, which is not surprising since no precaution was made to prevent conversion of the aluminas to alpha alumina by the 1200°C heat treatment.

De Boer, et al.[43] used the BET equation to determine monolayer coverage of water on the alumina of known surface area. The area of an adsorbed water molecule was determined to be 12.1 $Å^2$ on the alumina using this method.

A further study of water adsorption on alumina was reported by Morimoto, Nagao and Inai.[44] Their study made a comparison of SiO_2, Al_2O_3 and SiO_2-Al_2O_3 surfaces. Silica, which has been studied extensively,[45] shows different adsorption properties than alumina. As silica is heated at successively higher temperature the amount of water adsorption decreases, because of the formation of Si-O-Si linkages and the decrease of hydroxyl groups. Alumina, however, showed an increase in adsorption capacity with temperature of pretreatment. The BET equation was used to calculate the monolayer coverage and the area occupied by each adsorbed water molecule was calculated to

be 16.6Å^2. The amount of chemisorbed water was determined by the amount of water removed by heating at 30°C unlike that defined by de Boer, et al.[43] as water removed by heating at 120°C. An important point established by Morimoto and coworkers was that the area of the adsorbed water was constant, even though alumina showed increasing water adsorption with increasing heat treatment. Therefore, one can postulate that the adsorbed area does not change since H_2O can adsorb in two ways on an alumina surface as shown in Figure 3. Figure 3A shows water adsorption on a dehydroxylated surface and Figure 3B shows the adsorbed species on a hydroxylated alumina surface. Both adsorptions occur through the formation of strong hydrogen bonds. Peri's work[38] at elevated temperature showed that at high temperatures H_2O could form new hydroxyl groups on the alumina surface as illustrated in Figure 4.

The area of adsorbed water, 16.6Å^2, found by Morimoto, et al.[44] is in good agreement with Peri's model of the gamma alumina surface. However, no precaution was taken by Morimoto to insure that the alumina prepared by hydrolysis of aluminum isopropoxide was of a specific crystalline form, i.e., no X-ray powder diffraction results were reported.

One study of adsorption on alpha alumina was that of Carruthers, Payne, Sing and Stryker.[46] Studying alumina, silica and chromium oxide, these workers determined surface area and porosity using nitrogen and argon adsorption and α-plots. This procedure showed that of the aluminas studied, (α, θ and gibbsite calcined at 800°C), only

(A)

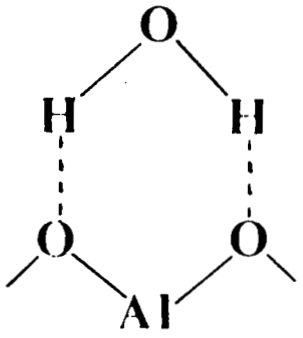

(B)

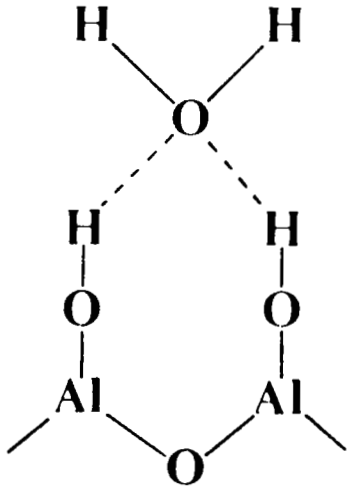

Figure 3. Nature of Water Adsorbed on Alumina Surface

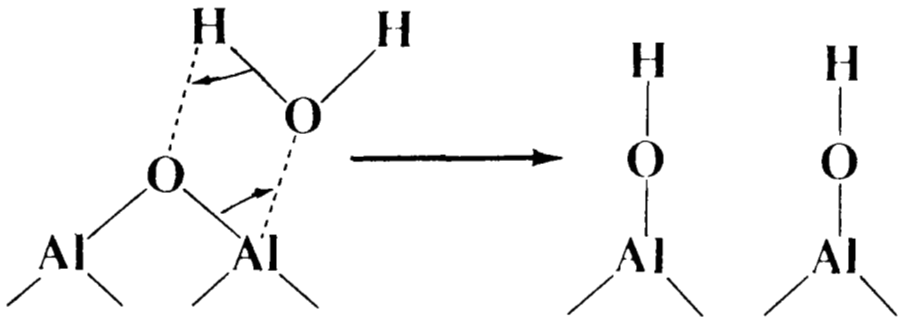

Figure 4. Formation of Hydroxyl Groups on Alumina Surface by Water Vapor Adsorption at Elevated Temperatures

the gibbsite was porous. By studying adsorption-desorption cycles of water the workers showed that dehydrated alumina surfaces do exhibit the type of hydrophobic character displayed by dehydroxylated silica. Comparison of water adsorption on alpha and theta alumina showed the alpha alumina adsorbed more water per unit area than the theta alumina. The authors concluded that alpha alumina has a high affinity for water with chemisorption taking place at low pressure to form hydroxyl groups and physical adsorption occurring on this hydroxylated surface. This high affinity exhibited by alpha alumina for water is associated with a marked tendency for exposed aluminum ions to be rehydrated, thus allowing dissociative chemisorption of water followed by physisorption.

A comparison of the adsorption properties of eta and gamma alumina was made by MacIver, Tobin and Barth.[47] Studying the hydration-dehydration cycle of the two aluminas, the workers found that eta and gamma alumina contained different amounts of pre-adsorbed water. Removal of this water produced surface acidity in the aluminas which was investigated using chemisorption of ammonia. A later paper by MacIver, Wilmot and Bridges[48] studied the influence of this acidity on the catalytic properties of the two aluminas.

Several workers have studied the heats of adsorption of water on alumina using calorimetric methods. Every, Wade and Hackerman[49] studied the heat of immersion in water of alpha, gamma and an amorphous alumina and the effect of particle size and outgassing temperature on the heats of immersion. The trend observed was that as particle

size decreased the heat of immersion increased. A dramatic difference in the heat of immersion for the alpha aluminas and the gamma aluminas was noted but could be due to a particle size effect. The alpha aluminas had larger particle sizes than the gamma aluminas.

The influence of outgassing temperature was studied by Every, et al.[49] by evacuation of alumina samples to 10^{-5} torr for 72 hours. The results showed that heats of immersion increased with increasing outgas temperature. This trend according to the authors seemed to indicate the existence of adsorbed water above 200°C.

In a later study Every, Wade, and Hackerman[50] investigated the difference in alpha and gamma alumina toward water, n-hexane and CH_3OH adsorption. Alpha alumina adsorbed more H_2O than gamma alumina per unit area, but no explanation of this difference was given. Also the quantity of water adsorbed increased with increasing outgas temperature.

Morimoto, Shiomi and Tanaka[51] studied the variation of surface area of alpha and gamma alumina and measured the heat of immersion in water. The surface area of gamma alumina began to decrease at 600°C, whereas the alpha alumina surface area remained constant. Heat of immersion data for both aluminas showed a dependence on outgas temperature initially increasing to a maximum at 600-650°C then decreasing.

Cochrane and Rudham[52] measured the heat of immersion of alpha alumina and gamma alumina in water after outgassing at 300°C. The heat of immersion for alpha alumina and gamma alumina were -773 and -648 mJ/m^2, respectively.

A later study of heats of immersion was that of Hendriksen, Pearce and Rudham[53] on alpha and gamma alumina outgassed from 100-600°C. Again a difference in heat of immersion was found for alpha and gamma alumina. The heat of immersion also increased with increasing outgas temperature, thus indicating that more surface hydration could be occurring. Contradictory to the results of Morimoto, et al.,[51] Hendriksen Pearce and Rudham[53] found that the surface of alumina outgassed at temperatures greater than 600°C did not anneal but returned to its initial state when re-exposed to water.

In summary, measurement of water adsorption on alumina has shown that the crystalline phase of alumina influences the adsorption properties. Several different mechanisms for water adsorption on alumina can take place depending on thermal pretreatments and the temperature of the adsorption. Water can form new hydroxyl groups, hydrogen bond to two hydroxyl groups or adsorb on oxygen ions on the alumina surface. The existence of two forms of adsorbed water (chemisorbed and physisorbed) has been reported.

F. Hydrogen Chloride Adsorption

Studies of hydrogen chloride adsorption on solid adsorbents have been limited due in part to the experimental difficulty of handling the corrosive HCl and the previous lack of recognition of the importance of the interaction. Studies of HCl adsorption on NaBr and KBr[54] rutile,[55,56] silica,[40] evaporated metal films,[57] metal chlorides supported on alumina[58] and aluminum[59] have been reported.

The infrared study by Parfitt, et al.[56] showed the chemisorption of hydrogen chloride on TiO_2 to occur by the reaction shown in Figure 5A. The existence of a surface species as in Figure 5B consisting of a water molecule coordinated to a titanium ion and in conjunction with a chloride ion gives rise to infrared absorption bands at 1565 and 3360 cm^{-1}.

Peri,[40] during adsorption studies on silica, found that HCl was not appreciably adsorbed on the silica surface.

G. Hydrogen Chloride Adsorption Studies on Alumina

In conjunction with his infrared study of the hydration and rehydration of the gamma alumina surface, Peri[42] studied the adsorption of HCl on silica-alumina and gamma alumina. Peri found that HCl adsorption on silica-alumina prevented adsorption of CO_2 on α-sites of the adsorbent. He stated that HCl, NH_3 and many other adsorbates react extensively with gamma alumina but no quantitative measurement of HCl adsorption was made. Peri postulates that the adsorption site or "α-site" is a "strained" oxide linkage. On alumina the α-site was postulated to be $Al^{+}O^{2-}Al+$ and on silica-alumina; $Al^{+}O^{-}$-Si. These sites chemisorb HCl to form Al-OH---Cl-Al.

In another paper Peri[7] made an infrared investigation of the hydrogen chloride reaction with the surface of gamma alumina. Using alumina aerogel plates outgassed at 800°C, Peri found that HCl adsorption at 50°C gave an absorption band at 3500 cm^{-1}, assignable to hydrogen bonded hydroxyl groups. Bands which would result from Cl-O and Al-Cl were not in the frequency range of the study. Desorption of HCl removed some of the OH groups. Using a deuterated

Figure 5A

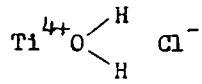

Figure 5B

Figure 5. Adsorption of Hydrogen Chloride on TiO_2

alumina surface, Peri observed that HCl did not react with the original deuteroxyl groups in strong preference to the bare oxide surface. Peri[7] also studied the adsorption of HCl at elevated temperatures (600°C), the effect of preadsorbed HCl on CO_2 adsorption and the catalytic activity of HCl treated alumina toward butene isomerization.

Tanaka and Ogasawara[9] investigated the influence of HCl pretreatment on the catalytic activity of alumina and silica. In agreement with Peri[7,42] they found that chemisorption of HCl on dry alumina procuces new hydrogen bonded hydroxyl groups on the surface. The adsorption on alumina outgassed at 500°C was very rapid and irreversible at room temperature, giving a maximum adsorption of 3×10^{14} molecules/cm^2. The new hydroxyl groups formed by HCl adsorption are protonic and participate in n-butene isomerization as Bronsted acid sites. Hydrogen chloride was adsorbed minimally on the silica surface and the isomerization of n-butenes on HCl-exposed silica did not occur.

Further studies of HCl-treated alumina catalysts were carried out by Ogasawara, Takagawa and Takahashi.[10] These studies showed that HCl treated gamma alumina increased the catalytic efficiency during diphenylammine synthesis.

Wightman[60] used a Calvet microcalorimeter to measure the heats of immersion of alpha and gamma alumina in water and hydrochloric acid.* The measurements were performed at different outgas temperatures and HCl concentrations. Heats of immersion of aluminas in water were found to increase with increasing outgas temperature. The heat of immersion of alpha alumina was less than that of gamma alumina. In hydrochloric acid, the heat of immersion increased from -888 mJ/m^2

---

*These calorimetric studies are described in detail in Appendix 12.

to -1829 mJ/m^2 as the outgas temperature was varied from 80° to 400°C for alpha alumina. Gamma alumina outgassed at 100° and 400°C gave -727 and -1728 mJ/m^2, respectively. Variation of the heat of immersion of alpha alumina outgassed at 200°C with HCl concentration was not as pronounced, giving -1134 mJ/m^2 for 0.001 M HCl and -1351 mJ/m^2 for 0.1 M HCl.

Tyree, in a series of reports,[61-63] studied the solution chemistry of the HCl-Al_2O_3 system. Measurement of vapor pressure changes in the system was used to determine which of the four reactions shown in Figure 6 would occur.

Using two different aluminas, theta alumina and mixed $Al(OH)_3$, significant differences in vapor pressure lowering were found upon addition of the aluminas to varying concentrations of hydrochloric acid. An obvious difference in the reactivity of the two aluminas was noted in the fact that a larger decrease in vapor pressure in a shorter time was observed for the mixed alumina, $Al(OH)_3$. Changes in pH of HCl/alumina slurries were also measured.

In summary the following conclusions can be made about the HCl/alumina interaction. HCl adsorbs on alumina rapidly and irreversibly to form hydroxyl groups. These hydroxyl groups are important in some catalytic reactions. Deuteration studies have shown that HCl reacts preferentially with the bare oxide surface. Again, as in the case of water adsorption, the heats of immersion show the importance of outgassing temperature on hydrogen chloride adsorption.

1. $H_2O(g) + Al_2O_3 \longrightarrow Al(OH)_3$ surface reaction

2. $Al_2O_3(s) + H_2O(g) \longrightarrow Al_2O_3(s) + H_2O(l)$ (on the $Al_2O_3(s)$)

3. $HCl(g) + H_2O(l) \longrightarrow HCl(aq)$

4. $HCl(aq) + Al(OH)_3(s) \longrightarrow AlCl_3(aq)$

5. $AlCl_3(aq) + Al(OH)_3(s) \longrightarrow Al(OH)_nCl_{3-n}(aq)$

6. $Al(OH)_nCl_{3-n}(aq) \longrightarrow Al(OH)_3(gibbsite) + AlCl_3(aq)$

Figure 6. Probable Reactions that Occur in a System Containing Aluminum Oxide, Water Vapor and Hydrogen Chloride (61-63)

H. ESCA Studies

The 1967 monograph by Siegbahn, et al.[64] described the analysis of photoelectrons as a probe of surface composition. The technique was designated ESCA, electron spectroscopy for chemical analysis. In ESCA, a solid sample is irradiated with X-rays followed by analysis of the kinetic energy of the photo-ejected electron. The kinetic energy of the electron (K.E.) is related to the energy level from which it was ejected by the equation:

$$K.E. = h\nu - B.E. - \phi$$

$h\nu$ is the energy of the incident X-rays, B.E. the binding energy of the photo-ejected electron and ϕ the work function of the spectrometer. Slight changes in the electronic environment produce a chemical shift in electron binding energy and the chemical shift can be used as a method of qualitative analysis.

The ESCA technique has found numerous application in studying surfaces and adsorbed species. Reviews have been presented by Hercules[65,66] and currently the use of ESCA as a quantitative surface technique is being studied.[67,68]

Kishi and Ikeda [69] reported an ESCA study of chlorine gas adsorbed on evaporated metal films of Fe, Ni, Pd, Ag, and Au. On exposure to Cl_2 gas the Cl 2p photoelectron line was recorded. For Cl_2 treated Au three peaks were observed in the Cl 2p region at binding energies 197.0, 199.4 and 201.4 eV, the Pd substrate showed only one peak, whereas all the other chlorine treated metal adsorbents showed two

peaks in the Cl 2p region. The Cl 2p binding energy was found to depend on the amount of adsorbed chlorine. Chemical shifts in the metals varied from +3.3 eV for the Fe $2p_{3/2}$ to -0.3 eV for the Ag $3d_{5/2}$. These chemical shifts were compared with the chemical shifts of known metal chloride compounds as a means of identifying the surface species.

An ESCA study of aluminum oxides was reported by Lidsay, et al.[70] These workers measured the Al 2p electron spectra of several anhydrous and hydrated aluminum oxides. The compounds and the results of the ESCA binding energy measurements are presented in Table I. The data shows a decrease in binding energy with an increase in the amount of positively charged ions in the solid. The trend was explained by the fact that the electronegativity of oxygen is higher than hydroxyl groups, thus the binding energy of the Al core electrons is higher than those of the aluminum hydroxides.

TABLE I

BINDING ENERGY, PEAK WIDTH, AND CHEMICAL SHIFT

OF Al (2p) ELECTRONS IN ALUMINUM OXIDES(70)

Compound	Full Width Half Max (eV)	Binding Energy (eV)	Chemical Shift (eV)
α-Al_2O_3	2.25	76.3 ± 0.1	
$MgAl_2O_4$	2.50	75.3 ± 0.1	1.0
α-AlO(OH)	2.26	74.8 ± 0.1	1.5
β-AlO(OH)	2.46	75.7 ± 0.1	0.6
α-$Al(OH)_3$	2.35	74.9 ± 0.1	1.4
β-$Al(OH)_3$	2.40	74.7 ± 0.2	1.6

III. EXPERIMENTAL

This section describes the materials, characterization techniques, and the experimental procedures used in this study. Data reduction procedures are also presented.

A. Description of Materials

1. Adsorbates: The adsorbates used were nitrogen, water and hydrogen chloride. Reagent grade (purity 99%) anhydrous hydrogen chloride was obtained from Matheson Company. Nitrogen used in the surface area measurements was of ultra high purity (99%) obtained from Matheson. Water vapor was produced by using distilled water which had been degassed by repeated freeze-thaw cycles on the vacuum system.

2. Adsorbents: Two aluminas were used as adsorbents. The gamma alumina was obtained from the Cabot Corporation, Boston, Massachusetts and is a high surface area alumina designated Alon-C. Alon-C is a fumed alumina produced by the hydrolysis of aluminum chloride in a flame process, similar to the method described by Fricke and Jockers.[71] According to the manufacturer, Alon-C is predominantly gamma alumina, having a surface area of approximately 100 m^2/g and an average particle size of 0.03 microns. X-ray powder diffraction patterns of Alon-C using Cu K_α radiation confirmed that Alon-C was indeed predominantly gamma alumina.

The alpha alumina used in the study was obtained from the Aluminum Company of America, Pittsburgh, Pennsylvania and designated A16SG. A16SG is produced by heating a transition alumina at 1537°C. According

to the manufacturer, Al6SG is an alpha alumina with a particle size <1 micron. X-ray powder diffraction patterns of Al6SG exhibited diffraction lines characteristic of alpha alumina, confirming that Al6SG is an alpha alumina.

B. Characterization Techniques

1. Surface Area Measurements: An important property to consider when studying the adsorption properties of solid adsorbents is the surface area. The surface areas of alpha alumina and gamma alumina were determined by the BET method described by Gregg and Sing.[72] The system and experimental procedure has been previously described by Hendley, O'Neal and Wightman.[73] Prior to the surface area measurements, the aluminas were outgassed for 2 hrs at 100, 200 and 400°C at (10^{-5} torr), which corresponded to the thermal pretreatment used in the hydrogen chloride and water vapor adsorption studies.

2. Nitrogen Adsorption-Desorption Measurements: Adsorption and desorption isotherms of nitrogen were measured on both aluminas. The same system and adsorption procedure as that described by Hendley, O'Neal and Wightman[73] was employed. Desorption measurements were made by successively increasing the volume of the system by a precalibrated amount using a gas buret. The initial pressure of the nitrogen adsorbate was approximately 1200 torr so that the adsorption - desorption cycle could be measured at relative pressure (P/P_o) values up to 0.95, thus causing capillary condensation in the pores. The method of calculating pore size distribution from nitrogen adsorption - desorption data is described by Gregg and Sing.[74]

3. Scanning Electron Microscopy (SEM): Particle size and topography were studied using an Advanced Metals Research Corporation Model 900 scanning electron microscope operating at 20 kV. Photomicrographs of alumina samples after various treatments were taken at 100X, 1000X and 5000X magnification. Energy dispersive X-ray analysis (EDAX) of the alumina particles was performed using an International Model 707A unit attached to the microscope.

Photomicrographs were taken of both aluminas, untreated and after outgassing, exposure to hydrogen chloride, washing with distilled water, and after contact with 0.1M hydrochloric acid. The samples were mounted on the SEM sample stubs with copper conductive tape. The alumina samples were subsequently vacuum coated with a thin film of Au/Pd alloy.

4. Electron Spectroscopy for Chemical Analysis (ESCA): Qualitative analysis of both adsorbents before and after exposure to hydrogen chloride and solution measurements was made with an AEI ES100 photoelectron pectrometer using Al K_{α} radiation (1486.6 keV) Data acquisition was accomplished with an AEI DS-100 data system and a Digital PDP-8/e computer.

The alumina samples were mounted on copper sample probes, by applying finger pressure. The sticking difficulty encountered in the infrared disk preparation as described in Appendix 1 was used as an advantage in mounting the alumina samples on the ESCA probe.

Studies to insure that the two aluminas were pure and did not contain a surface coating were accomplished by wide scan ESCA spectra.

Wide scan spectra from 0 eV to 743 eV binding energy were obtained on untreated alumina and on alumina which had been washed three times with distilled water.

The nature of the adsorbed hydrogen chloride species was investigated using narrow scan ESCA spectra. ESCA spectra for Al $2s_{1/2}$, Al 2p, O $1s_{1/2}$ and Cl 2p peaks were obtained on alumina before and after treatment with hydrogen chloride. The same peaks of the model compound, $AlCl_3$, were also studied. Calibration of the binding energy of the samples was performed by monitoring the C $1s_{1/2}$ peak.

C. Adsorption Measurements

1. System: Gas adsorption measurements were performed in the vacuum system shown schematically in Figure 7. The pyrex vacuum system could be evacuated to a base pressure of 10^{-5} to 10^{-6} torr by use of a mechanical pump (MP) and a mercury diffusion pump (DP). Pressure was measured using an ionization gauge (IG). The pumps were isolated from the system with a liquid nitrogen trap (LNT). The reservoir bulbs (RA), (RB), (RC), (RD), and (RE) were used for storing gases introduced into the system through valve (VG).

The section of the system below valve (V6) was used to introduce and remove gases from the system. This section consisted of a gas tank (G), mercury manometer (M), helium inlet (HE), liquid nitrogen trap (NT), a trap containing saturated sodium hydroxide (BT), potassium sulfate traps (ST1, ST2) immersed in liquid nitrogen, Teflon valves (V6), (V7), (V8), (V9) and valves (V10) and (VG) and a mechanical pump (SP).

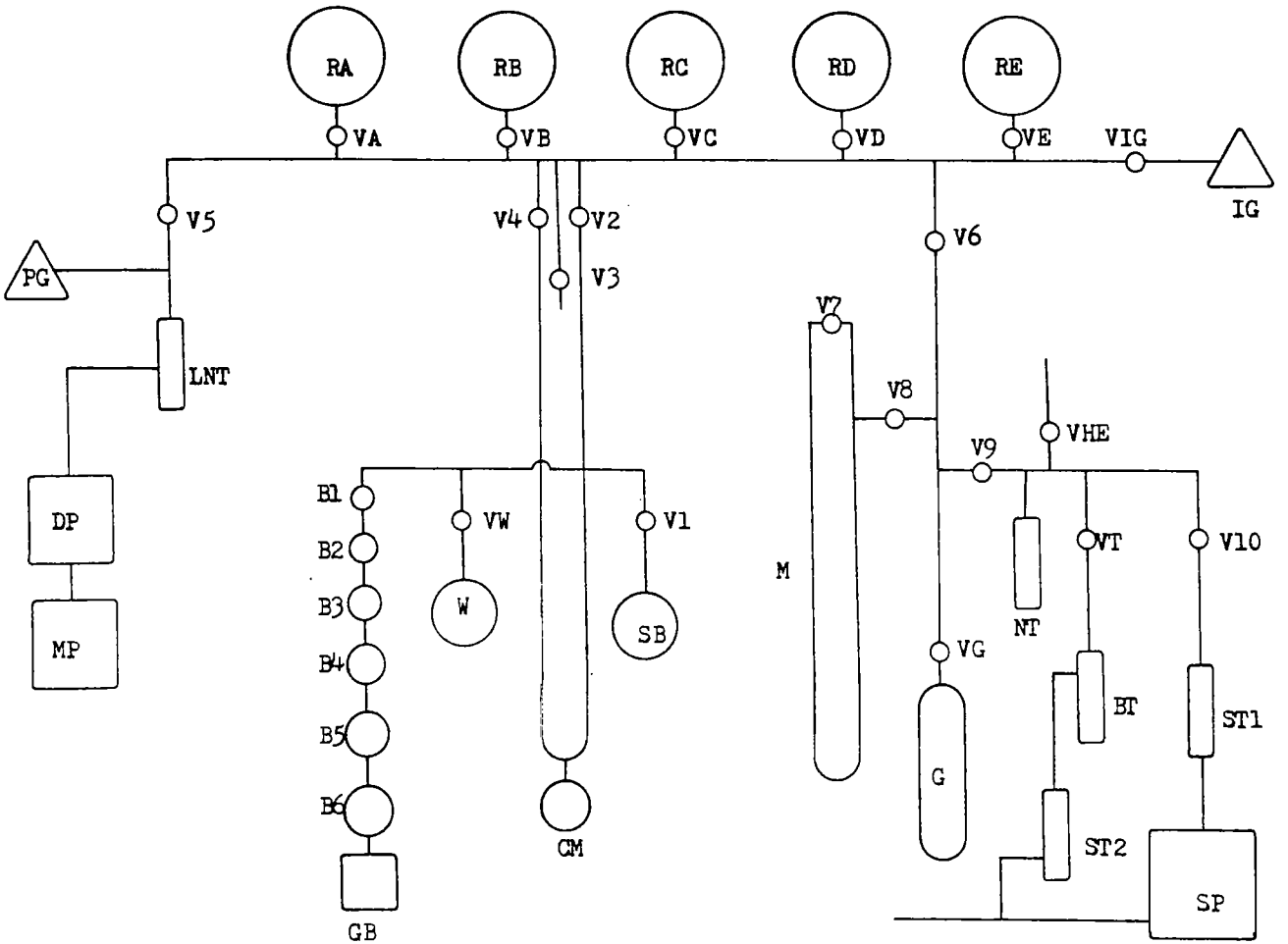

Figure 7. Schematic of Adsorption Apparatus

The system below valves (V2) and V4) was the critical section where the adsorption measurements were performed. This section consisted of Teflon stopcocks (V1), (V2), (V4), and (VW), a constant volume manometer (CM), a gas buret (GB) consisting of a series of precalibrated bulbs (B1 - B6), a bulb containing degassed water (W) and the sample bulb (SB). The sample bulb could be surrounded by either a constant temperature bath or a furnace. The bath temperature was controlled using a mercury thermoregulater connected to a Fischer Model 51 Unitized Bath Control. The sample heater was a tube furnace (Hoskins Electric Company) placed in a vertical position, the temperature was controlled by use of a powerstat and stabilized by connection to a constant voltage transformer. The temperature of the heater was measured using a chromel-alumel thermocouple attached to the wall of the sample bulb and connected to a Thermo Electric MiniMite thermocouple controller.

2. Introduction and Removal of Gases from the System: Gases were introduced into the pre-evacuated system by the following procedure: with stopcocks (V8) and (V10) opened and all the other stopcocks closed gas was introduced into the section between stopcocks (V6) and (V9) by opening (VG) to the gas tank. The pressure was measured on manometer (M), then (V6) was opened and the gas was transferred to the main manifold. Typically 760 torr of gas would be stored in the reservoir bulbs by opening valves (VA - VE).

Hydrogen chloride was removed from the system through a series of traps. Valves were closed except (V1), (V2), (V6), (V9), and (V8). The hydrogen chloride was condensed into trap (NT) surrounded by liquid

nitrogen, (V9) was then closed and helium was introduced into the system between (V9), (VT), (V10), to atmospheric pressure. Valve (VT) was then opened and the liquid nitrogen slowly removed from (NT), the condensed hydrogen chloride expanded and flowed into trap (BT) containing a saturated NaOH solution. Any hydrogen chloride that was not neutralized was then trapped in the potassium sulfate trap (ST2) surrounded by liquid nitrogen. After all the hydrogen chloride had evaporated, the system was purged with helium for several minutes, valve (VT) was closed and valve (V10) to the secondary pump was opened.

3. Sample Outgassing and Pretreatment: In a typical adsorption determination approximately 0.1g of gamma alumina or approximately 1.0g of alpha alumina was weighed into the quartz sample bulb (SB). The sample was pretreated before the adsorption measurement by the following procedure. The entire system between valves (V6) and (V1) was evacuated to 10^{-5} to 10^{-6} torr. The sample bulb (SB) was placed on the system and valve (V1) opened slowly until the Hastings vacuum gauge (PG) measured <0.5 torr. The heater was then placed around the sample bulb and heated for 2 hrs under vacuum at the outgas temperature measured by the thermocouple. After heating, the sample was immersed in the constant temperature bath at the desired adsorption temperature. Preliminary experiments using water vapor adsorption on gamma alumina established this pretreatment procedure.

4. Gas Adsorption Measurement: The gas adsorption measurements were performed in the constant volume system below valves (V2) and (V4). After pretreatment of the sample the following adsorption procedure was

used. With all stopcocks closed the volume of the system was adjusted using the gas buret (GB), usually the mercury level was fixed between bulbs (B5) and (B6). Helium was introduced into the system through valves (VHE), (V9), (V6) and (V2). Valve (V2) was then closed and the initial pressure measured using the constant volume manometer (CM). A cathetometer (Gaertner Scientific) was used to read the manometer (precision $\pm$ 0.05mm). Valve (V1) was opened and helium expanded into the sample bulb. The final pressure was measured and by use of the ideal gas law the final volume was calculated. The initial volume was known from previous calibration with helium. After this volume calibration, valve (V2) was opened and the system evacuated to 10^{-5} to 10^{-6} torr. The adsorption measurement was performed in the same manner. The adsorbate was introduced from a reservoir bulb through valve (V2) with valve (V1) closed, the initial pressure was measured. Valve (V1) was opened and after equilibrium was established the experimental pressure was read using the manometer and cathetometer. The sample bulb stopcock (V1) was then closed and another dose of adsorbate introduced and the pressure was measured. Valve (V1) was then opened, the equilibrium pressure measured and the second adsorption point was obtained. This procedure was continued until an entire isotherm was obtained.

By this procedure, the initial and final volumes are known from the helium calibration. The initial and equilibrium pressures are determined. Using these parameters and the ideal gas law one can calculate the ideal pressure assuming that only gas expansion occurred. The difference between the equilibrium pressure and the ideal pressure

can be related to the amount of gas adsorbed by use of the ideal gas law. A sample calculation of an adsorption isotherm using the experimental data is presented in Appendix 2.

5. Readsorption Procedure: The reversibility of the hydrogen chloride and water vapor adsorption was tested by performing readsorption experiments. The readsorption experiment consisted of evacuating the sample bulb after the initial adsorption isotherm was obtained. The evacuation typically lasted 18 to 20 hrs and was carried out at the adsorption temperature, then another adsorption isotherm was measured.

D. Solution Measurements

In conjunction with calorimetric studies performed by Wightman[60] some solution properties of the aluminas were measured. pH changes of hydrochloric acid solutions upon addition of alumina were determined as well as solubilities of the alpha and gamma alumina in hydrochloric acid and distilled water.

1. Solubility Measurement: A stock solution of 0.1N HCl was prepared by dilution of a Hellige standard hydrochloric acid solution R1193C to 1000 cc with double distilled, deionized water. 40cc aliquots of this stock solution or water were placed in a flask, 0.1g of alumina was introduced, the solution was heated to near boiling for 15 minutes and then stirred for two hours. The alumina/0.1N HCl or alumina/water solution was then centrifuged and filtered. The concentration of aluminum in these filtered solutions was determined using a Perkin Elmer Model 503 Atomic Absorption spectrometer equipped with

automatic digital readout of concentration. A single element hollow cathode lamp (Perkin Elmer) was employed in the determination of the aluminum. Standards were prepared by dilution of a stock 1000 ppm solution, as described by Smith and Parsons.[75] To insure that no aluminum contamination was present in the HCl solutions and distilled water the aluminum concentration of blank solutions of water and 0.1N HCl, treated in the same manner but containing no alumina, was measured. The results of the solubility measurements are presented in Appendix 3.

2. pH Measurement: The change in pH of dilute hydrochloric acid solutions and water upon addition of alumina was recorded using an Orion Research Model 701 pH Meter and Thomas Universal Combination Electrode. Approximately 0.1 g of gamma alumina or 1.0 g of alpha alumina was weighed and heated in a lab oven at 100°C for one hour. These weighed alumina samples were placed in 5 cc of solution and stirred constantly throughout the experiment. The pH was measured before addition of the alumina and at time intervals of 10, 60 and 180 minutes.

E. Data Reduction Procedures

1. Adsorption Isotherms: Experimental data obtained in the adsorption system was reduced to the amount of gas adsorbed by employing equations based on the ideal gas law. The amount adsorbed was calculated by the following equations:

$$R_1 - R_0 = P1 \tag{1}$$

$$R_2 - R_0 = P_{EXP} \tag{2}$$

$$P_{CAL} = \frac{P1 \text{ X } VI + P2 \text{ X } VSB}{VT} \tag{3}$$

$$P = P_{CAL} - P_{EXP} \tag{4}$$

$$N_i = \frac{P \text{ X } VT}{R \text{ X } T \text{ X } W} \tag{5}$$

$$N_S = \sum_{i}^{n} N_i \tag{6}$$

where: R_0 = Zero point setting of cathetometer.

R_1 = Initial cathetometer reading before sample stopcock was opened.

R_2 = Cathetometer reading after equilibrium is established.

P2 = Pressure in sample bulb after V1 was closed for next dose of gas. P2 is equal to P_{EXP} in previous determination and P2 is zero in initial adsorption.

VI, VSB and VT = The initial volume, sample bulb volume and total volume, respectively, which were determined using helium expansion.

R = Ideal gas law constant in appropriate units.

T = Adsorption temperature.

W = Sample weight.

The following parameters are calculated using equations 1 - 6:

P1 = Initial pressure of adsorbate.

P_{EXP} = Equilibrium pressure (experimental).

P_{CAL} = Calculated pressure if only expansion occurred.

N_i = Number of moles of adsorbate/gram adsorbent adsorbed on the sample after each dose.

N_S = Total number of moles adsorbate/gram adsorbent adsorbed.

A typical data table and sample calculation is given in Appendix 2.

2. Monolayer volume and Adsorbate Area: The monolayer volume is defined as the quantity of adsorbate required to cover the adsorbent with a monomolecular layer. The monolayer volume is used to determine surface areas of finely divided and porous solids. The adsorbate area is defined as the area occupied by an adsorbate molecule on the adsorbent surface. The adsorbate area was calculated using the monolayer volume of the adsorbate and the nitrogen surface area of the adsorbent. Several methods [11,14,74] of calculating monolayer volume from adsorption data have been described including the BET method and Langmuir treatment.

The Brunauer, Emmett, and Teller method (BET) was used to calculate the monolayer volume of water adsorbed on gamma alumina (Alon-C) and alpha alumina (A16SG). The BET equation was used in the following form:

$$\frac{X}{N(1 - x)} = \frac{1}{N_m c} + \frac{(c - 1)X}{N_m c} \qquad (7)$$

where $X = \frac{P}{P_0}$

and P = Equilibrium pressure of water vapor

P_o = Vapor pressure of water at the adsorption temperature.

N = Number of moles H_2O/gram adsorbent at each pressure.

c = A constant related to the heat of adsorption and is characteristic of the gas/solid system.

N_m = Monolayer capacity in moles H_2O/gram adsorbent.

$$N_m = \frac{1}{m + Y} \tag{8}$$

where Y and m are the y-intercept and slope of a plot of x/N (1-x) vs. P/P_o. The slope and y-intercept were evaluated using a linear least squares computer program on a Digital PDP 8/I computer.

The area of the adsorbed water on the alumina was calculated by the following equation:

$$A = \frac{\Sigma}{N_m \cdot N_o} \tag{9}$$

where: N_m = Monolayer capacity of the adsorbate

N_0 = Avogadro's number.

Σ = BET nitrogen surface area of the adsorbent in appropriate units.

and therefore, A is the area occupied by each adsorbed water molecule in square angstroms.

The monolayer capacity of adsorbed hydrogen chloride on the alumina was calculated using the following form of the Langmuir equation:

$$\frac{P}{N} = \frac{1}{bN_m} + \frac{P}{N_m} \tag{10}$$

where: P = Equilibrium pressure of hydrogen chloride.

N = Number of moles of HCl/gram adsorbent.

b = Constant characteristic of the system.

N_m = Monolayer capacity in moles HCl gram adsorbent.

The monolayer capacity is equal to the reciprocal of the slope of the line obtained by plotting P/N vs P. The adsorbate area of HCl is calculated from the monolayer capacity in the same way as the area of the adsorbed water molecule (see equation 9).

3. Isosteric Heat Calculation: The thermodynamic properties of a gas/solid system can be determined either directly from gas phase calorimetry or indirectly by mathematical analysis of several adsorption isotherms. In this study adsorption isotherms at three temperatures were used to calculate isosteric heats of adsorption at various surface coverages. The isosteric heat is a differential quantity calculated using the isotherm data and the Clausius Clapeyron equation in the following form

$$-q_{st} = R\left[\frac{\ln P}{(1/T)}\right]_N \qquad (11)$$

where: q_{st} = Isosteric heat of adsorption.

R = Ideal gas constant.

P = Equilibrium pressure.

T = Adsorption temperature.

N = Moles adsorbate/gram adsorbent

The isosteric heat was calculated from a plot of ln P vs 1/T at constant coverage. The slope of this linear plot is equal to $-q_{st}/R$.

Accurate determination of values of ln P at constant coverage was facilitated by computer fitting the isotherm data. Clark, Holm, and

Blackburn[76] used a Freundlich plot (log P vs log N) to fit isotherm data of ammonia adsorption on silica-alumina in the calculation of thermodynamic properties. A comparison of hydrogen chloride and water vapor isotherm data by the BET, Langmuir and Freundlich equations showed that the Freundlich equation gave the best fit, that is the least deviation from linearity, of the experimental data. A "Focal" computer program for calculating N vs ln P from experimental data using the Freundlich equation is shown in Appendix 4. The computer program used to calculate the isosteric heat of adsorption using the Freundlich parameters is described in Appendix 5.

IV. RESULTS AND DISCUSSION

A. Characterization of Adsorbents

1. Crystalline phase: X-ray powder diffraction patterns of Alon-C using Cu K_α radiation exhibited diffraction lines at 1.98 and 1.39 Å characteristic of gamma alumina. Intense lines at 2.087, 2.555 and 1.601 Å were observed in the X-ray powder pattern of Al6SG. Several other less intense line were also seen. The entire pattern was characteristic of alpha alumina.

2. Surface areas: A typical BET plot for the low temperature nitrogen adsorption on gamma alumina outgassed at 100°C is shown in Figure 8. A similar plot for nitrogen adsorption on alpha alumina outgassed at 100°C is shown in Figure 9. These figures show a reasonable fit of the adsorption data to the BET equation. The results of the BET surface area determination for alpha alumina are given in Table II. The surface areas were determined after outgassing the sample at 100, 200 and 400°C. The alpha alumina has a surface area of 8.1 ± 1.8 m^2/g. The surface area is constant between 100-400°C in agreement with the results of Morimoto, Shiomi and Tanaka.[51] This lack of outgas temperature dependence is reasonable since alpha alumina is the high temperature modification of alumina and does not undergo a phase transistion in the temperature range studied (100-400°C).

The surface area of gamma alumina shows a significant dependence on outgas temperature as seen in Table III. A 10% loss in surface area is seen for gamma alumina outgassed at 400°C. This loss of surface area was also observed by Morimoto, Shiomi and Tanaka.[51] The decrease

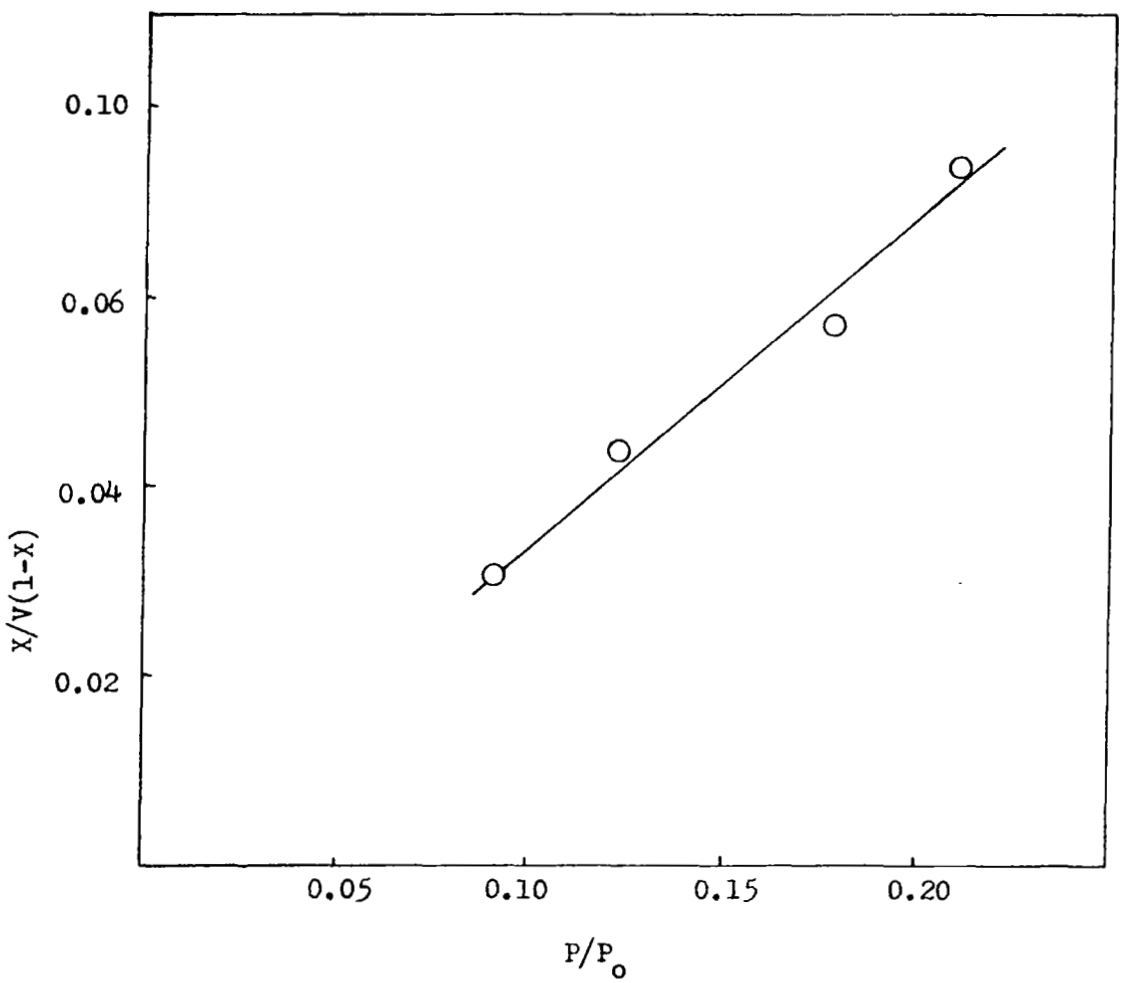

Figure 8. Typical BET Plot for Nitrogen Adsorption on Gamma Alumina

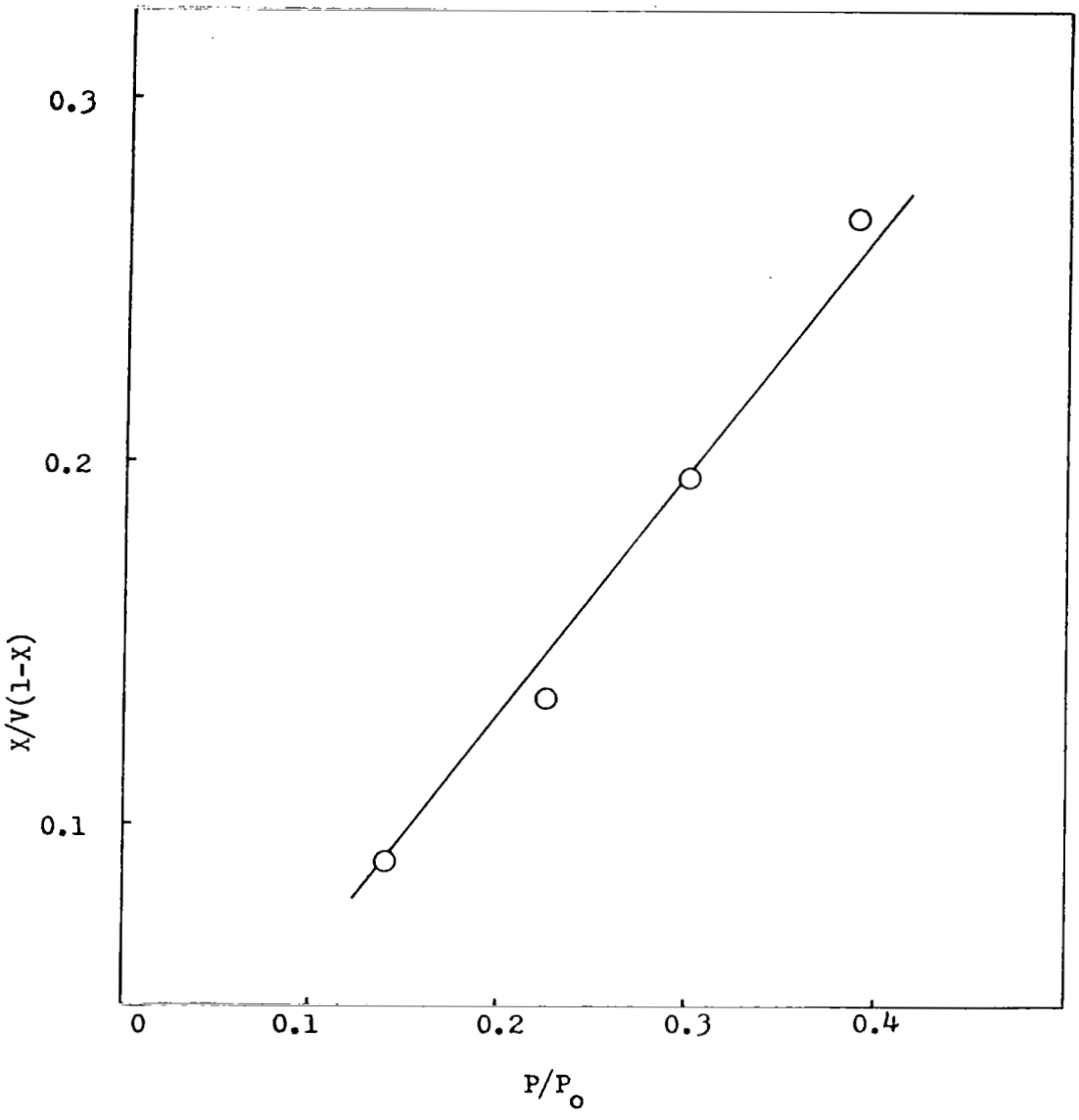

Figure 9. Typical BET Plot for Nitrogen Adsorption on Alpha Alumina

TABLE II

BET NITROGEN SURFACE AREA OF ALPHA ALUMINA

Outgas Temperature (°C)	Surface Area (m^2/g)
100	8.1
200	9.2
200	8.4
200	7.4
400	6.3
400	8.4
400	9.1
	Average 8.1 ± 1.8

TABLE III

BET NITROGEN SURFACE AREA OF GAMMA ALUMINA

Outgas Temperature (°C)		Surface Area (m^2/g)
100		94.0
100		97.1
100		92.9
200		95.4
200		97.7
	Average	95.4 ± 3.4
400		81.3
400		87.1
400		82.9
400		88.7
400		87.8
	Average	85.6 ± 3.9

in surface area may be due to sintering accompanying the onset of a phase transition. Gamma alumina is a low temperature transitional alumina, capable of undergoing phase changes at elevated temperature. Werfers and Bell[23] report the transition from gamma to delta alumina occurring near 900°C under conditions of moist atmosphere, pressure greater than one atmosphere, heating rate greater than 1°C/min and particle size greater than 100 microns. Although the gamma alumina was outgassed at only 400°C, conditions of pressure, atmosphere and particle size are different and may favor formation of delta alumina at lower temperatures.[77,78]

The surface area of the two aluminas given in Table II and Table III is related to the particle size of the two aluminas. If one assumes spherical non porous particles having a density of 3.6 g/cc for gamma alumina, an average particle size of 0.02 microns is calculated. The manufacturer's value is given as 0.03 microns. A calculated particle size of 0.18 microns is obtained for alpha alumina using a density of 3.9 g/cc.

3. Nitrogen Adsorption and Desorption on Alumina: The results of nitrogen adsorption - desorption measurements on gamma alumina are shown in Figure 10. No hysteresis was seen in the desorption cycle of nitrogen. This lack of hysteresis was due to an absence of micropores (<200 Å) in the gamma alumina in which nitrogen could condense.

Figure 11 shows the low temperature nitrogen adsorption-desorption isotherm on alpha alumina. Again the desorption cycle shows no hysteresis, indicating the absence of micropores. The lack of micropores is

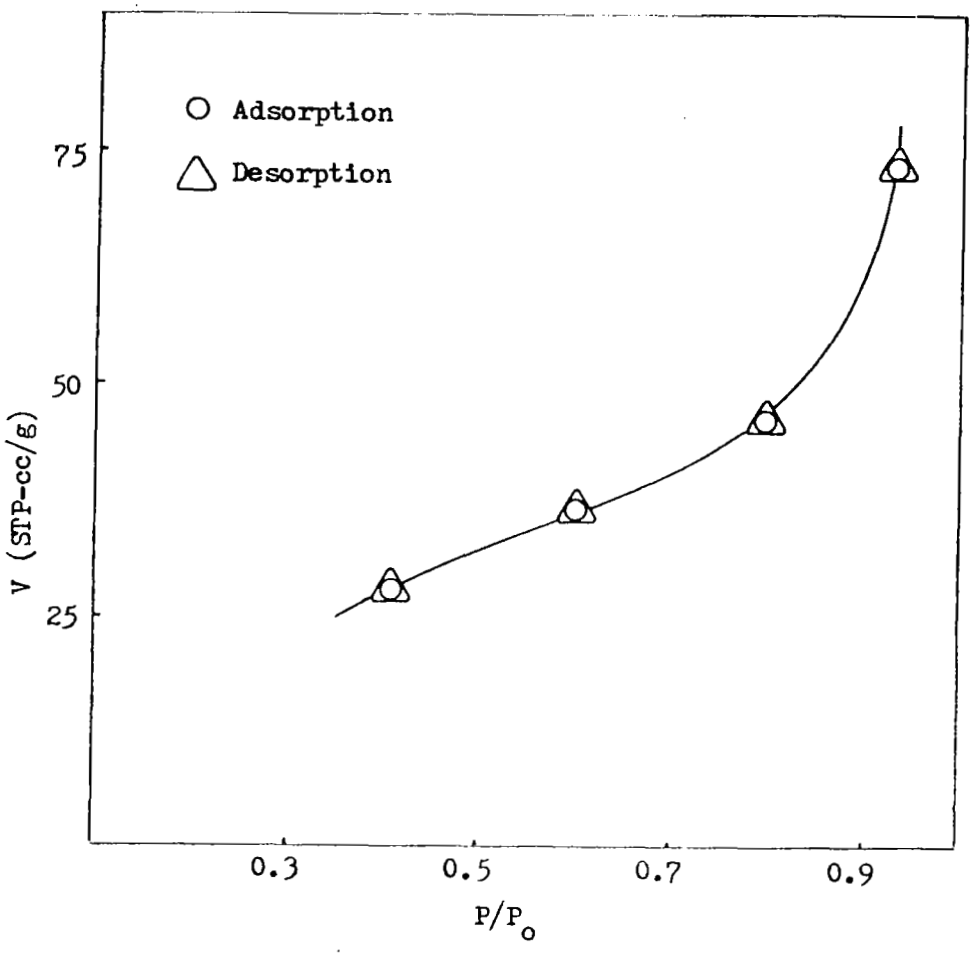

Figure 10. Adsorption and Desorption of Nitrogen on Gamma Alumina at 77°K

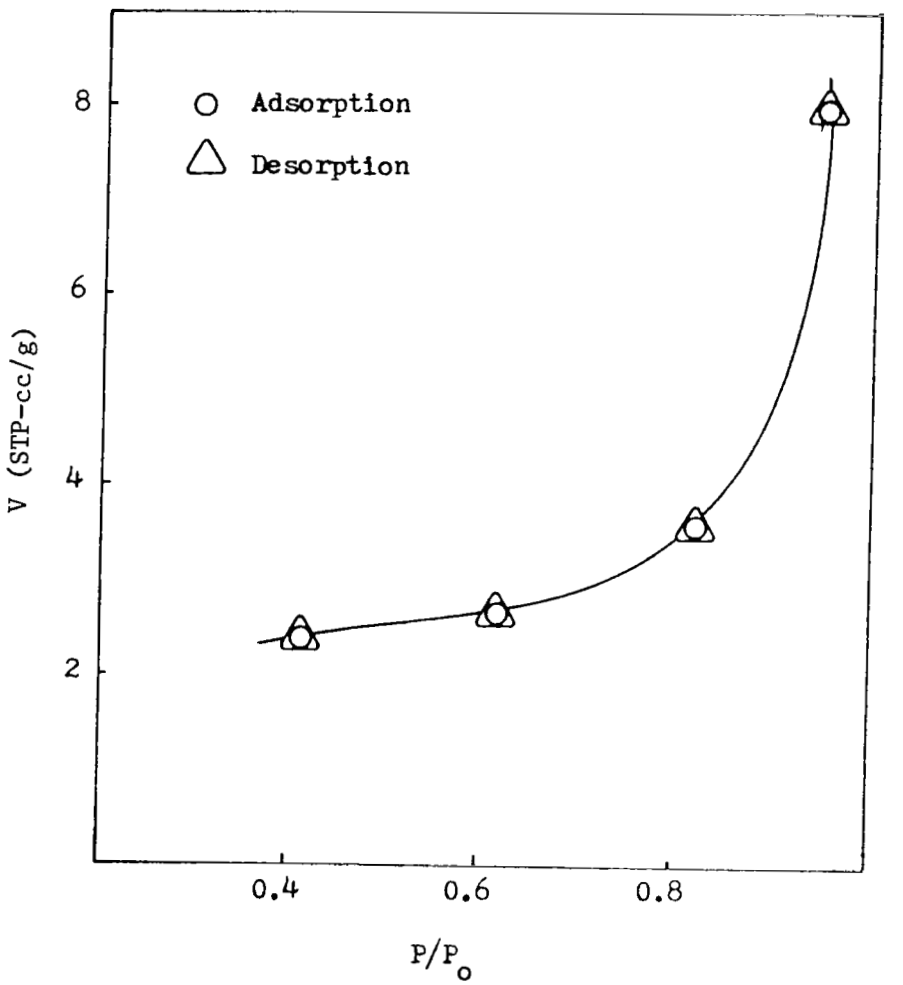

Figure 11. Adsorption and Desorption of Nitrogen on Alpha Alumina at 77^{o}K

not unexpected since alpha alumina had been heated to 1537°C and gamma alumina is prepared in a high temperature flame. The results of the adsorption-desorption studies reinforces the validity of the calculation of relative particle size using surface areas and density where it was assumed that both adsorbents did not contain micropores.

4. Surface Topography and SEM Studies: A 100X scanning electron photomicrograph of untreated gamma alumina is shown in Figure 12. A 100X photomicrograph of alpha alumina is reproduced in Figure 13. A cursory comparison of the particle size in these two figures might lead to the conclusion that gamma alumina consists of larger particles than alpha alumina. However, inspection of the photomicrographs taken at 5000X magnification shown in Figure 14 and Figure 15 leads to a different conclusion. The gamma alumina consists of small primary particles clustered together to give the larger secondary particles observed at lower magnification. Excessive charging of the particles lead to a loss of resolution at magnifications greater than 5000X and prevented studies of the topography of the individual alumina particles.

The results of an SEM experiment to account for the observed decrease in surface area of gamma alumina at high pretreatment temperature are shown in Figure 16 and Figure 17. No significant differences are seen on comparing the photomicrographs of untreated gamma alumina, Figure 12 and Figure 14 with those of gamma alumina taken after outgassing at 400°C. These results show that the changes in gamma alumina associated with the measured 10% decrease in surface area cannot be observed using scanning electron microscopy.

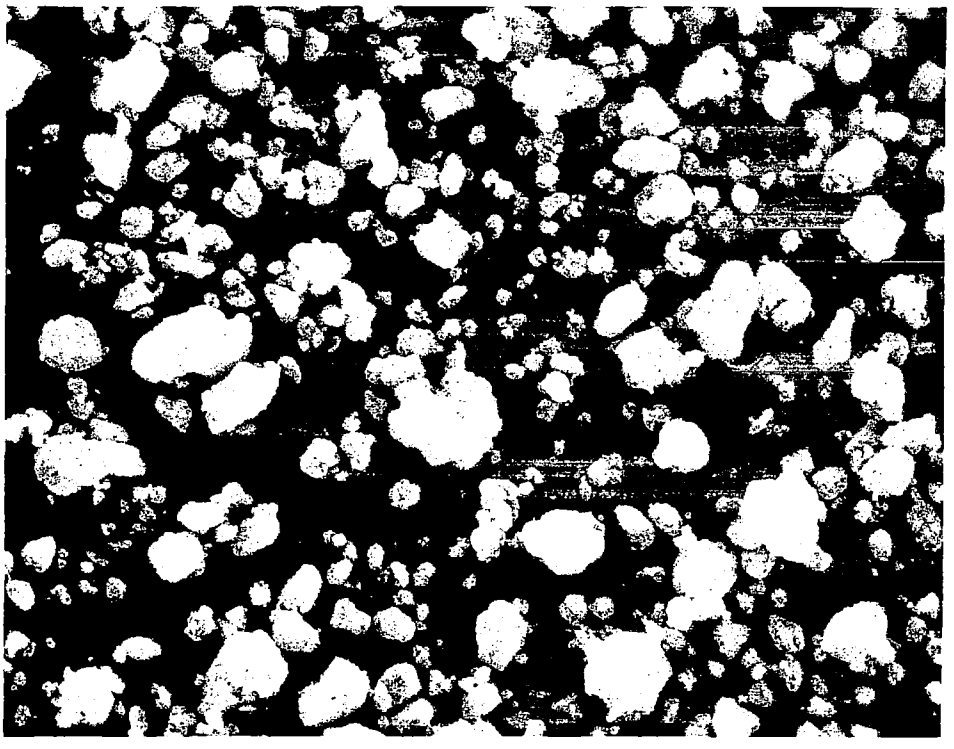

Figure 12. Photomicrograph of Untreated Gamma Alumina at 100X

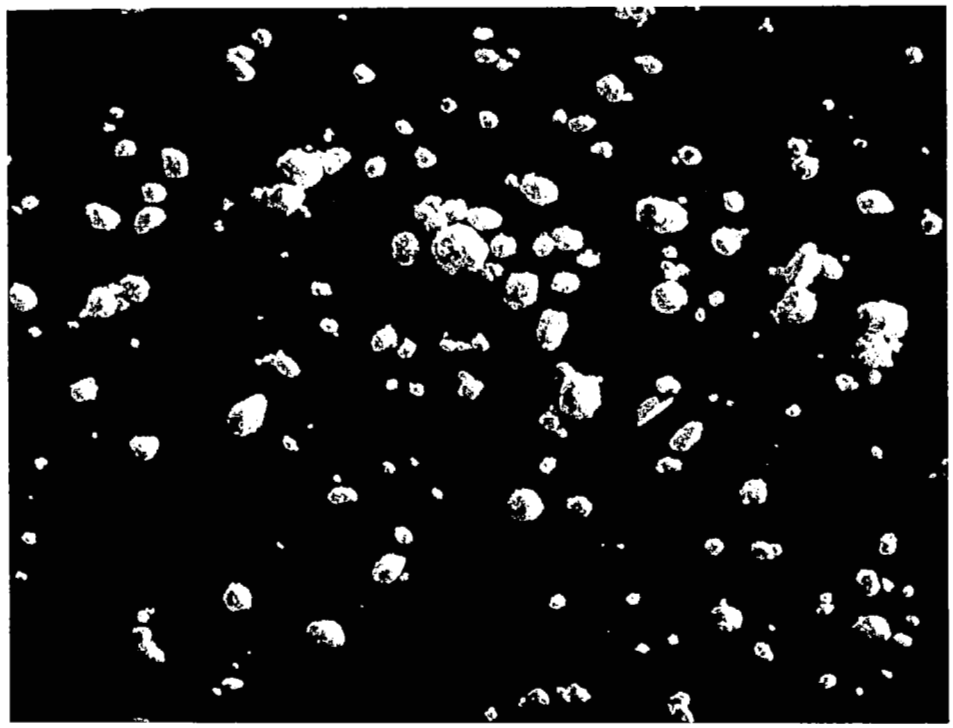

Figure 13. Photomicrograph of Untreated Alpha Alumina at 100X

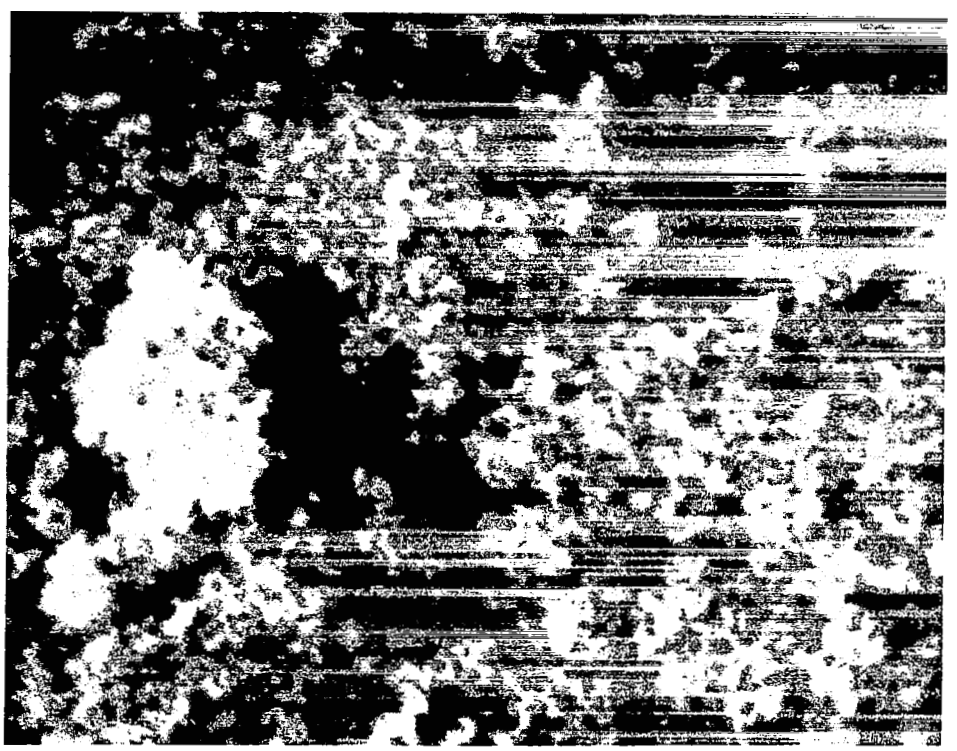

Figure 14. Photomicrograph of Untreated Gamma Alumina at 5000X

Figure 15. Photomicrograph of Untreated Alpha Alumina at 5000X

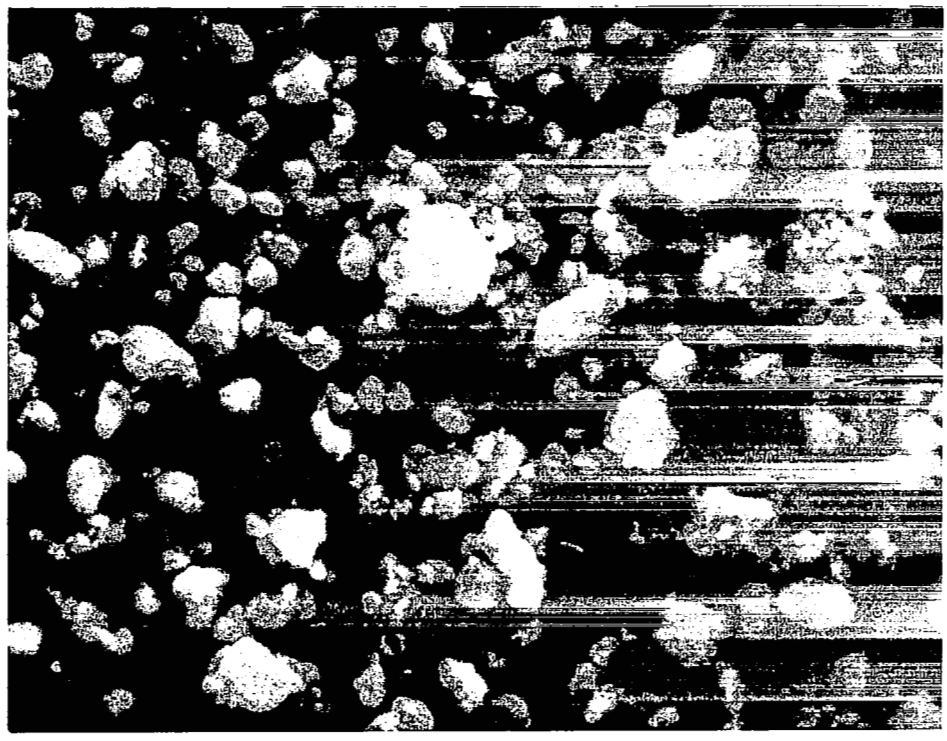

Figure 16. Photomicrograph of Gamma Alumina Outgassed at 400°C at 100X

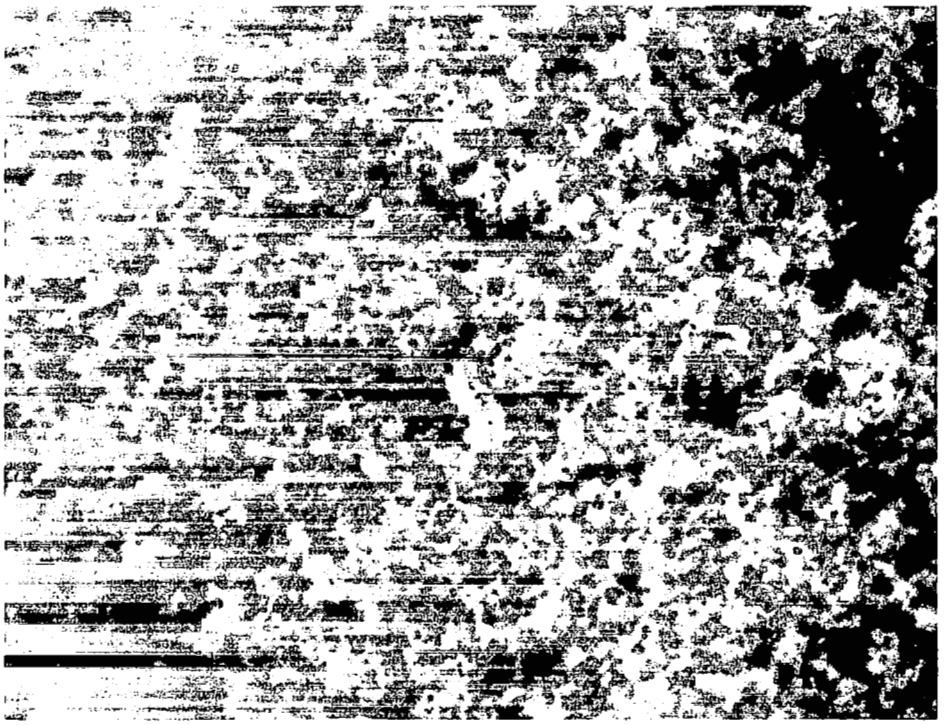

Figure 17. Photomicrograph of Gamma Alumina Outgassed at 400°C at 5000X

The results of energy dispersive analysis of X-rays (EDAX) of untreated gamma alumina is shown in Figure 18. The only peaks seen are those resulting from the Au-Pd coating and aluminum. Other elements of interest such as chlorine, sodium and silicon were not detected. The same results were obtained on a sample of untreated alpha alumina.

5. ESCA Surface Analysis: A qualitative study of the surface composition of alpha and gamma alumina was carried out using wide scan ESCA. Figure 19 shows the wide scan ESCA spectrum of an untreated alpha alumina sample. The largest peaks in the spectrum correspond to the O $1s_{1/2}$ (532 eV), C $1s_{1/2}$ (284 eV), Al 2p (74 eV) and Al $2s_{1/2}$ (118 eV) levels and to an Auger peak of Cu. A small peak at 200 eV may be due to chlorine contamination. The C $1s_{1/2}$ peak is a result of contamination from the oil diffusion pumps of the spectrometer. The Auger peak for copper is not surprising since the copper sample probe may not have been completely covered.

Figure 20 shows a wide scan ESCA spectrum of untreated gamma alumina. Again the observed peaks can be assigned to an Auger transition for Cu and to the O $1s_{1/2}$, Al 2p, Al $2s_{1/2}$ and C $1s_{1/2}$ levels. A small peak at 200 eV is again assignable to chlorine which is not unexpected since $AlCl_3$ is the starting material for the preparation of gamma alumina. The fact that other intense peaks are not observed is evidence for the absence of any surface coating on both alumina surfaces.

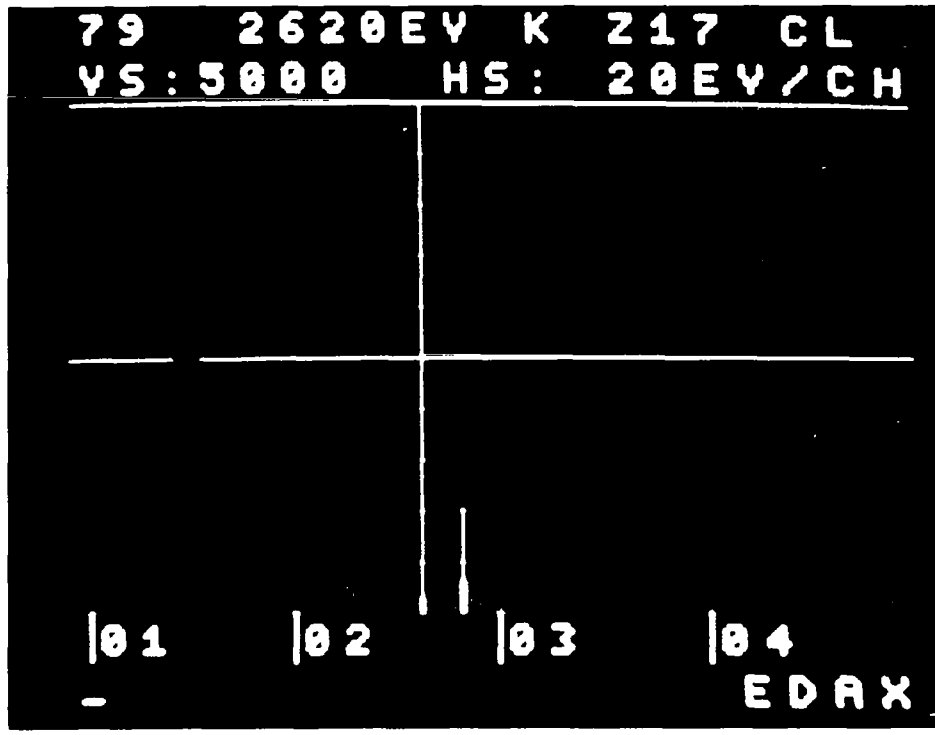

Figure 18. EDAX of Untreated Gamma Alumina

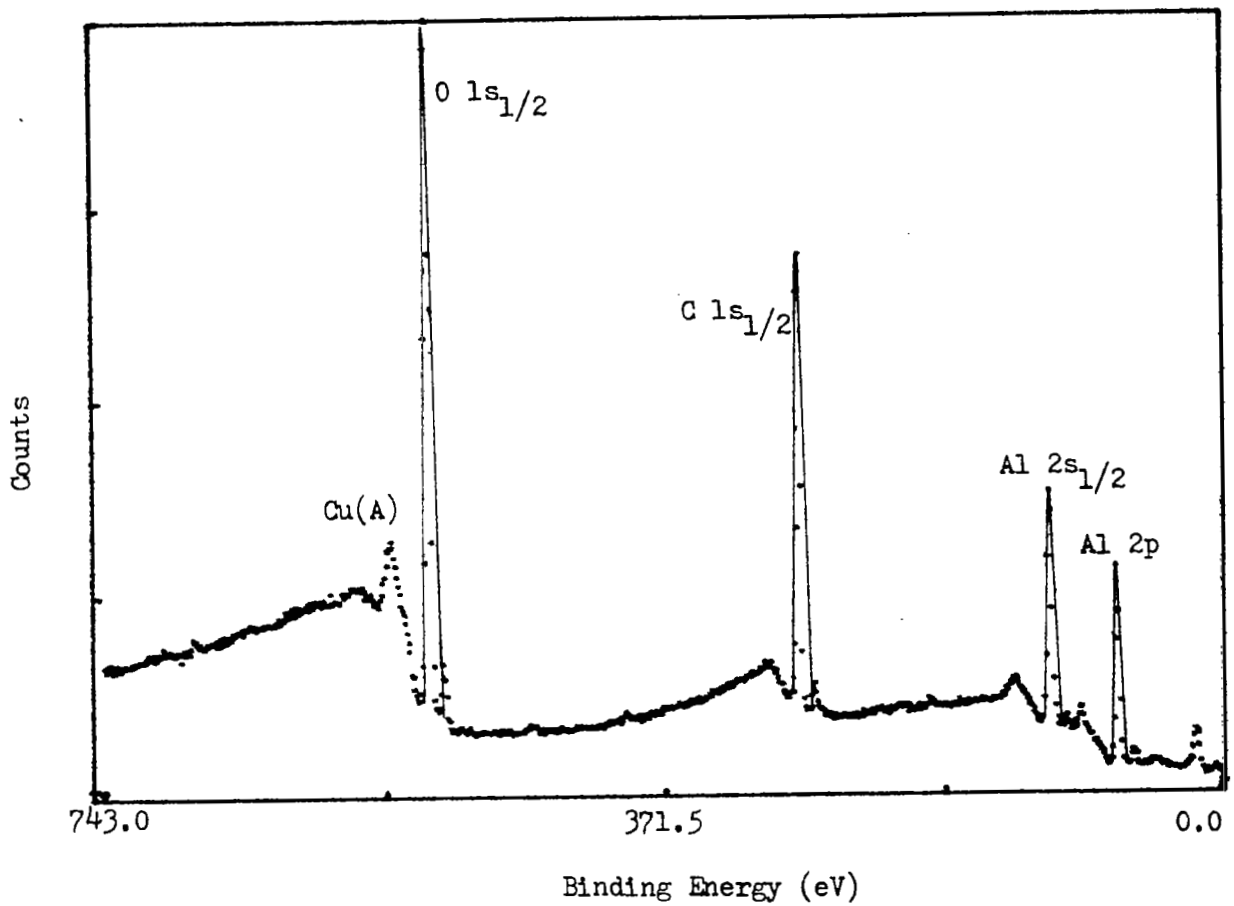

Figure 19. Wide Scan ESCA Spectrum of Untreated Gamma Alumina

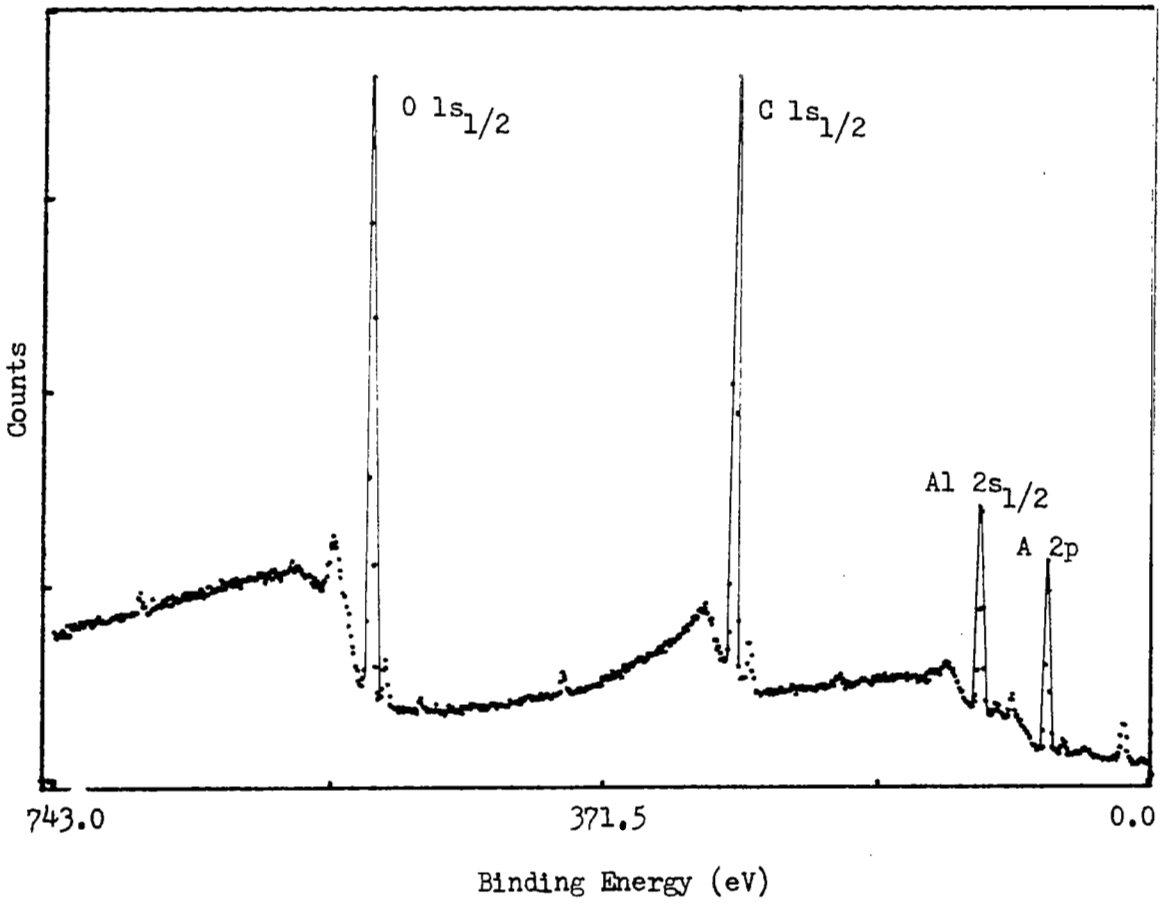

Figure 20. Wide Scan ESCA Spectrum of Untreated Alpha Alumina

B. Preliminary Adsorption Studies:

The reproducibility of the adsorption properties of gamma alumina was studied as a function of temperature and the time of heating of the sample in the constant volume adsorption apparatus. Results of water adsorption at room temperature on gamma alumina outgassed for 2 hr at three different temperatures are shown in Figure 21. The temperature of the pretreatment is critical in defining the adsorption capacity.

Figure 22 shows the effect of the pretreatment time on the adsorption capacity of gamma alumina outgassed at 60°C for time periods from 2 to 19 hours. No change in adsorption capacity over this range of pretreatment time is observed. After these preliminary studies of the effects of pretreatment time and temperature on the adsorption capacity of alumina, all samples were evacuated for 2 hrs at a specified outgas temperature and then cooled for 2 hrs to the adsorption temperature. The good reproducibility of this technique is seen in Figure 23, in which six separate HCl adsorption isotherms (50°C) are shown on gamma alumina samples outgassed at 80°C for two hrs.

The amount of both HCl and H_2O adsorbed on the walls of the sample bulb was determined to be negligible. This result is reasonable since the sample bulbs (15cc) have a small surface area compared to the surface areas of alpha and gamma alumina.

C. Water Vapor Adsorption on Gamma Alumina

The results of the previous section showed that outgas temperature was critical in defining the adsorption capacity of gamma alumina. A

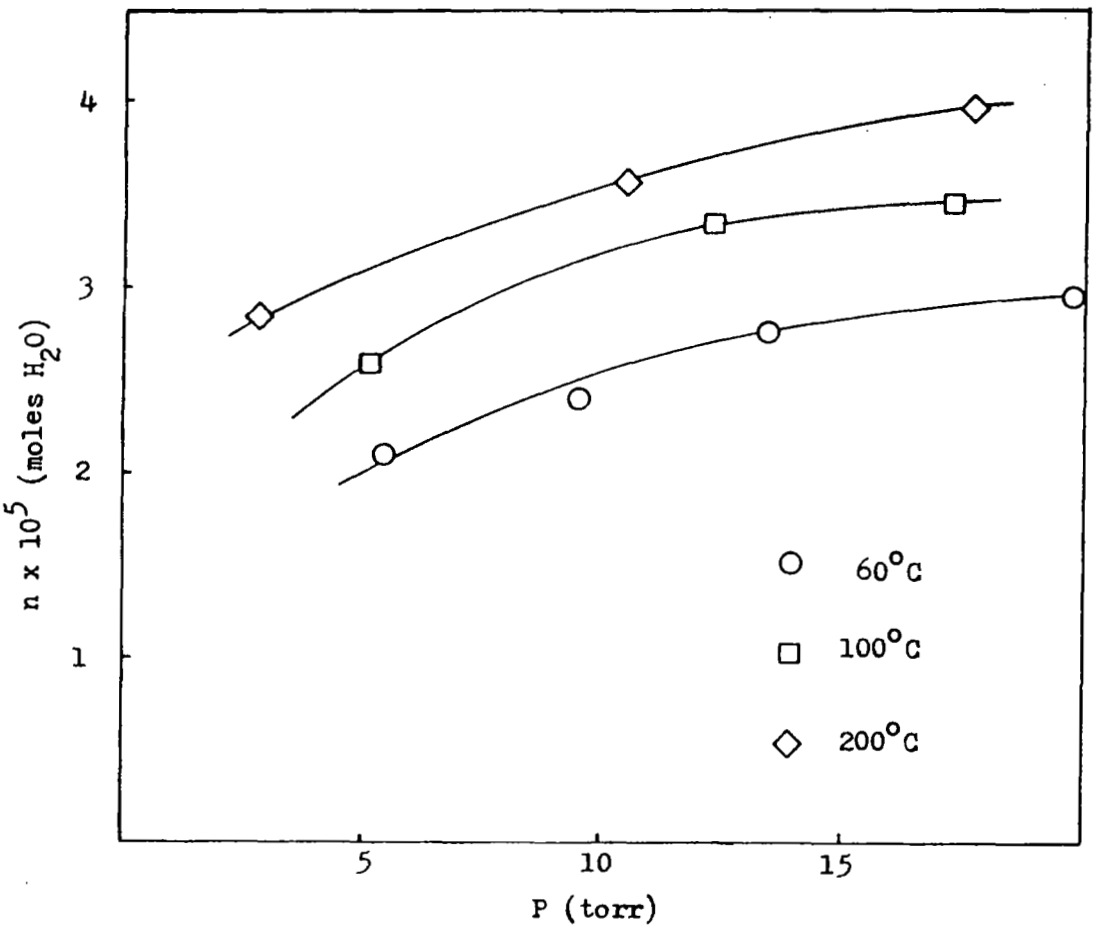

(1 torr = 133.32 Pa)

Figure 21. Influence of Outgas Temperature on Water Vapor Adsorption on Gamma Alumina

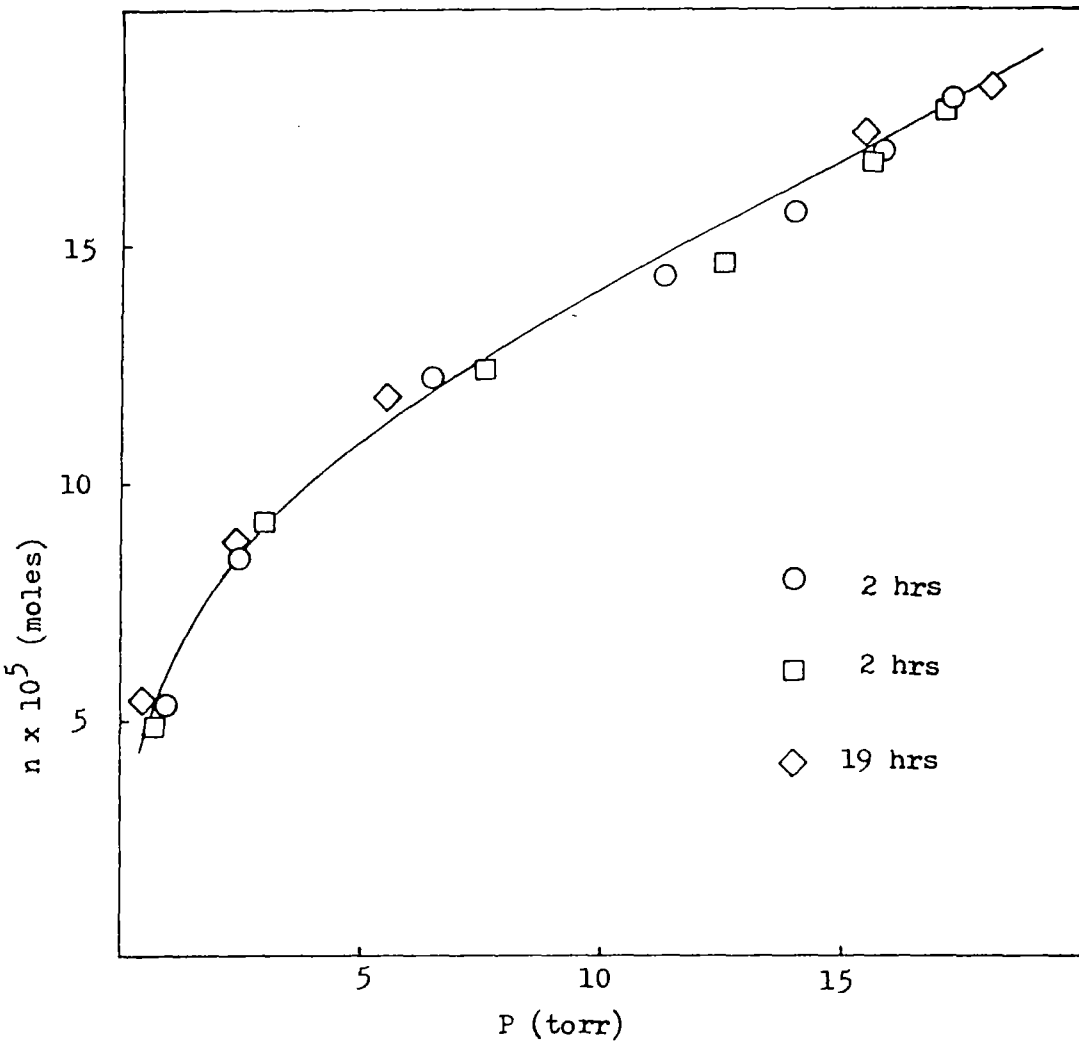

Figure 22. Effect of Heating Time on Adsorption Capacity of Alumina

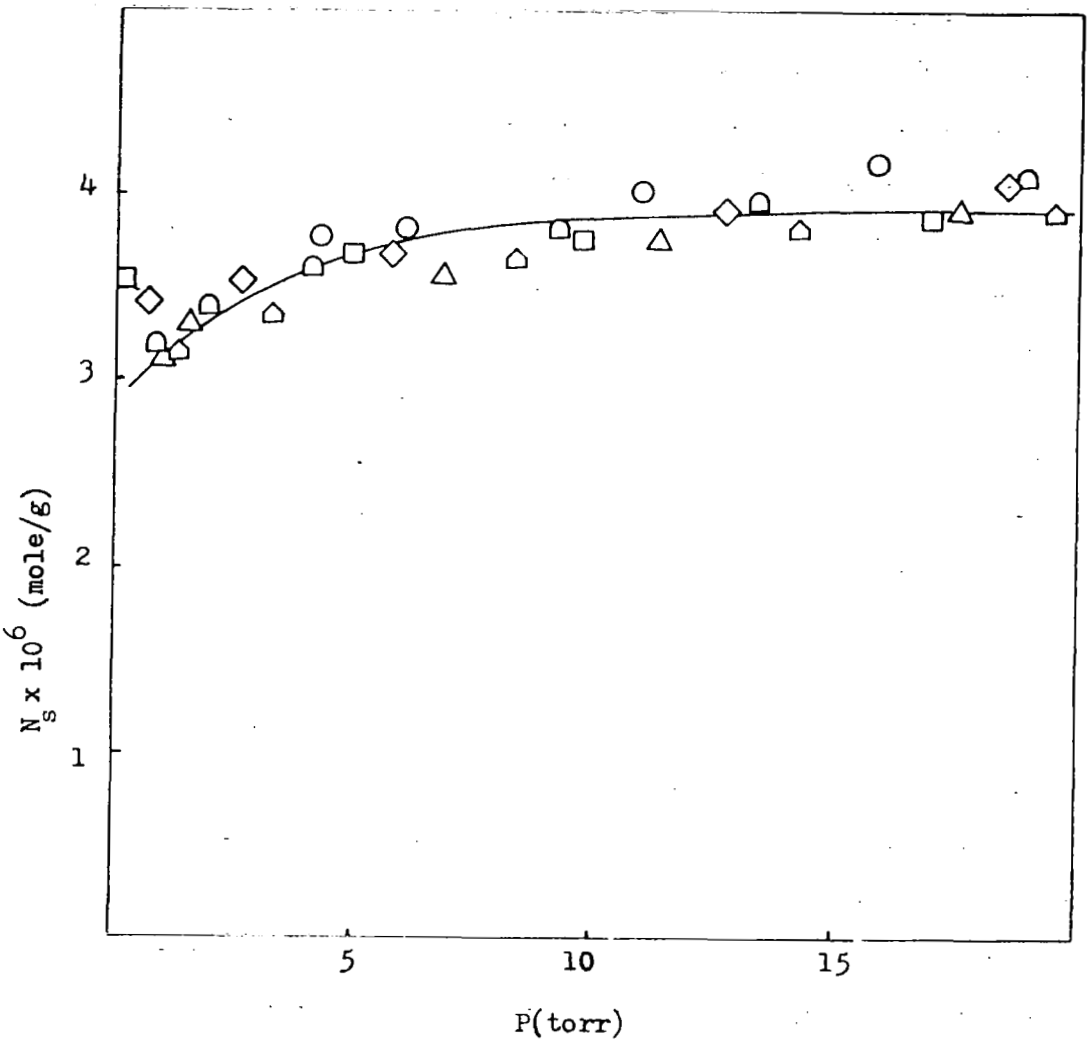

Figure 23. Reproducibility of HCl Adsorption at 50°C on Six Different Gamma Alumina Samples

matrix of experimental parameters based on outgassing temperature and adsorption temperature was developed to further study this temperature influence. Water vapor adsorption was measured on gamma alumina outgassed at 80, 200 and 400°C. Adsorption isotherms were measured at 30, 40, and 50°C. The data for water vapor adsorption on gamma alumina is presented in Appendix 6.

The results of the outgas temperature study are shown in Figure 24 for H_2O adsorption at 40°C on gamma alumina. The amount of water adsorption increases with increasing outgas temperature due probably to removal of physisorbed water. Similar results were obtained at 30 and 50°C.

The temperature dependence of water adsorption on gamma alumina outgassed at 80°C is shown in Figure 25. An inverse relationship between H_2O adsorption capacity and adsorption temperature is observed. Similar results were obtained after outgassing at 400°C.

The adsorption data was linearized using the BET equation. The use of the BET equation allows the calculation of the average area occupied by an adsorbed water molecule. Table IV gives the cross-sectional area (σ) of the adsorbed water molecule calculated from the water vapor isotherms. The σ values appear to fall into two groups. An average σ value of 16.2 $Å^2$/molecule is obtained for gamma alumina outgassed at 80°C or 200°C. Water adsorbed on gamma alumina outgassed at 400°C gives an average area of 12.4 $Å^2$/molecule. Peri's idealized model[41] of the gamma alumina surface (see Figure 1) would yield an adsorbed area of 16 $Å^2$/molecule assuming that each adsorbed

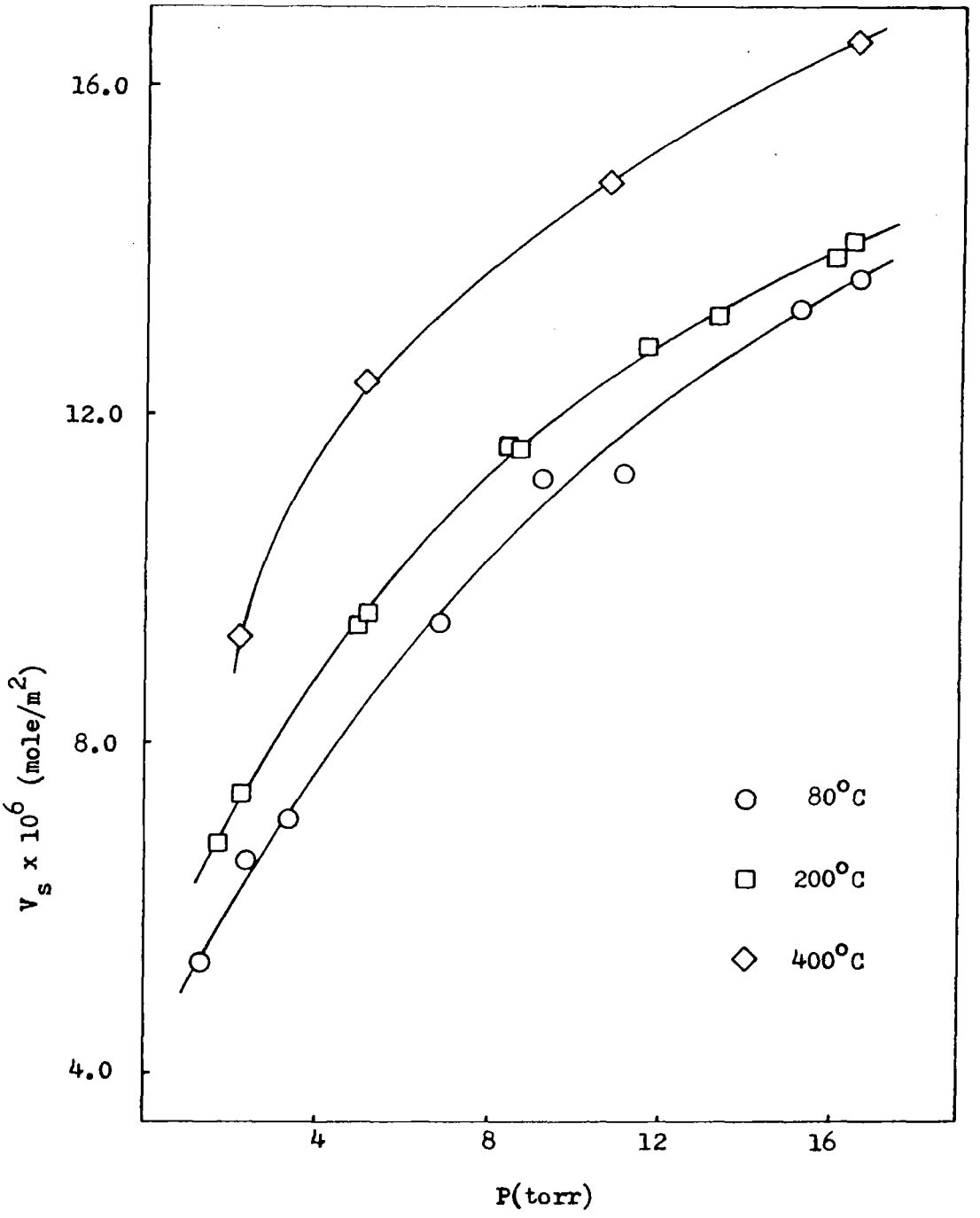

Figure 24. Influence of Outgas Temperature on Water Vapor Adsorption on Gamma Alumina at 40°C

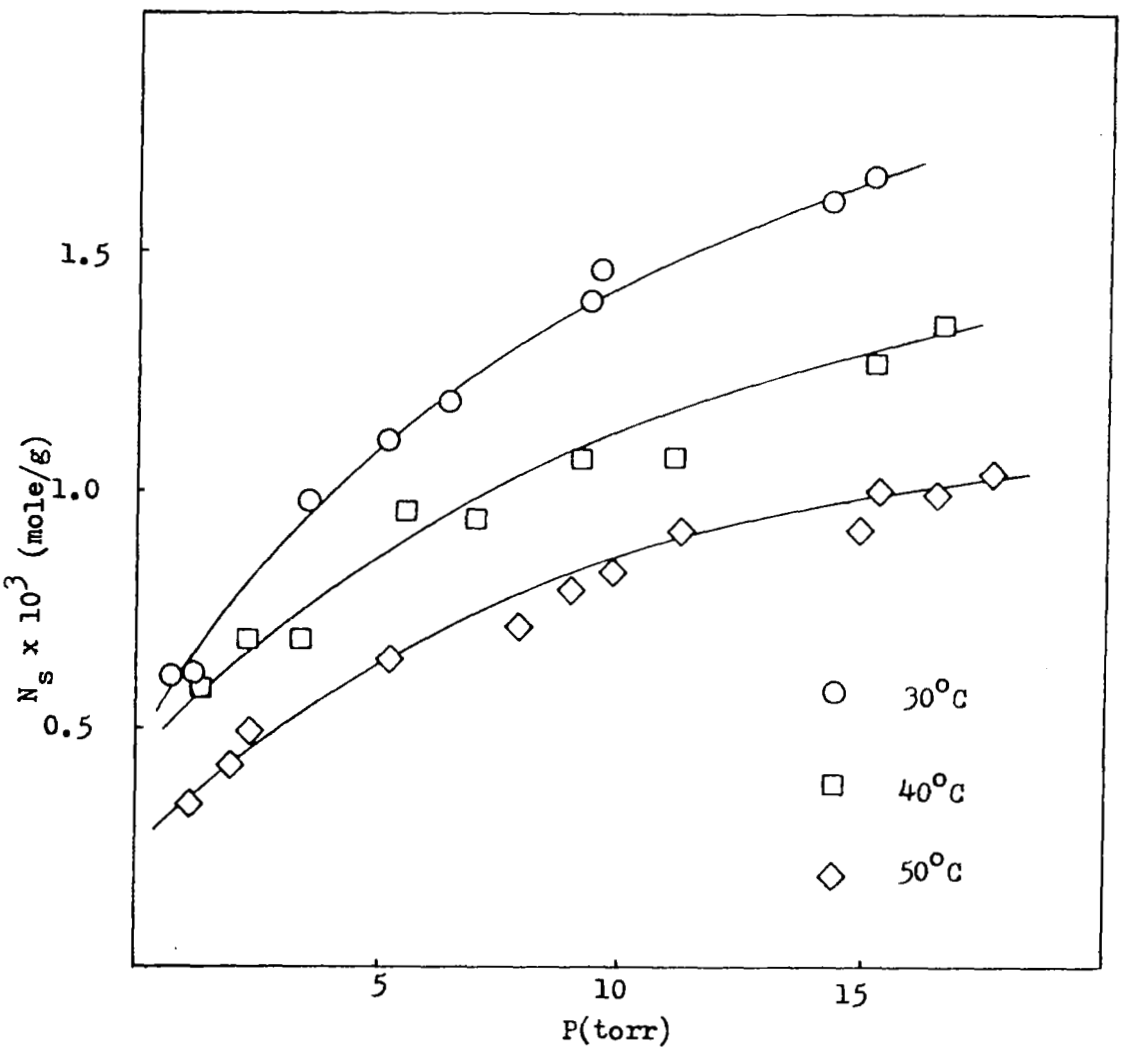

Figure 25. Temperature Dependence of Water Vapor Adsorption on Gamma Alumina Outgassed at 80°C

TABLE IV

CROSS-SECTIONAL AREAS OF WATER ADSORBED ON GAMMA ALUMINA

Outgas Temperature (°C)	Isotherm Temperature (°C)		H_2O Area ($Å^2$/molecule)
80	30		15.2
80	40		16.0
80	50		17.9
200	40		15.8
		Average	16.2 ± 1.2 (7%)
400	27		11.9
400	40		13.8
400	50		11.5
		Average	12.4 ± 1.2 (10%)

water molecule requires two oxygen ions or two surface hydroxyl groups as an adsorption site. The smaller area for water adsorbed on the 400°C outgassed gamma alumina is consistent with a phase transition occurring at 400°C as was previously postulated to explain the 10% loss in surface area. The transition from gamma alumina to higher temperature modifications results in a closer packing of oxygen ions in the alumina lattice. Figure 26 shows an ideal alpha alumina surface assuming fracture of alpha alumina to occur between alternate layers. In this surface each oxygen ion occupies an area of 6.5 Å^2. The area of an adsorbed water molecule on this surface would then be 13 Å^2.

De Boer et al.[43] found an area of 12.2 Å^2/molecule for water adsorbed on alumina pretreated at 1200°C in agreement with the model of an alpha alumina surface. The value of 12.4 A^2/molecule for gamma alumina heated at 400°C in this study is in good agreement with the value obtained by de Boer et al.[43] and that calculated for the ideal alpha alumina surface model.

The significance of the area of the adsorbed water molecule is that it supports IR evidence reported in the literature[25,37] for adsorbed states similar to those shown in Figure 3. Here an adsorbed water molecule is hydrogen bonded to either two surface hydroxyl groups or to two oxygen ions.

The result of a readsorption study of water adsorption on gamma alumina is shown in Figure 27. Between the original isotherm and the readsorption isotherms the sample was outgassed in vacuum at 10^{-5} torr for 18 hrs. The readsorption points fall on the original isotherm.

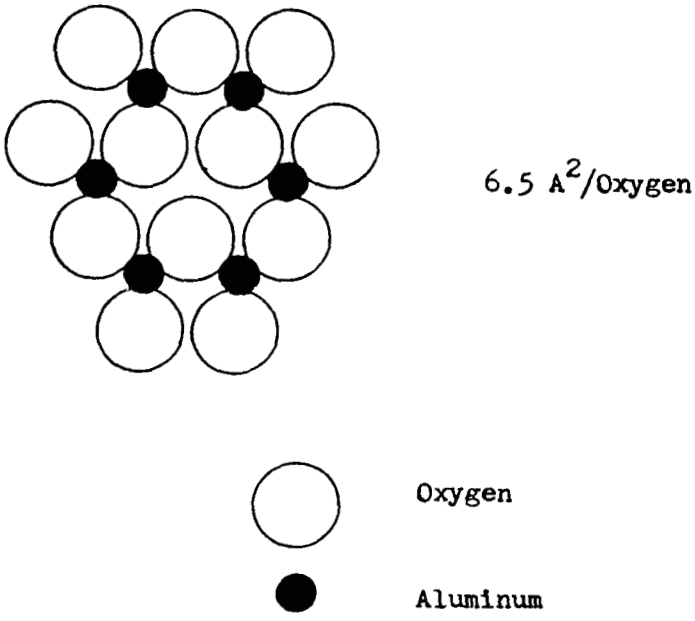

Figure 26. Ideal Alpha Alumina Surface

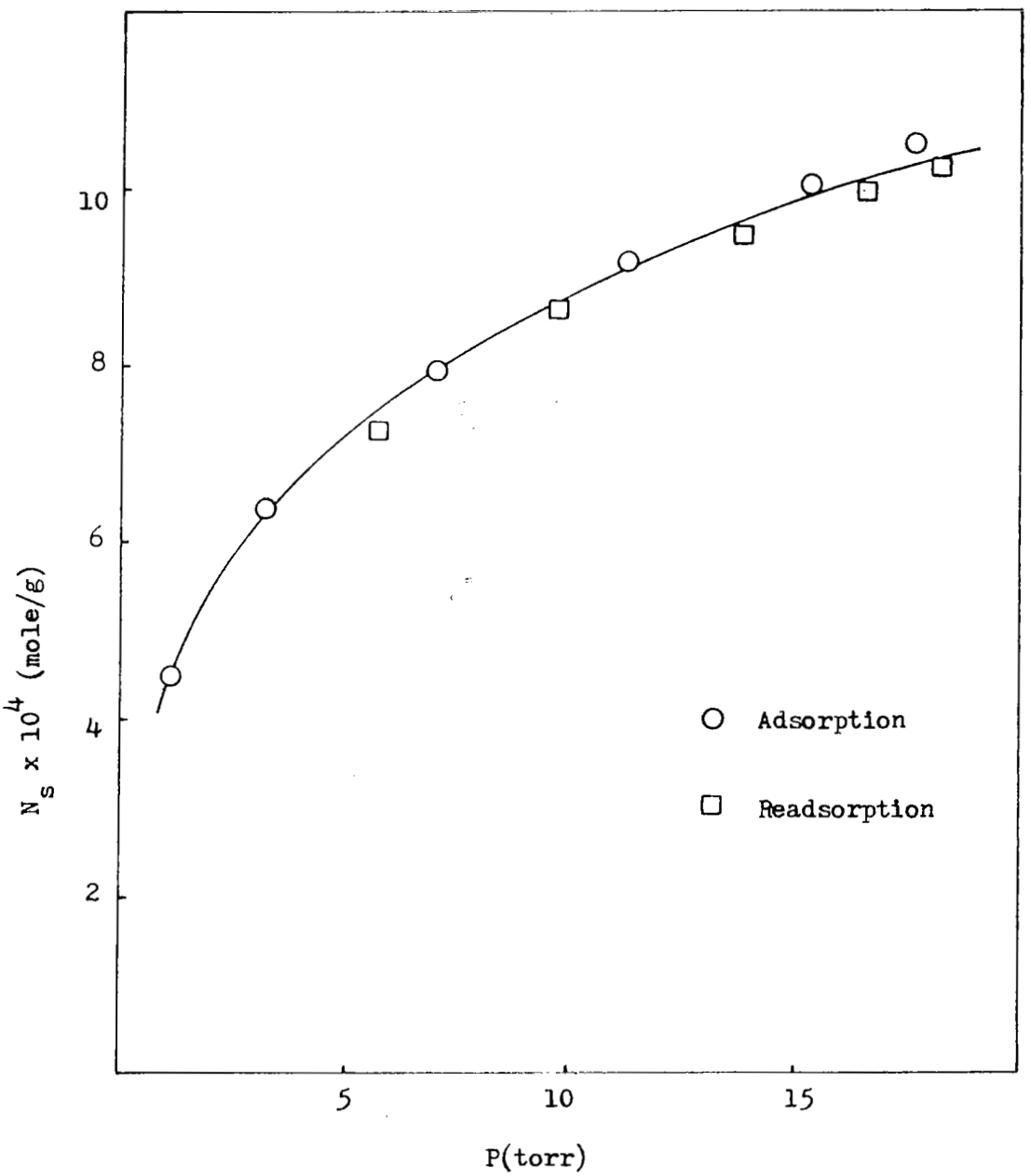

Figure 27. Readsorption of Water Vapor on Gamma Alumina at 50°C

Water adsorption on gamma alumina outgassed at 80°C is thus completely reversible. This reversibility indicates that water adsorption on alumina can be characterized as a physisorption process. Formation of hydroxyl groups by reaction with the bare oxide surface to form new hydroxyl groups is ruled out because of this reversibility.

D. Water Vapor Adsorption on Alpha Alumina

The dependence of adsorption capacity on outgas temperature for water adsorption on alpha alumina at 40°C is shown in Figure 28. Similar results were obtained at 30 and 50°C and are presented in Appendix 7. The influence of outgas temperature seems to be more uniform for the alpha alumina than for gamma alumina, possibly because of the stability of the alpha alumina in the outgas temperature range studied.

The BET equation applied to H_2O/alpha alumina isotherms again gave good linear fits. The result of the BET analysis is given in Table V for all the isotherms in the matrix. The results may indicate a dependence of the cross-sectional area on outgas temperature, but further studies are needed to establish this dependence. The average cross-section area (σ) is 12.4 A^2/molecule on alpha alumina. This area agrees with the results of de Boer et al.[43] and the model surface of alpha alumina (see Figure 26). The consequence of the differences in the adsorbed area of the water molecule can be seen in Figure 29 which shows that the amount of water adsorbed per unit area is greater for alpha alumina than for gamma alumina.

The result of the study of the temperature dependence of water adsorption on alpha alumina outgassed at 80°C is shown in Figure 30.

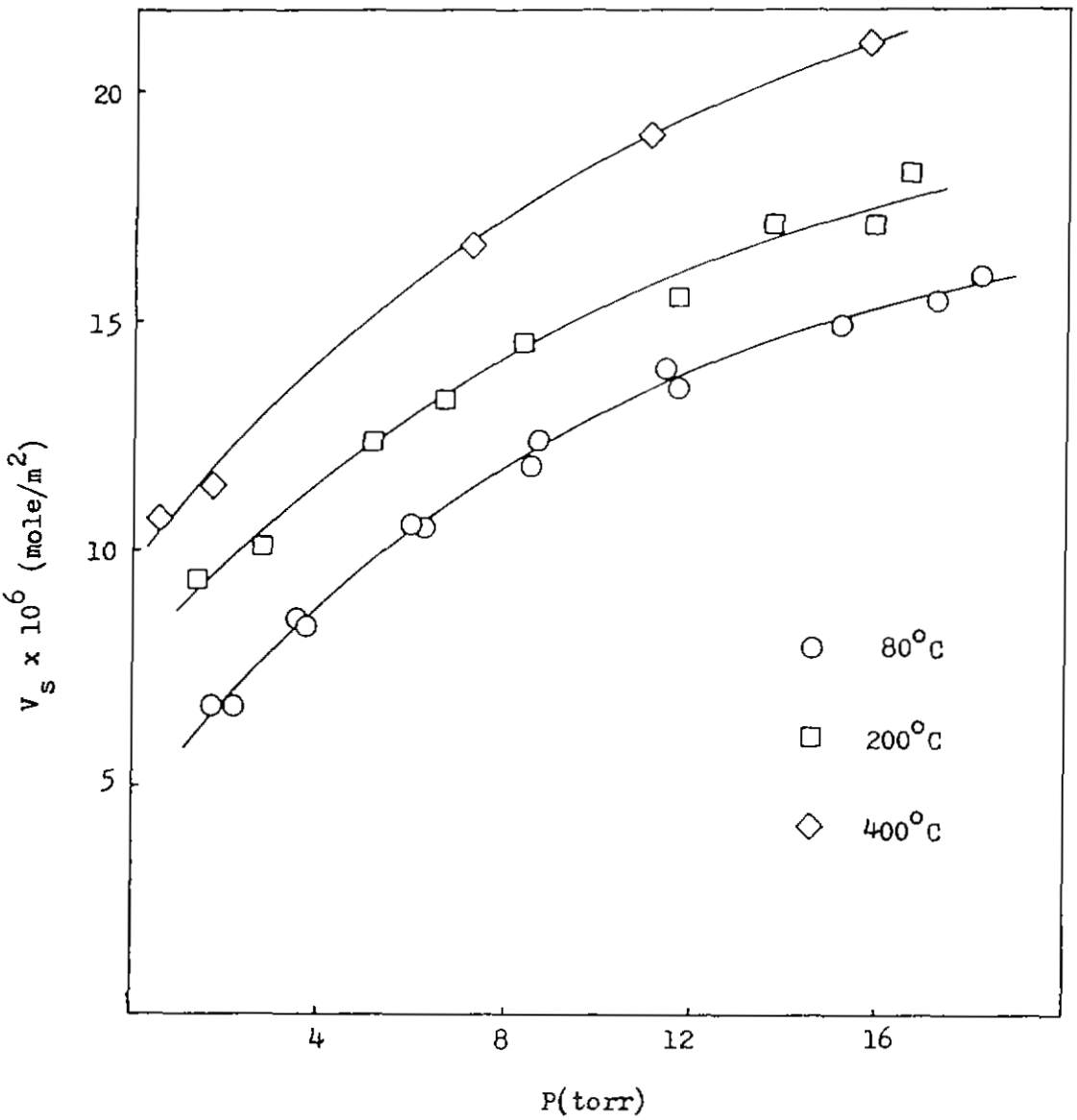

Figure 28. Influence of Outgas Temperature on Water Vapor Adsorption on Alpha Alumina at 40°C

TABLE V

CROSS-SECTIONAL AREAS OF WATER ADSORBED ON

ALPHA ALUMINA

Outgas Temperature (°C)	Isotherm Temperature (°C)	H_2O Area (A^2/molecule)
80	27	12.4
80	40	12.8
80	50	19.8
200	40	13.0
400	30	9.0
400	40	10.1
400	50	10.0
	Average	12.4 ± 3.3 (26%)

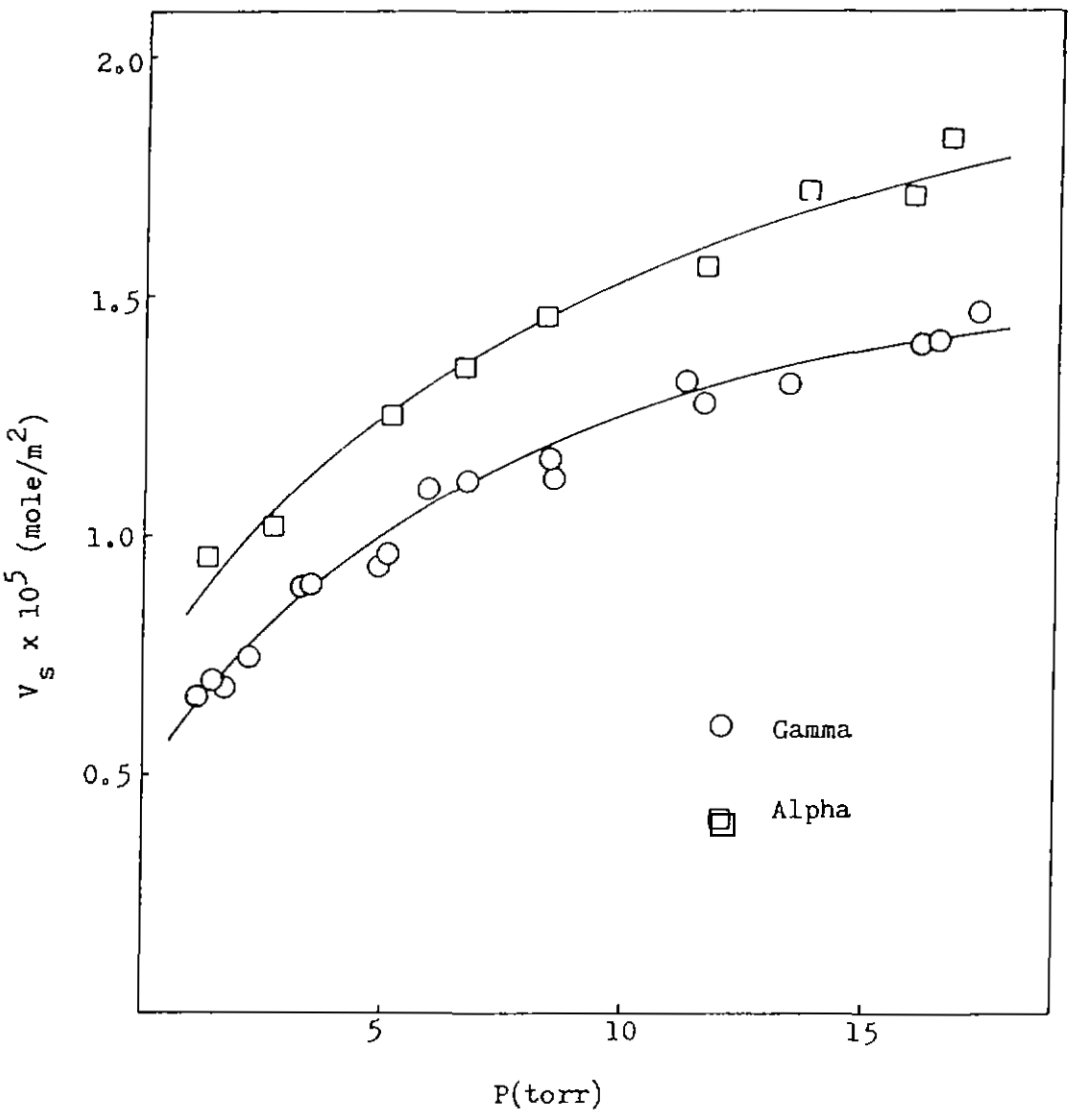

Figure 29. Comparison of Water Vapor Adsorption at 40°C on Alpha and Gamma Alumina Outgassed at 200°C

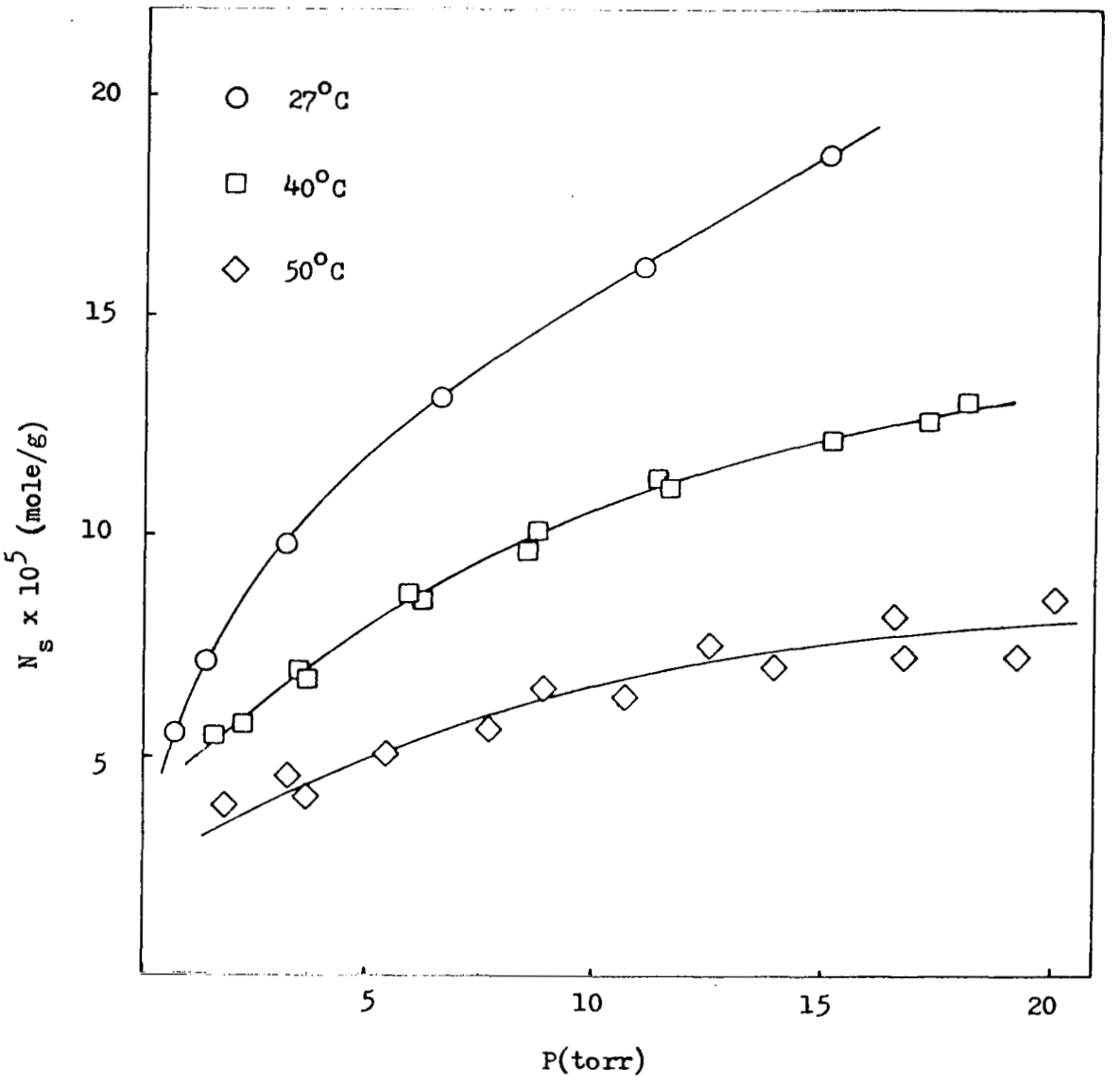

Figure 30. Temperature Dependence of Water Vapor Adsorption on Alpha Alumina Outgassed at 80°C

Results obtained after outgassing at 400°C were similar. As in the case of water adsorption on gamma alumina, an inverse relationship is seen between adsorption temperature and the amount of water adsorbed on alpha alumina. This temperature dependence was used to calculate the isosteric heat of adsorption for water vapor on both aluminas.

Water adsorption on alpha alumina, like water adsorption on gamma alumina, was completely reversible as seen by the results of the readsorption experiment on alpha alumina shown in Figure 31.

As the above results indicate, alpha and gamma alumina show similar behavior towards water vapor adsorption. The water adsorption capacity of both aluminas is increased with increasing outgas temperature. Reversibility of water vapor adsorption on both alpha and gamma is observed. The same adsorption temperature dependence is exhibited by the two aluminas. The most notable difference between the two aluminas is their adsorption capacity for water vapor. Alpha alumina adsorbs more water per unit area than gamma alumina (see Figure 29). Carruthers, Payne, Sing and Stryker[46] had found greater water adsorption on alpha alumina than on the transitional theta alumina. Differences in adsorption capacity can be explained on the basis of the packing of oxygen ions in the idealized surfaces of alpha and gamma alumina. This same packing difference and the amount of pre-adsorbed water on the two aluminas may influence the adsorption of hydrogen chloride on the two aluminas.

E. Hydrogen Chloride Adsorption on Gamma Alumina

Outgas temperature had a strong influence on water adsorption

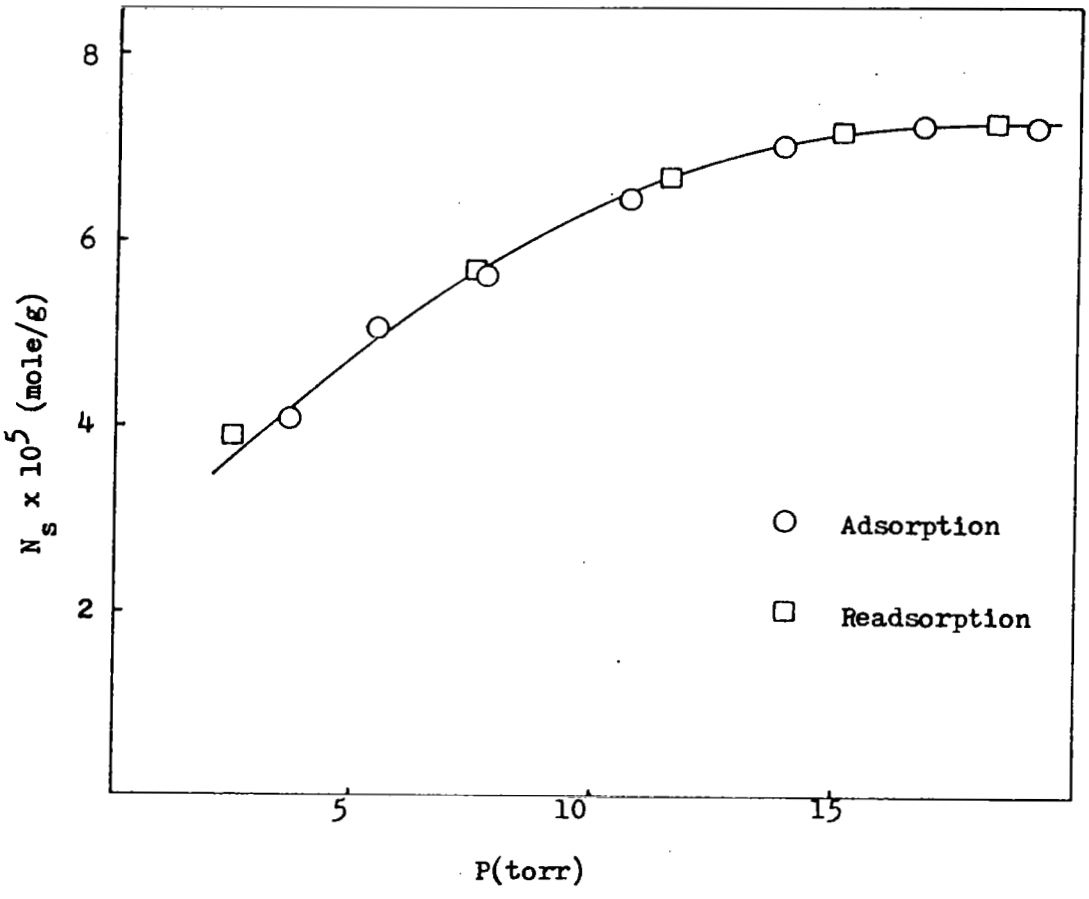

Figure 31. Readsorption of Water Vapor on Alpha Alumina at 50°C

on gamma alumina. Increasing the outgas temperature of gamma alumina also increased the amount of hydrogen chloride adsorbed on gamma alumina as shown in Figure 32. This increase is probably due to the removal of water molecules from sites needed for hydrogen chloride adsorption.

A readsorption study of the reversibility of hydrogen chloride adsorption was carried out on gamma alumina. Here the sample was evacuated at the adsorption temperature for 18 hours at 10^{-5} - 10^{-6} torr. Figure 33 shows the results of the readsorption study on gamma alumina initially outgassed at 80°C and the adsorption measured at 40°C. Hydrogen chloride adsorption is only partially reversible on gamma alumina, whereas water adsorption was completely reversible. The reversible part of the adsorption may correspond to a solution process of the hydrogen chloride in the physisorbed water on the gamma alumina. A test of this hypothesis based on a thermodynamic analysis of the adsorption is given in a later section. The irreversible part of the adsorption may be due to the formation of a bond between the hydrogen chloride and the alumina surface.

The temperature dependence of hydrogen chloride adsorption on gamma alumina outgassed at 80°C is summarized by the results presented in Figure 34. Isotherms on gamma alumina outgassed at 200 and 400°C showed similar temperature behavior as the adsorption data in Appendix 8 indicates.

Hydrogen chloride adsorption was primarily irreversible. This irreversibility indicates a chemisorption process and thus the probable formation of bonds between the hydrogen chloride and alumina surface,

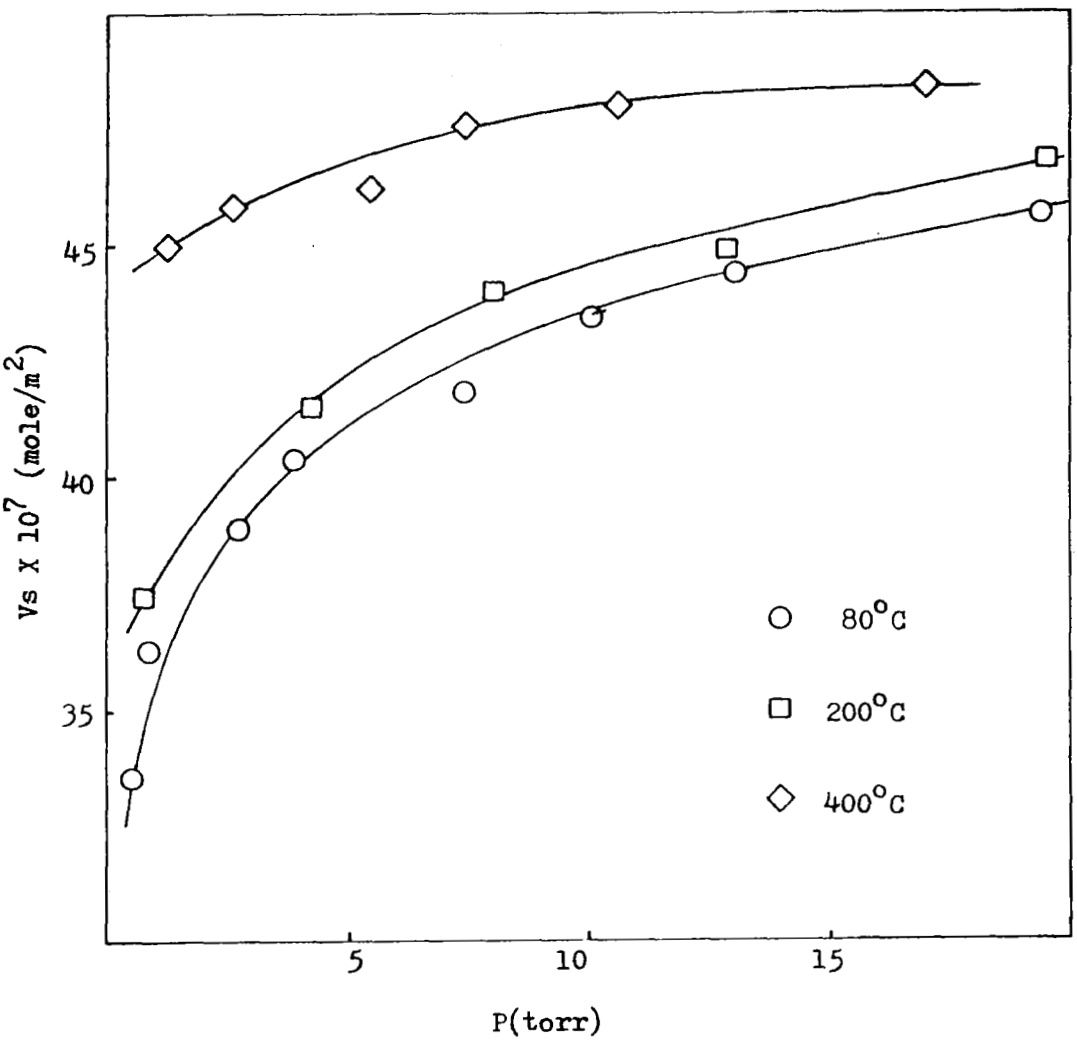

Figure 32. Influence of Outgas Temperature on Hydrogen Chloride Adsorption on Gamma Alumina at 40°C

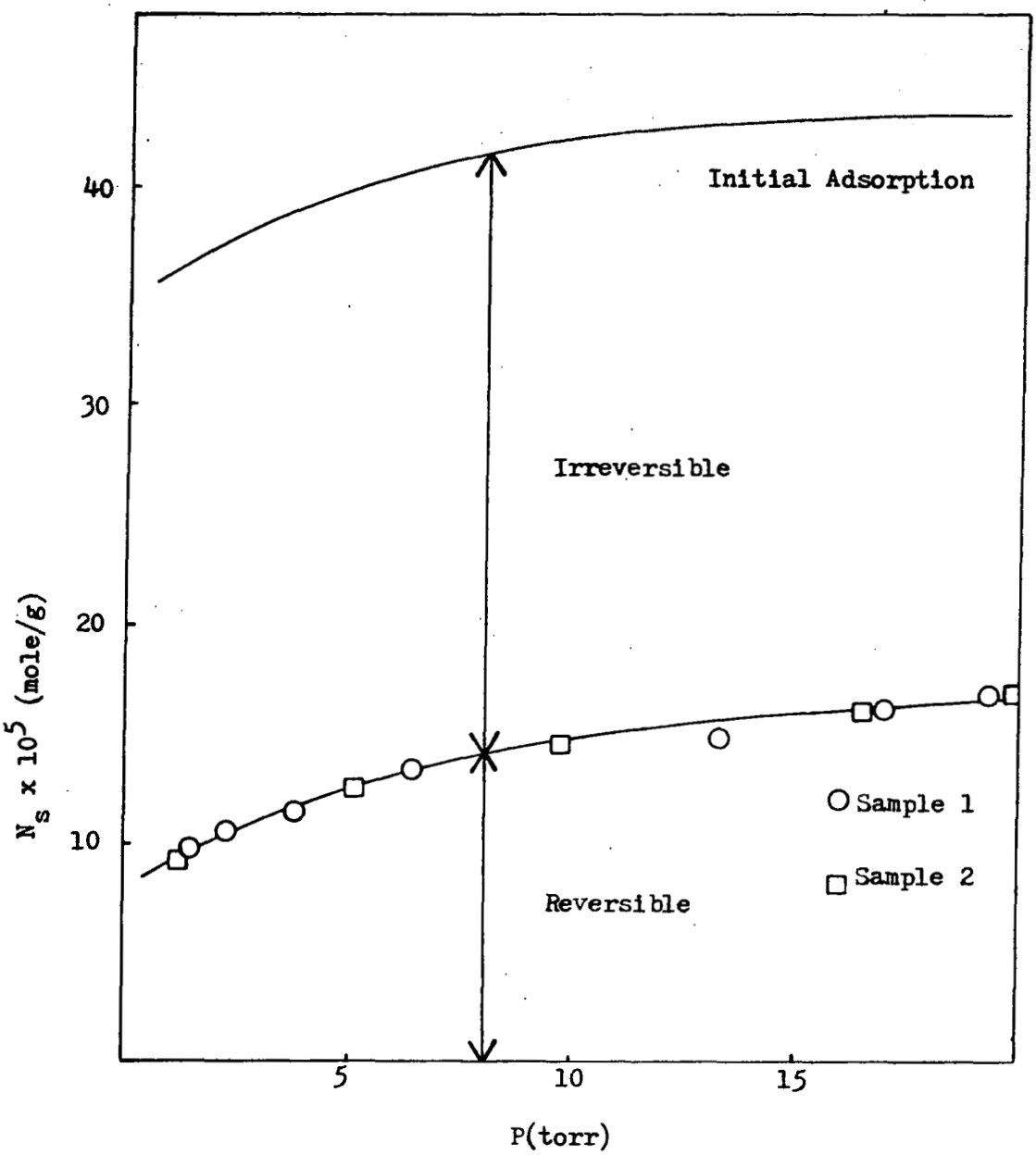

Figure 33. Readsorption of Hydrogen Chloride on Gamma Alumina at 40°C after Outgassing for 18 hours

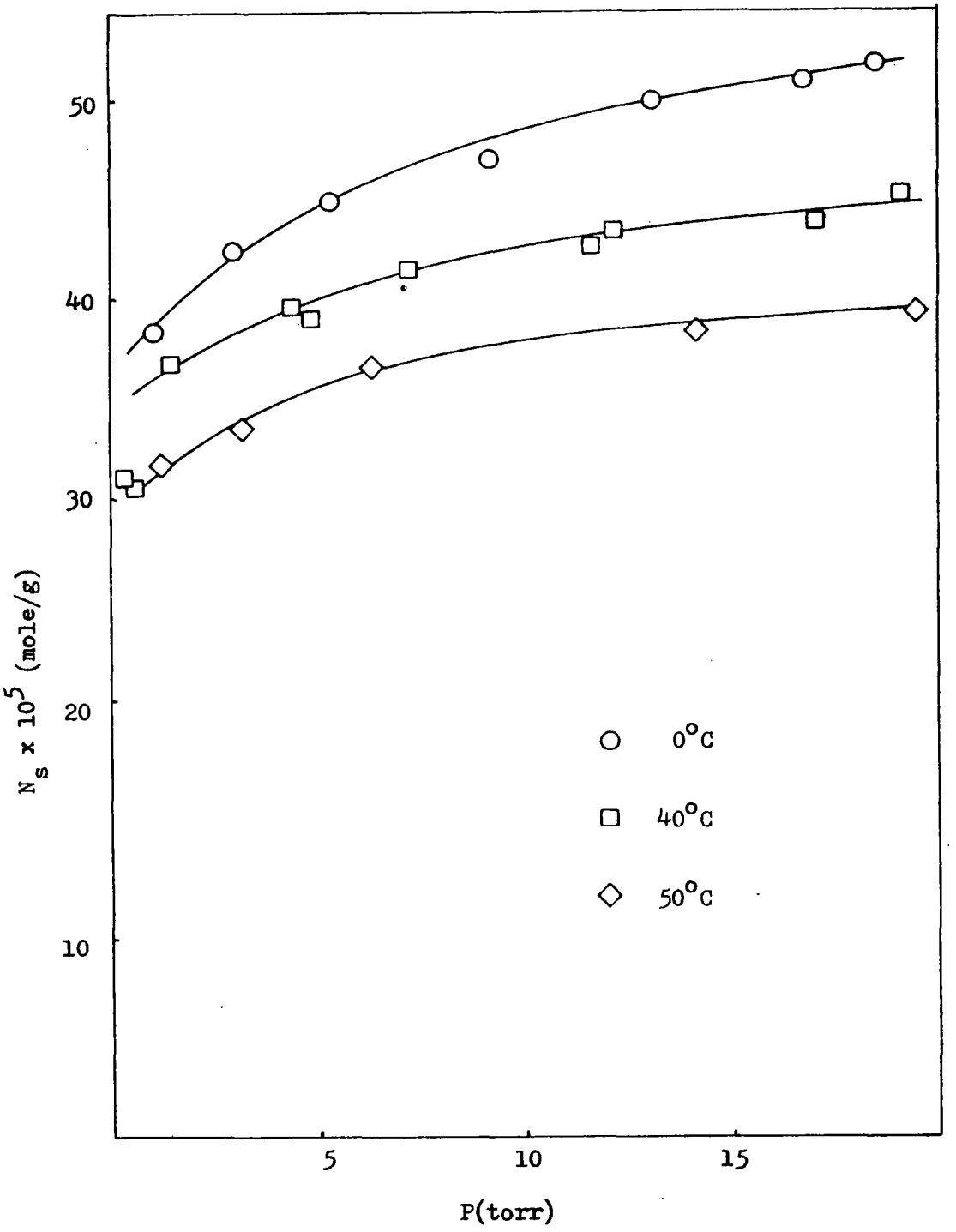

Figure 34. Temperature Dependence of Hydrogen Chloride Adsorption on Gamma Alumina Outgassed at 80°C

i.e., localized adsorption. The Langmuir equation which is based on localized adsorption was thus appropriate to linearize the adsorption data.

Table VI shows the calculated surface area of gamma alumina from the Langmuir model and the area of each adsorbed HCl molecule on the gamma alumina surface calculated from the data given in Appendix 8. Using 16.6 $\mathring{A}^2$ as the area of the hydrogen chloride molecule obtained from liquid density calculations, the surface area of gamma alumina based on HCl adsorption was 48.2 m^2/g. Comparison of this surface area with the BET nitrogen surface area of 95.4 m^2/g shows that the hydrogen chloride adsorbs on approximately half the gamma alumina surface. This gives added support to a chemisorption process occurring on distinct sites on the gamma alumina.

The nature of the hydrogen chloride adsorption site can be elucidated by considering the area occupied by the adsorbed hydrogen chloride molecule and the ideal gamma alumina surface in Figure 1. In the ideal gamma surface each aluminum ion is surrounded by four oxide ions, thus the area of this group is 32 $\mathring{A}^2$. Assuming that the adsorption site for hydrogen chloride is an aluminum ion in the surface, the area of the adsorbed HCl would be 32 $\mathring{A}^2$. Work by Parfitt[56] on HCl adsorption on TiO_2 and by Peri[37-42] on alumina showed that the metal ion was the active site in these systems. Adsorption of hydrogen chloride at every aluminum ion in the ideal surface would give an area of 16 A^2. The area of the HCl molecule is 16.6 $\mathring{A}^2$ and hence would be expected to adsorb on every other aluminun ion. The average HCl

TABLE VI

CROSS-SECTIONAL AREAS OF HYDROGEN CHLORIDE ADSORBED ON GAMMA ALUMINA

Outgas Temperature (°C)	Isotherm Temperature (°C)	HCl Surface Area (m^2/g)	HCl Area (A^2/molecule)
80	0	53.1	29.8
80	40	46.5	34.1
80	50	41.0	38.7
200	0	59.7	26.5
200	40	44.7	35.4
200	50	44.1	35.9
	Average	48.2	33.4 ± 4.5

adsorbed area is 33 $Å^2$ in Table VI in good agreement with the description that alternating aluminum ions are the adsorption sites for HCl adsorption on gamma alumina. Figure 35 is a representation of the gamma alumina surface after exposure to hydrogen chloride.

F. Hydrogen Chloride Adsorption on Alpha Alumina

The effect of outgas temperature on hydrogen chloride adsorption on alpha alumina is shown in Figure 36. The points on the 80°C isotherm are from two different samples, the lower points may be due to non equilibration of the system before the measurement was taken. The amount of hydrogen chloride adsorption on alpha alumina increases significantly between 80 and 200°C outgas. The difference between 200 and 400°C does not appear to be significant.

Typical results for the temperature dependence of HCl adsorption on alpha alumina are shown in Figure 37. As the results demonstrate, increasing adsorption temperature decreased the amount of hydrogen chloride adsorbed on alpha alumina. This is similar to the behavior noted for HCl adsorption on gamma alumina.

Hydrogen chloride adsorption on alpha alumina was only partially reversible as the results of the readsorption experiment shown in Figure 38. A study of the temperature dependence of this reversibility was performed by heating the sample during the outgassing step in the readsorption experiment after the initial adsorption. As Figure 39 indicates more of the adsorbed hydrogen chloride is removed at elevated temperature. Even at the highest temperature (341°C), some of the hydrogen chloride remains on the alpha alumina originally outgassed at 80°C.

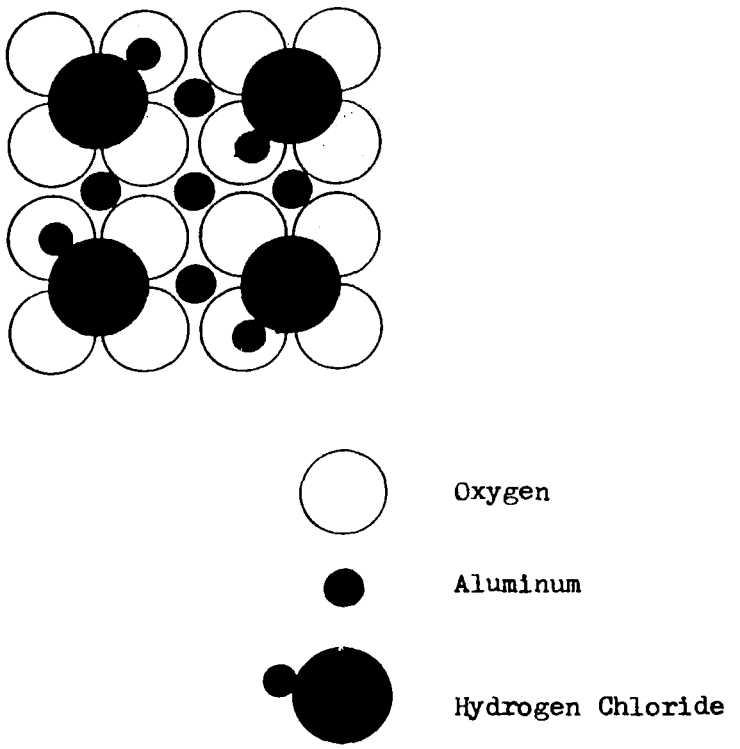

Figure 35. Ideal Gamma Alumina Surface After Hydrogen Chloride Adsorption

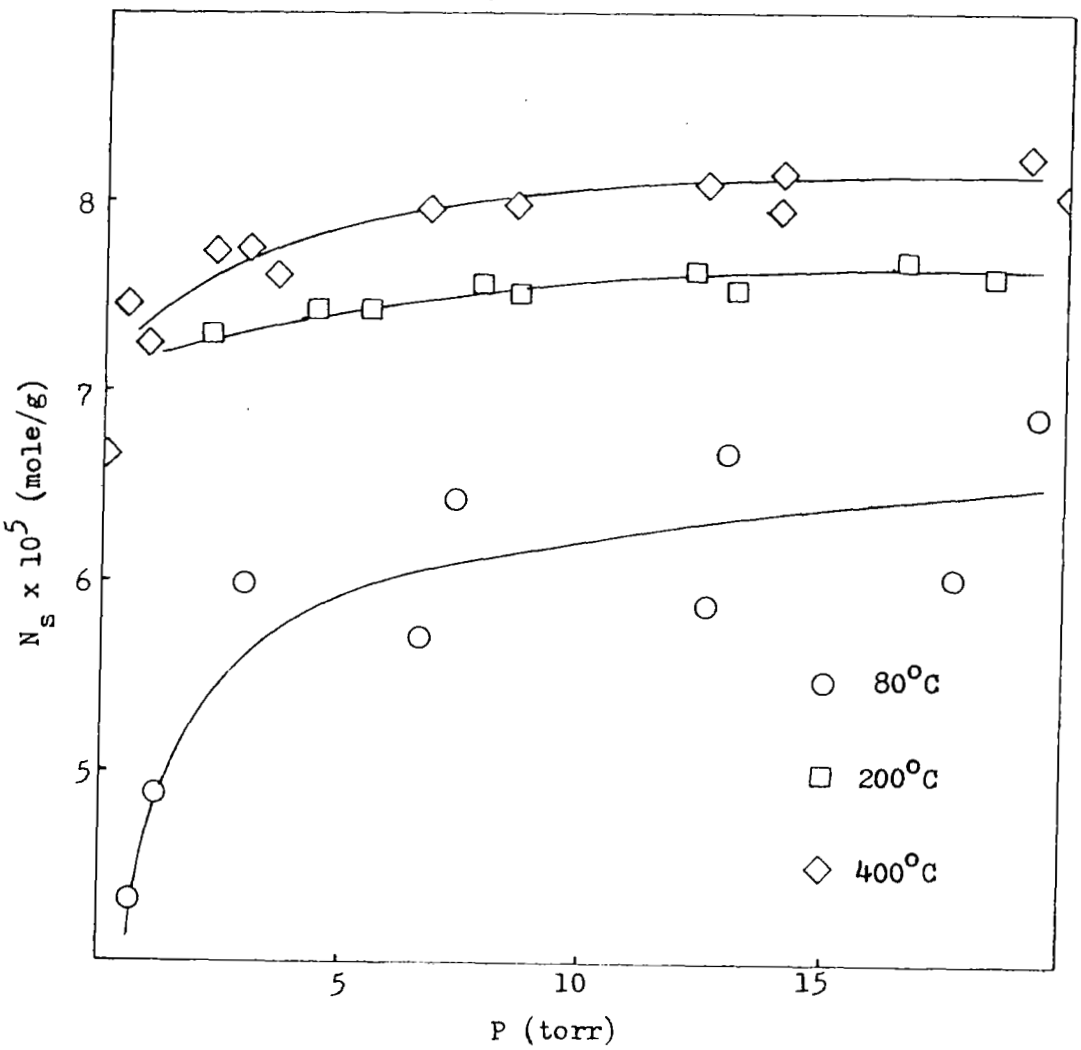

Figure 36. Influence of Outgas Temperature on Hydrogen Chloride Adsorption on Alpha Alumina at 40°C

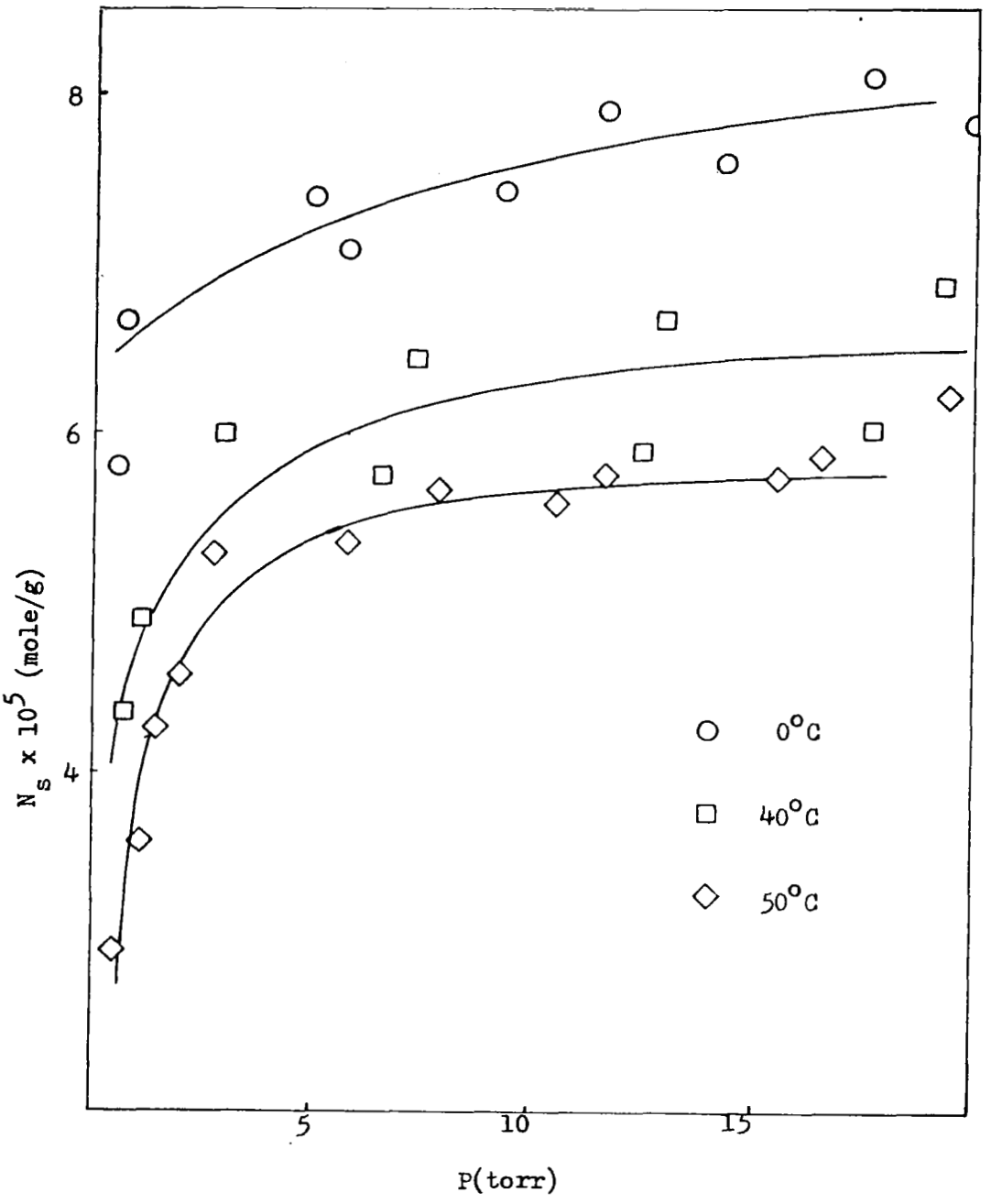

Figure 37. Temperature Dependence of Hydrogen Chloride Adsorption on Alpha Alumina Outgassed at 80°C

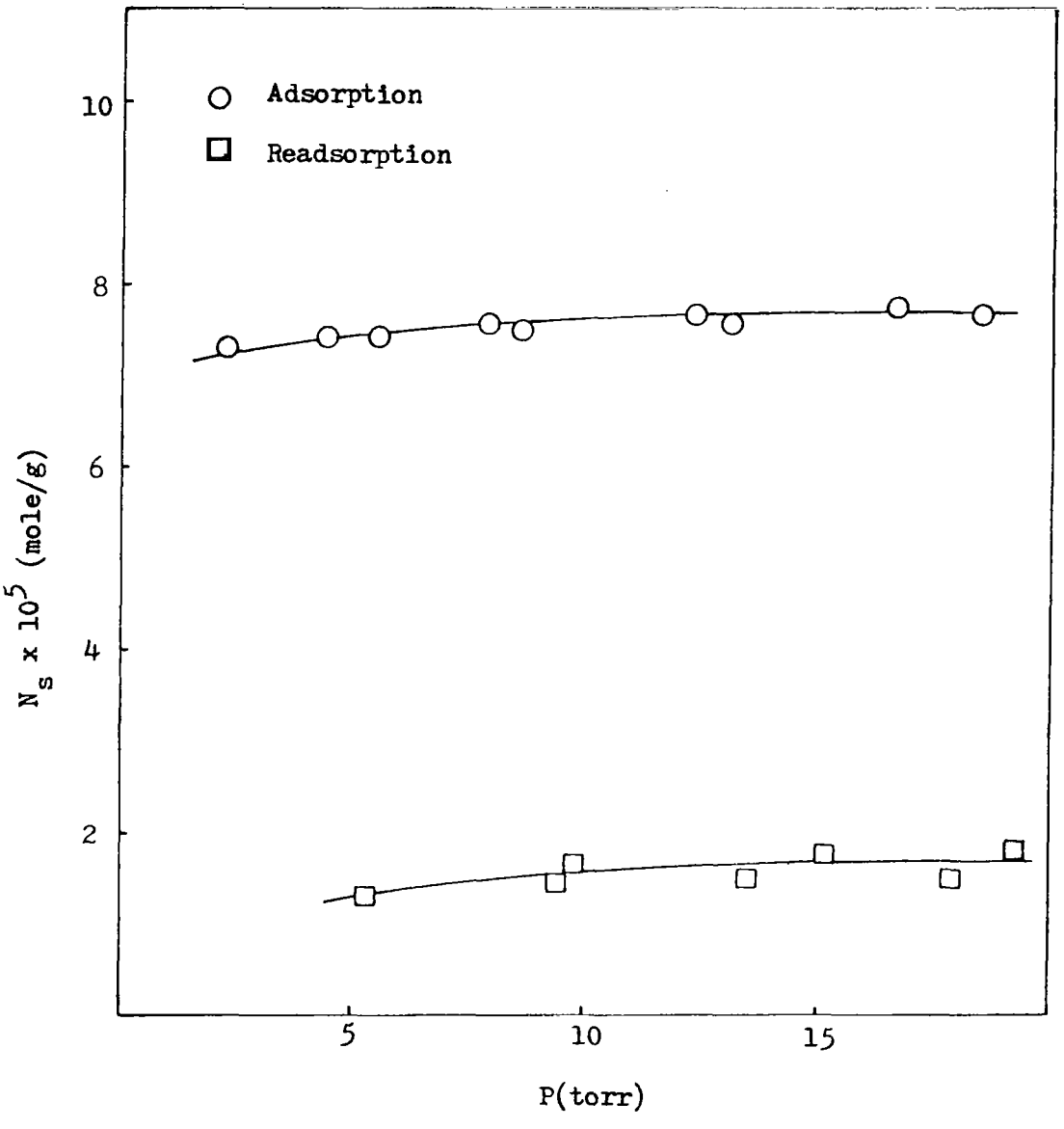

Figure 38. Readsorption of Hydrogen Chloride at 40°C on Alpha Alumina Outgassed at 200°C

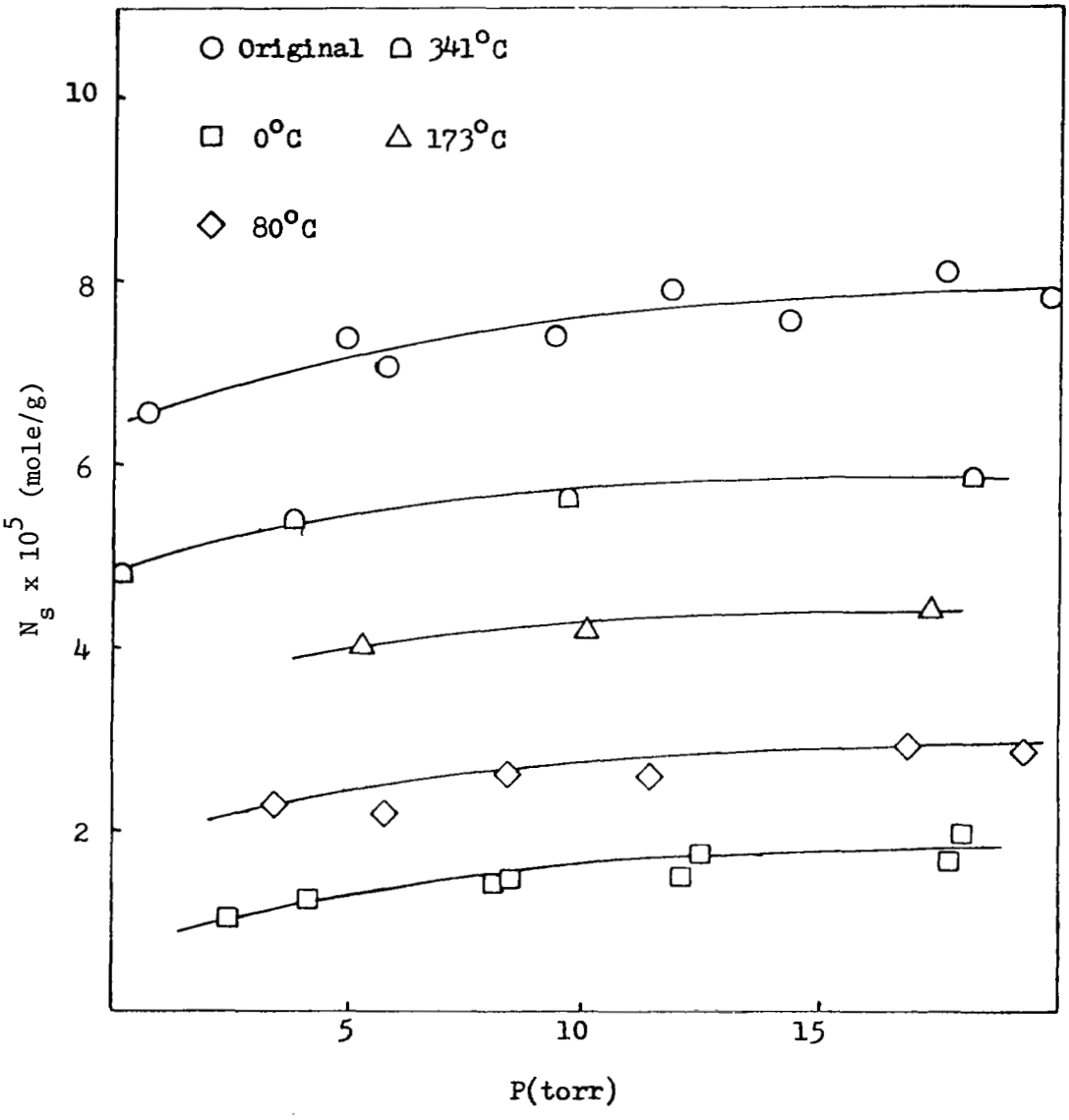

Figure 39. Temperature Dependence of Hydrogen Chloride Readsorption at 0°C on Alpha Alumina Initially Outgassed at 80°C

The irreversibility of hydrogen chloride adsorption on alpha alumina indicates that alpha alumina could act as an effective sink for hydrogen chloride since it has the ability to adsorb HCl and not release it. This irreversibility, as in the adsorption of HCl on gamma alumina, indicates that chemisorption of hydrogen chloride on alpha alumina is occurring.

Analysis of the HCl adsorption isotherms on alpha alumina using the Langmuir equation gave the results shown in Table VII. The HCl surface area of 7.9 m^2/g was approximately the same as the BET nitrogen surface area (8.1 m^2/g) on alpha alumina. This agreement of the hydrogen chloride surface area and the BET nitrogen surface area showed that most of the alpha alumina surface is accessible for adsorption of the hydrogen chloride. The cross-sectional areas of hydrogen chloride adsorbed on alpha alumina, which are shown in Table VII, may indicate a dependence on outgas temperature and adsorption temperature. The areas increase with increased adsorption temperature and decrease with increased outgas temperature. Further studies using a wider range of temperatures are needed to establish if this dependence actually exists. The average area of an adsorbed hydrogen chloride molecule was 17.5 $Å^2$. The significance of this area is seen on referring to the ideal alpha alumina surface in Figure 26. If, again, surface aluminum ions are the adsorption site, then the ideal HCl adsorbed area would be 19.5 $Å^2$ in agreement with the area obtained from the hydrogen chloride adsorption data on alpha alumina.

Hydrogen chloride adsorption on alpha alumina is influenced by outgas temperature and adsorption temperature in similar ways to that

TABLE VII

CROSS-SECTIONAL AREAS OF HYDROGEN CHLORIDE ADSORBED ON ALPHA ALUMINA

Outgas Temperature (°C)	Isotherm Temperature (°C)	HCl Surface Area (m^2/g)	HCl Area ($Å^2$/molecule)
80	0	8.0	16.9
80	40	6.4	21.1
80	50	6.1	22.3
200	0	9.1	14.7
200	40	7.6	17.5
200	50	7.6	17.7
400	0	9.9	13.6
400	40	8.1	16.6
400	50	8.0	16.8
		Average 7.9	Average 17.5 ± 2.8

of hydrogen chloride adsorption on gamma alumina. Increased outgas temperature and thus decreased amounts of pre-adsorbed water increased hydrogen chloride adsorption. This trend seems to indicate that water vapor and hydrogen chloride compete for similar adsorption sites on the two aluminas.

The most significant difference in the adsorption of hydrogen chloride on alpha and gamma alumina is the amount adsorbed per unit area. Alpha alumina adsorbs more hydrogen chloride per unit area than gamma alumina as shown in Figure 40. The difference in adsorption capacity can again be explained on the basis of the packing of aluminum and oxide ions in the ideal surfaces of alpha and gamma alumina. On a mass basis, however, gamma alumina has a greater adsorption capacity than alpha alumina for hydrogen chloride because of its greater surface area.

G. Isosteric Heat of Adsorption for Water Vapor on Alumina

Water vapor adsorption on alpha and gamma alumina was temperature dependent as shown in Figure 25 and Figure 30. This temperature dependence was used to calculate the isosteric heat of adsorption for water vapor on both aluminas.

Although the BET equation was previously used to linearize the experimental data to obtain surface areas, it did not adequately fit the experimental data at low surface coverage as seen in Figure 41 where use of a Freundlich plot (ln N vs ln P) gave a better fit of the experimental data. Table VIII shows the errors produced in fitting the H_2O adsorption data on gamma alumina outgassed at $80^{o}C$ by use of the BET and the Freundlich equations.

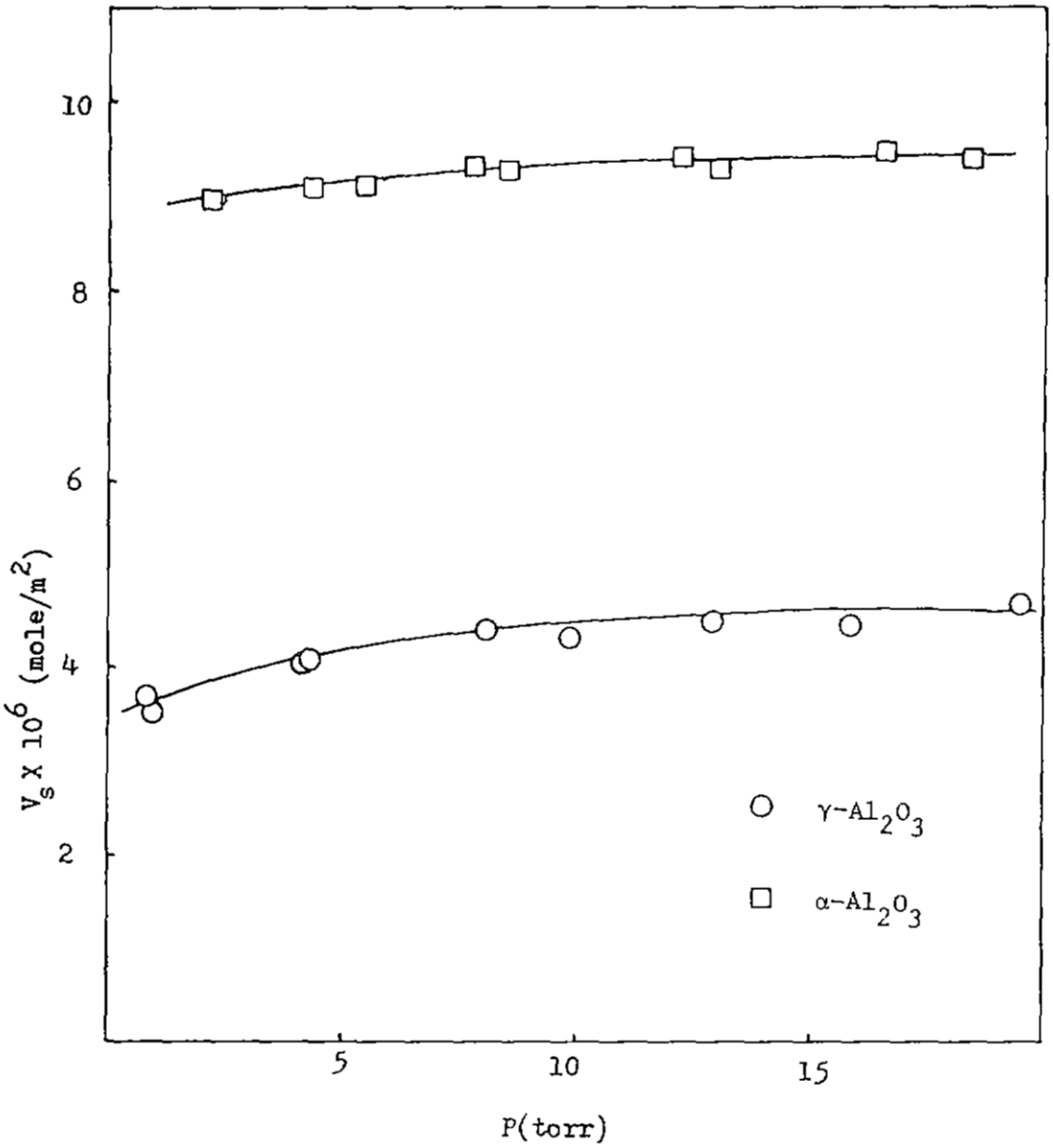

Figure 40. Comparison of Hydrogen Chloride Adsorption at 40°C on Alpha and Gamma Alumina Outgassed at 200°C

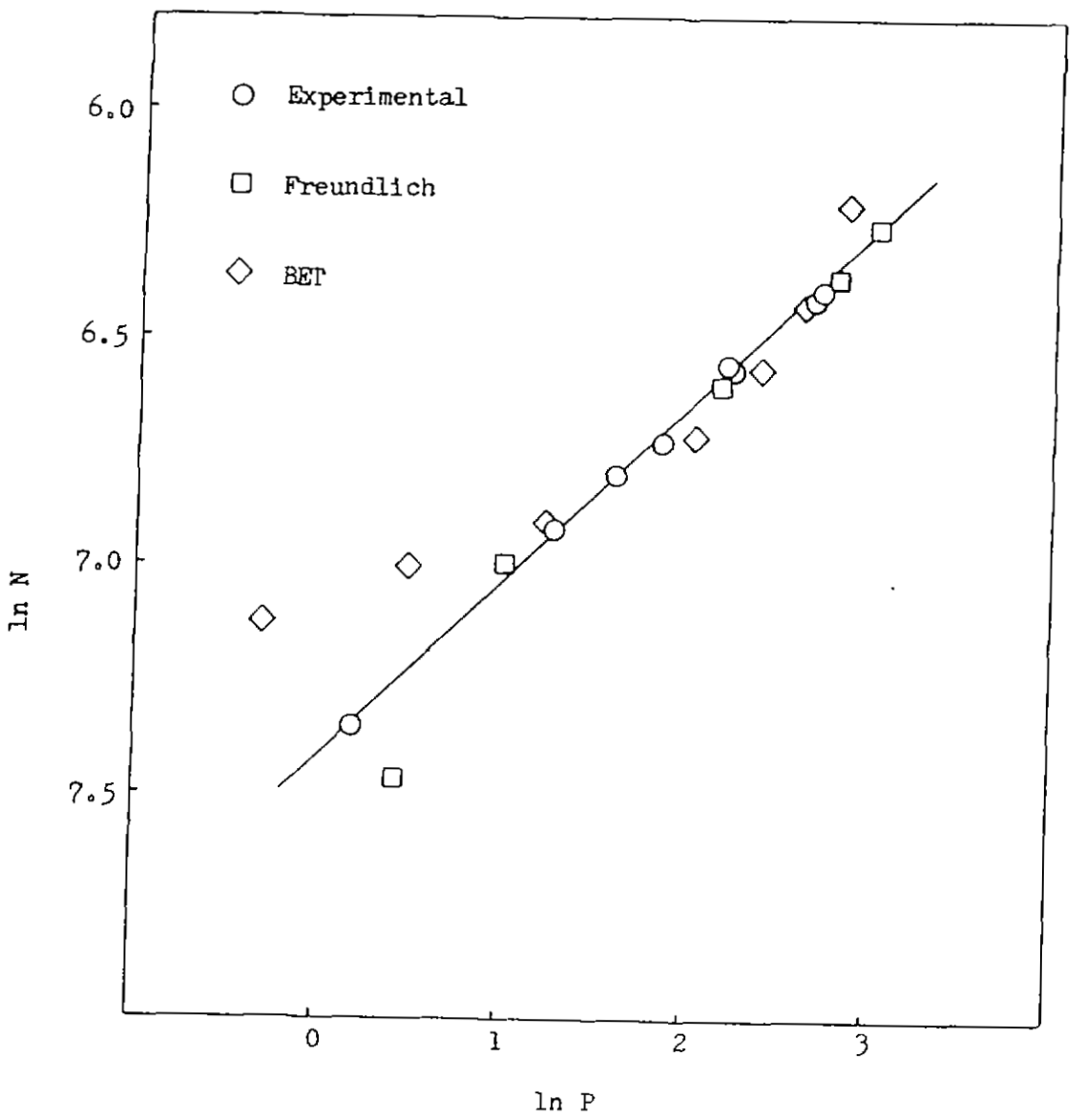

Figure 41. Comparison of BET and Freundlich Equations for Fitting Experimental Data of HCl Adsorption on Gamma Alumina

TABLE VIII

ERROR FOR FIT OF H_2O ADSORPTION ISOTHERM ON GAMMA ALUMINA USING THE BET AND FREUNDLICH EQUATIONS

	Slope (%)	Y-Intercept (%)
BET	3.7	242
Freundlich	0.9	0.06

The results of the analysis of the temperature dependence data is shown in Table IX. As the isosteric heats indicate, water adsorption on alumina is an exothermic process. Alpha alumina had a higher isosteric heat of adsorption than gamma alumina. In support of this conclusion, Wightman[60] found higher heats of immersion in water for alpha alumina than for gamma alumina. Every, Wade and Hackerman[50] also reported higher heats of immersion for alpha alumina than for gamma alumina. The larger heat of immersion for alpha alumina results from the larger number of H_2O molecules adsorbed per unit area on alpha alumina than on gamma alumina.

H. Thermodynamic Model of Hydrogen Chloride Adsorption on Alumina

In order to correlate the experimental data for the adsorption of water vapor and hydrogen chloride on alumina, a water layer model was tested using Wightman's calorimetric data.[60] The model consists of describing the adsorbent as an alumina particle surrounded by several layers of pre-adsorbed water as shown in Figure 42. This description is consistent with Peri's infrared results[37-42] which showed molecular water to be present on the surface of alumina up to 400°C. Since water vapor adsorption increased with increasing outgas temperature as shown in Figures 24 and 28, successive water layers are postulated to be removed from the alumina particle as the outgas temperature is raised. An untreated alumina particle contains a water layer of the thickness represented by the distance N - T_3 in Figure 42. Outgassing the alumina at a temperature T_1 removes part of the water layer represented by the distance N - T_1 in Figure 42. The temperature T_3 at which no water

TABLE IX

ISOSTERIC HEAT OF ADSORPTION FOR WATER VAPOR ON ALUMINAS

Adsorbent	Outgas Temperature (°C)	θ	Isosteric Heat (kcal/mole)
Gamma	80	0.58	13.9 ± 2.8
Gamma	80	0.98	14.5 ± 1.2
Gamma	400	1.03	11.0 ± 4.8
Alpha	80	0.52	16.7 ± 2.3
Alpha	80	0.86	19.6 ± 2.4
Alpha	400	0.81	17.2 ± 7.4
Alpha	400	1.04	19.2 ± 5.6

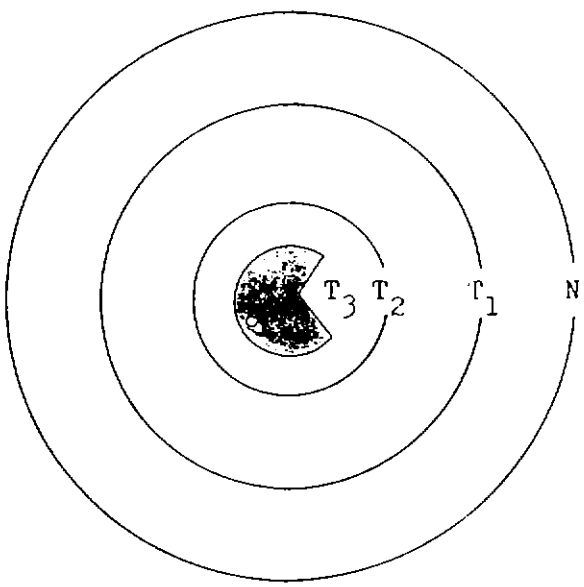

$$N_{T_1} = N - T_1$$

$$N_{T_2} = N - T_2$$

$$N_{T_3} = N - T_3$$

Figure 42. Alumina Particle with Surrounding Layers of Water

surrounds the alumina particle was taken as 400°C since Peri's infrared work[37-42] indicated the absence of molecular water on gamma alumina at 400°C. The amount of water present on alpha and gamma alumina after a given outgas temperature was taken as the difference in the amount of water adsorbed on alumina outgassed at 400°C and that adsorbed on alumina outgassed at any lower temperature.

The adsorption of hydrogen chloride on alumina can be described as a two step process as shown in Figure 43. The initial step in the adsorption process (Reaction 1) is the solution of the hydrogen chloride gas in the layer of water surrounding the alumina particle. The second step (Reaction 2) is the adsorption of the dissolved hydrogen chloride on the alumina particle.

The energetics of the two step process are represented by the following equation:

$$\Delta\bar{H}_{ADS} = \int Q_{st}\,d\theta = \Delta\bar{H}_{sol} + \Delta\bar{H}_{HCl/Al_2O_3} \qquad (I)$$

where: $\Delta\bar{H}_{ADS}$ = the integral heat of adsorption for HCl(g) on Al_2O_3

Q_{st} = the isosteric heat of adsorption

$d\theta$ = the incremental change in surface coverage

$\Delta\bar{H}_{sol}$ = the integral heat of solution for HCl in water

$\Delta\bar{H}_{HCl/Al_2O_3}$ = the integral heat of interaction between HCl and alumina

A test of the water layer model is a comparison of the integral isosteric heat of adsorption $\int Q_{st}d\theta$ determined by gas phase measurements and the heat of immersion of alumina in hydrochloric acid. The two values differ only by the integral heat of solution, $\Delta\bar{H}_{sol}$. Each

1. $HCl(g) + H_2O\ (l) \longrightarrow HCl$ in X moles H_2O

2. $HCl(aq) + Al_2O_3\ (s) \longrightarrow HCl \text{ --- } Al_2O_3$

Figure 43. Possible Mechanism for Hydrogen Chloride Adsorption on Alumina

of the parameters in equation (I) was determined experimentally as described below.

The heats of immersion of alpha and gamma alumina in 0.1 N HCl has been measured by Wightman[60] and the results are shown in Table X. A study of the change in pH of hydrochloric acid solutions of varying concentration upon addition of alumina was used to establish if Wightman's results were determined at monolayer coverage of hydrogen chloride. Table XI and Table XII show the change in pH of hydrochloric acid solutions upon addition of alpha and gamma alumina, respectively. pH_o is the pH before addition of the aluminum and pH_{10}, pH_{60} and pH_{180} is the pH of the solution after 10, 60 and 180 minutes, respectively. No significant pH change is observed after addition of alumina to 0.1 N HCl solutions. This absence of change in pH is a good indication that a 0.1 N HCl solution has a sufficient concentration of HCl for saturation of the alumina surface.

The integral heat of solution of HCl in water was determined by linear extrapolation of the data in Table XIII. The number of moles of adsorbed water was determined as described above.

The isosteric heat of adsorption (Q_{st}) was determined from the temperature dependence of the hydrogen chloride adsorption shown in Figure 34 and Figure 37. The experimental results were linearized on a ln N vs ln P plot. Figure 44 shows a comparison of the experimental data with results calculated using the Langmuir and the Freundlich equations to fit the data. After fitting and extrapolating the data the isosteric heat was calculated using hydrogen chloride isotherms

TABLE X

HEATS OF IMMERSION OF ALPHA AND GAMMA ALUMINA IN 0.1N HCl AT 30°C

	Outgas Temperature (°C)	$-\Delta_w H$ (mJ/m^2)	$-\Delta_w H$ (J/g)
Alpha	80	888	7.23
	100	949	7.73
	200	1351 ± 17(1.2%)	11.0 ± 0.1
	300	1732 ± 38(2.2%)	14.1 ± 0.3
	400	1829 ± 60(3.3%)	14.9 ± 0.5
Gamma	100	727 ± 40(5.5%)	69.3 ± 3.8
	400	1728	148

TABLE XI

pH OF SLURRIES OF ALPHA ALUMINA AND HYDROCHLORIC ACID

Outgas (°C)	C_{HCl} (mole-l^{-1})	pH_0	pH_{10}	pH_{60}	pH_{180}
100	0.1	1.43	1.49		1.47
200	0.001	3.37	10.03	9.76	9.39
200	0.01	2.30	5.17	5.76	6.03
200	0.016	2.09	3.95		4.14
200	0.032	1.74	2.11	2.33	2.62
200	0.1	1.25	1.33	1.36	1.32

TABLE XII

pH OF SLURRIES OF GAMMA ALUMINA AND HYDROCHLORIC ACID

Outgas (°C)	C_{HCl} (mole-l^{-1})	pH_0	pH_{10}	pH_{60}	pH_{180}
100	0.1	1.42	1.42	1.41	1.36
200	0.001	3.16	4.51	4.65	4.69
200	0.01	2.14	3.38	3.93	4.00
200	0.016	2.01	2.38	3.54	3.93
200	0,032	1.68	1.82	1.95	2.10
200	0.1	1.26	1.27	1.29	1.29

TABLE XIII

INTEGRAL HEATS OF SOLUTION FOR HCl IN WATER AT 25°C

Moles of H_2O per mole HCl	Integral Heat (kcal/mole)
	-18.003
20,000	-17.978
5,000	-17.952
3,000	-17.940
1,000	-17.893
400	-17.839
200	-17.778
100	-17.693
50	-17.557
25	-17.315
15	-17.01
10	-16.651
8	-16.35
6	-15.79
4	-14.67
3	-13.63
2	-11.71
1	- 6.31

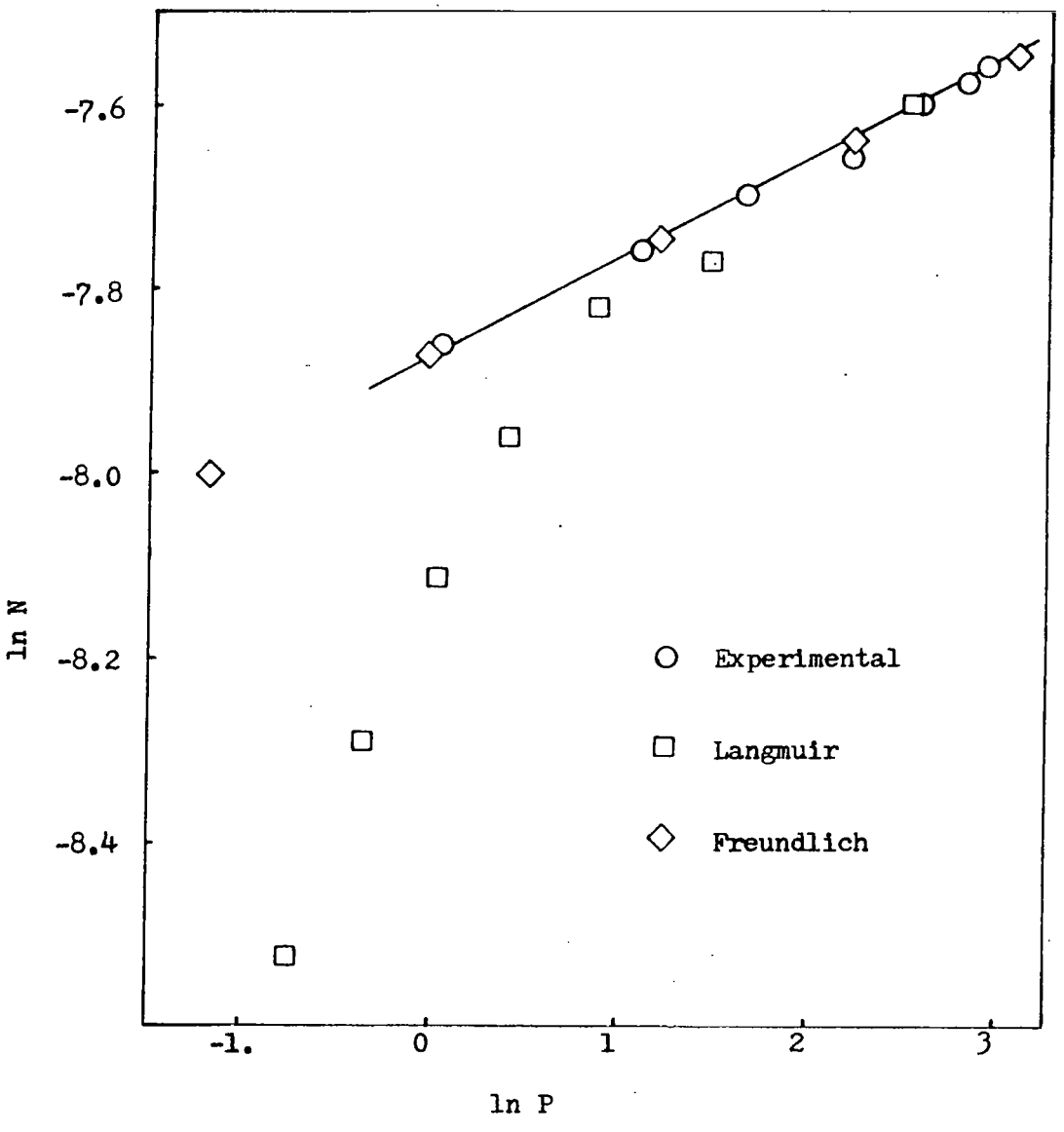

Figure 44. Comparison of Experimental Data with Results Calculated Using the Langmuir and Freundlich Equations for HCl Adsorption at 0°C on Gamma Alumina Outgassed at 80°C

determined at 0, 40 and 50°C and Equation 11. Figures 45 and 46 show the isosteric heat curves as a function of surface coverage for HCl adsorption on gamma alumina and alpha alumina, respectively. Evaluation of the integral isosteric heat of adsorption ($\int Q_{st} d\theta$) was facilitated by obtaining a quadratic equation describing the heat curve using a non-linear least square fit of the Q_{st} vs θ data as described in Appendix 10. Integration of the equation between $\theta = 0$ and $\theta = 1$ then gave the integral isosteric heat of adsorption.

The results of the water layer model analysis for hydrogen chloride adsorption are shown in Table XIV. The agreement between the heat of adsorption determined calorimetrically, ΔH_L, and the heat of adsorption determined from the gas phase adsorption, ΔH_G, is reasonably good for alpha alumina outgassed at 80 and 200°C. The difference in ΔH_L and ΔH_G on alpha alumina outgassed at 400°C may be an indication that not all the pre-adsorbed water was removed at 400°C.

The poor agreement for the heats of adsorption on gamma alumina may be attributed to the presence of water on gamma alumina at 400°C. Further there is considerable uncertainty in the extrapolation of the integral heat of solution curve to very low concentrations where the heat of solution is not reported.

A comparison of the calorimetric heat and integral isosteric heat of adsorption for hydrogen chloride adsorption on alpha alumina suggests that hydrogen chloride adsorption may involve a two step process with initial solution in pre-adsorbed water layers surrounding the alumina particle. However, further work is needed to establish the thermodynamic validity of this model.

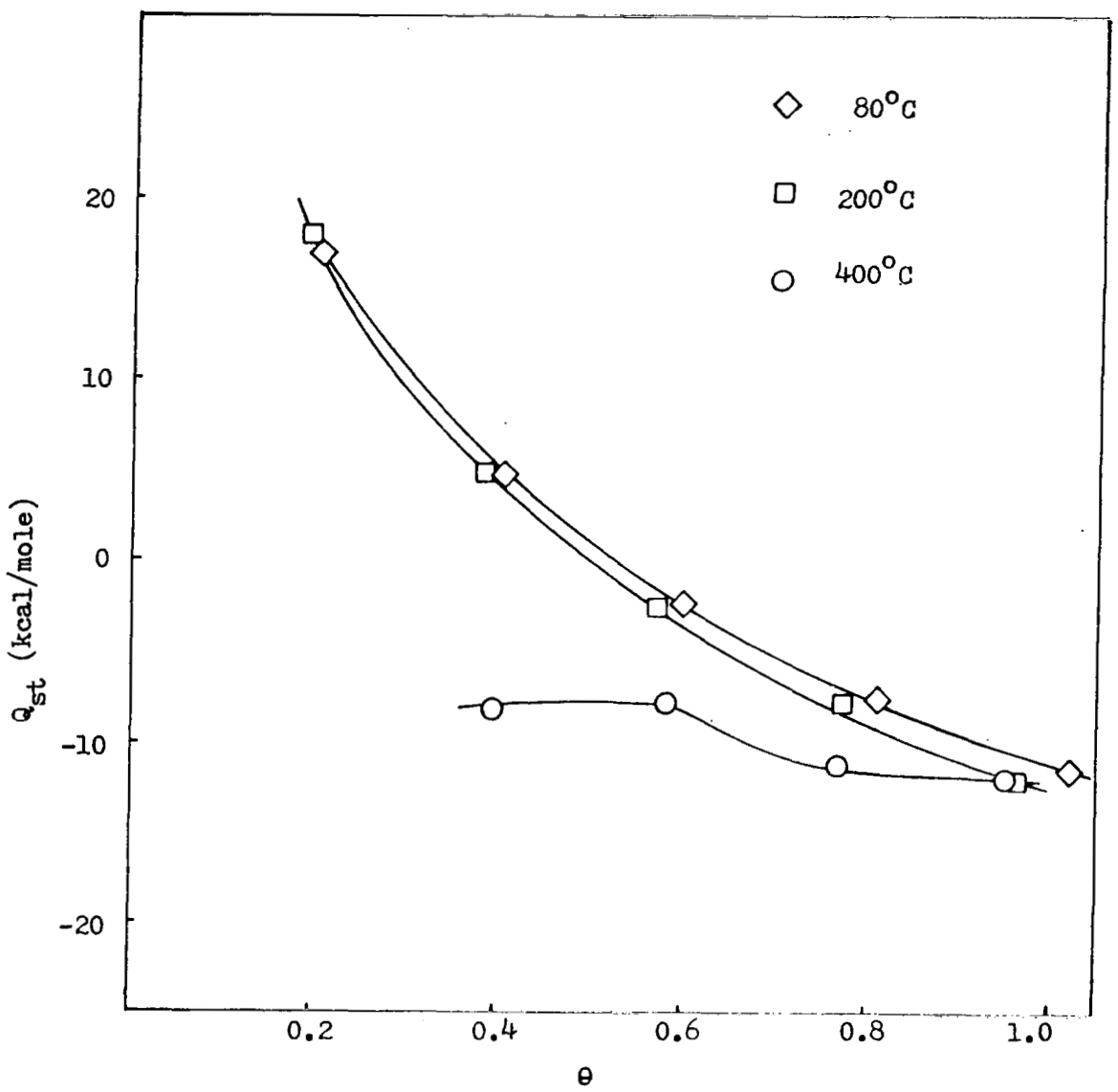

Figure 45. Isosteric Heat of Adsorption for HCl on Gamma Alumina

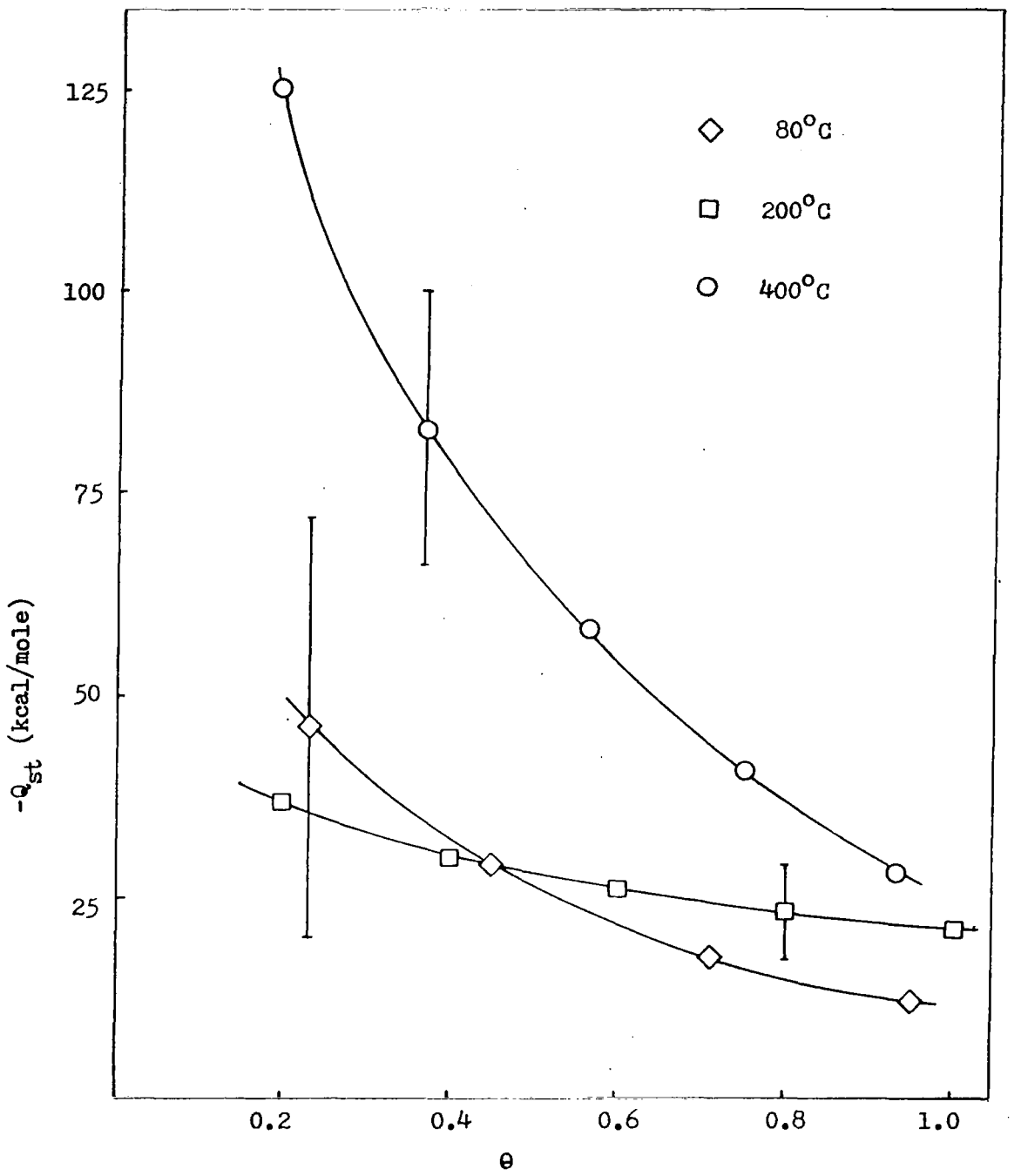

Figure 46. Isosteric Heat of Adsorption for HCl on Alpha Alumina

TABLE XIV

RESULTS OF WATER LAYER MODEL TREATMENT

Adsorbent	ΔH_{ADS} kcal mole	X mole H_2O mole HCl	ΔH_{sol} kcal mole	ΔH_L kcal mole	ΔH_G kcal mole
Gamma-80	3.8	0.23	-2.3	-33.4	6.13
Gamma-200	3.1				
Gamma-400	-8.5	0.0	0.0	-79.9	-8.5
Alpha-80	-31.0	0.69	-4.7	-28.3	-26.3
Alpha-200	-29.5	0.44	-3.4	-32.2	-26.2
Alpha-400	-76.3	0.0	0.0	-40.9	-76.3

I. ESCA Studies:

In order to elucidate the nature of the adsorption site and structure of the adsorbed species, narrow scan ESCA spectra were obtained on both alpha and gamma alumina before and after exposure to hydrogen chloride.

Figure 47 shows the Cl 2p ESCA peak for untreated gamma alumina. Untreated gamma alumina contains some chlorine contamination as seen in Figure 47, which is not unexpected since it is prepared from $AlCl_3$. The narrow scan ESCA spectra of the Al $2s_{1/2}$, Al 2p, O $1s_{1/2}$ and Cl 2p peaks are shown in Figures 48 through 51 for untreated alpha alumina. One sees a significant signal for chlorine in Figure 51. This large signal, however, was obtained by counting the spectra in a ratio of 6:3:3:2:2 for the Cl 2p, Al $2s_{1/2}$, Al sp, O $1s_{1/2}$, and C $1s_{1/2}$, thus the chlorine signal was counted twice the time as long as the Al $2s_{1/2}$ and Al 2p signals. The sensitivity of photoelectron spectroscopy for chlorine is approximately three times greater than its sensitivity for aluminum as shown by Wagner.[67] Thus, because of the greater sensitivity and longer counting time, the chlorine signal does not represent a large chlorine concentration. An ESCA spectra of an untreated theta alumina prepared in an independent laboratory[79] by a precipitation method also gave a significant chlorine peak as shown in Figure 52.

Narrow scan ESCA spectra of the two aluminas after outgassing at 400°C and exposure to 20 torr of hydrogen chloride at 0°C, surprisingly showed no increase in the chlorine signal nor any significant change

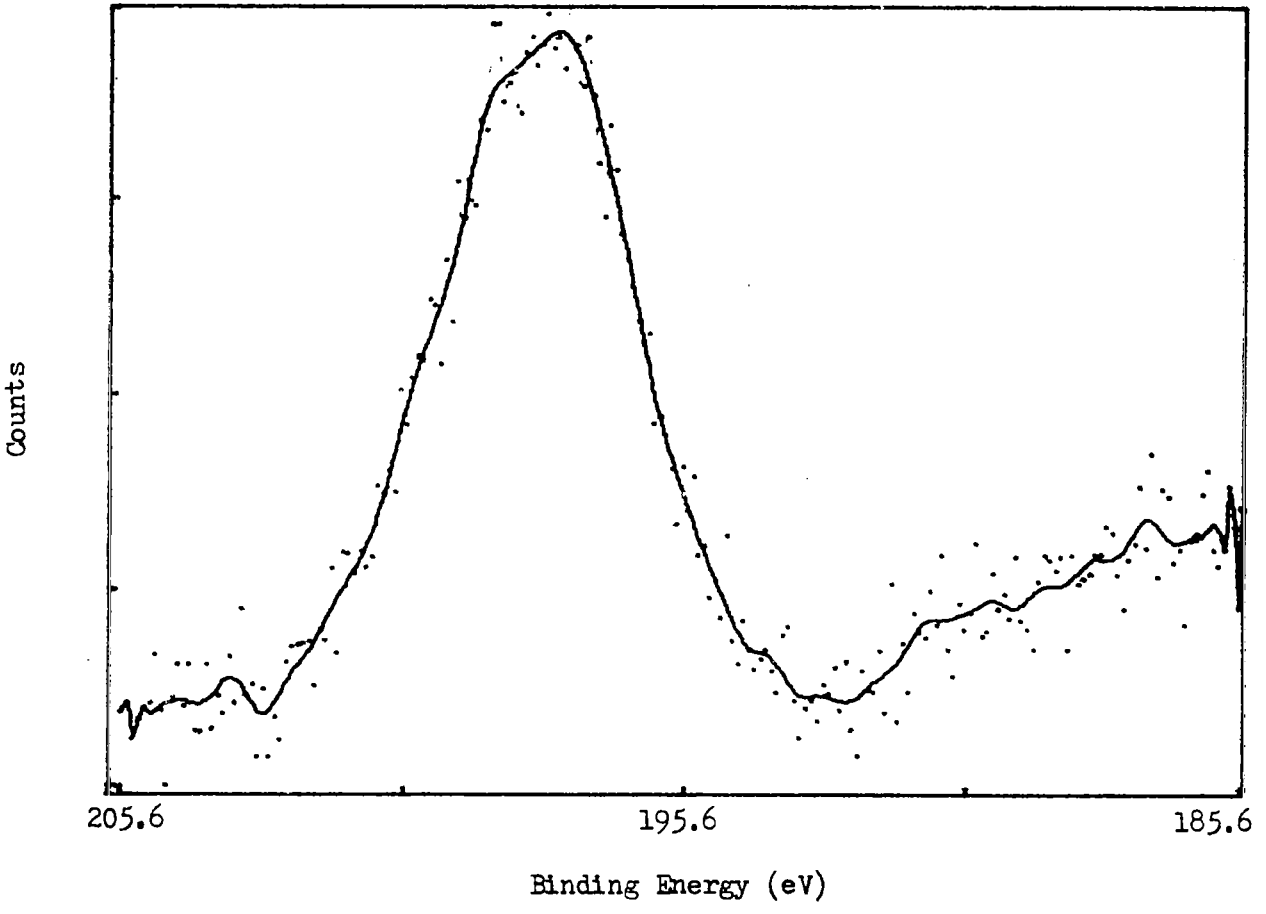

Figure 47. ESCA Spectrum of Chlorine 2p Electrons Obtained from Untreated Gamma Alumina

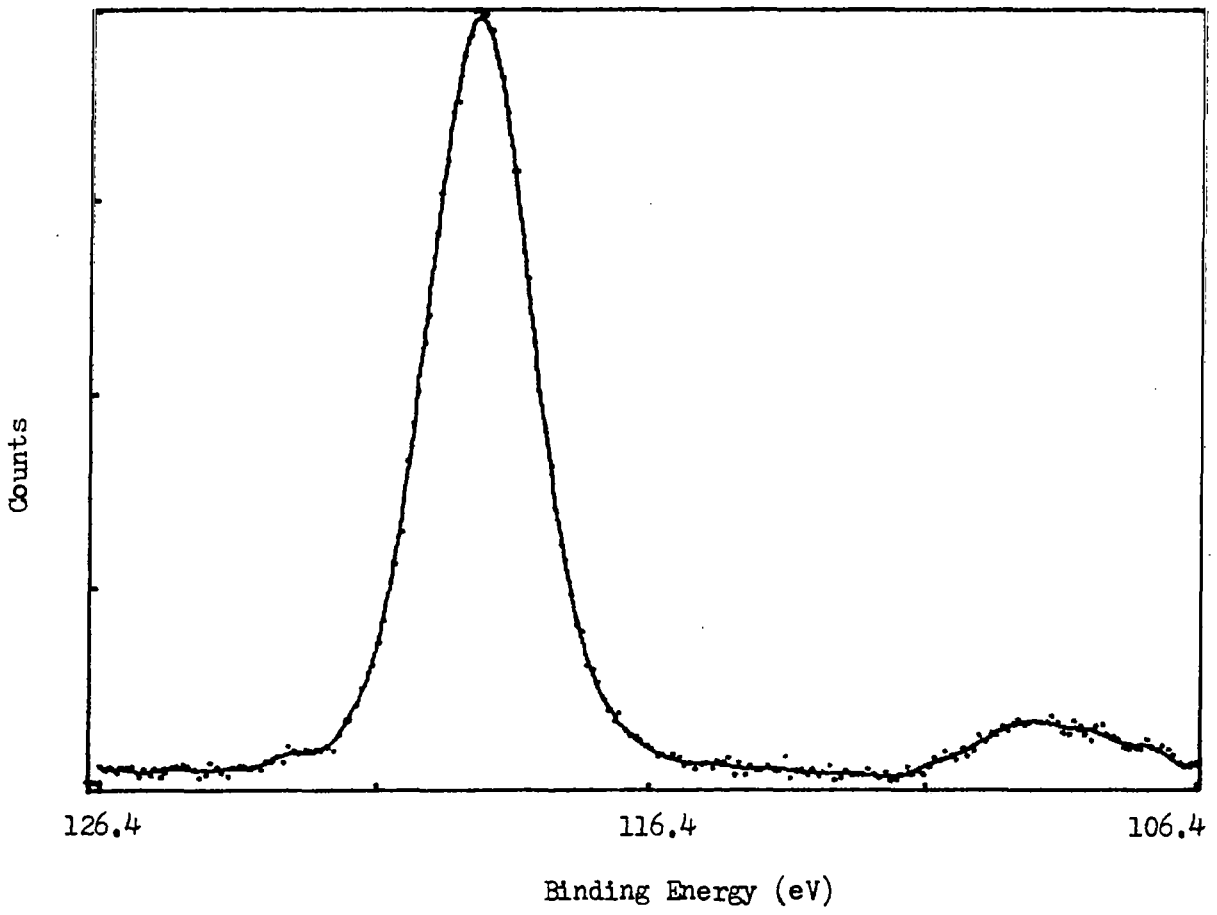

Figure 48. ESCA Spectrum of Aluminum 2s Electrons Obtained from Untreated Alpha Alumina

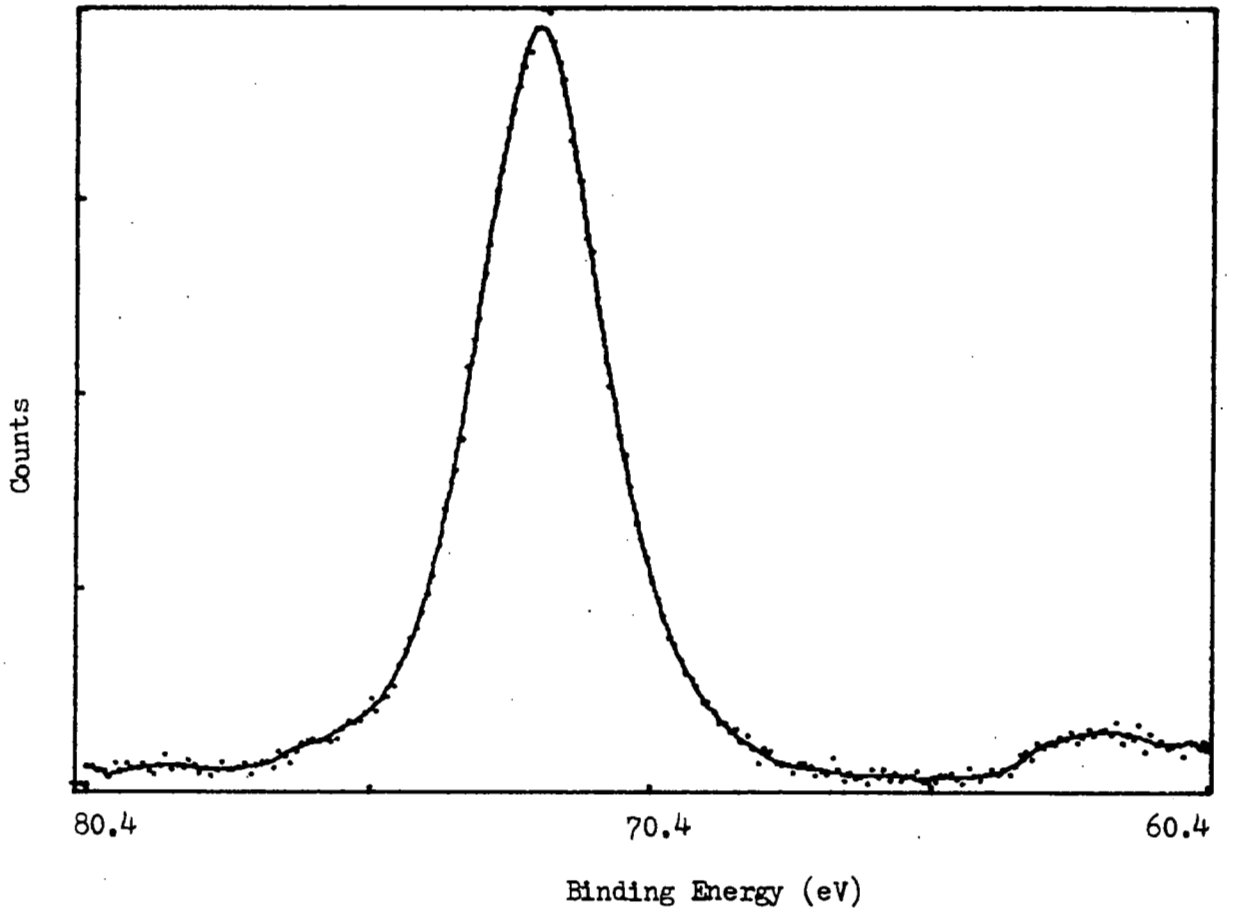

Figure 49. ESCA Spectrum of Aluminum 2p Electrons Obtained from Untreated Alpha Alumina

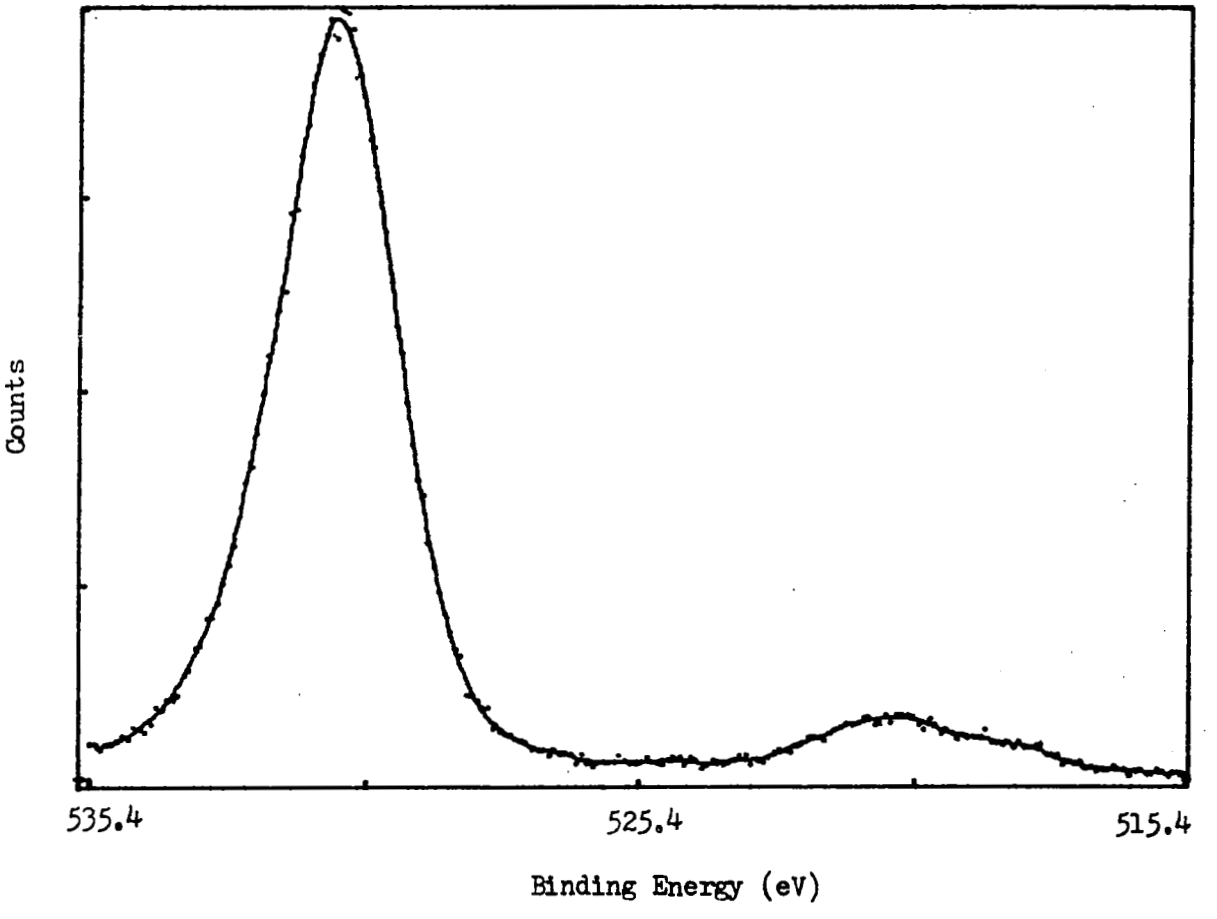

Figure 50. ESCA Spectrum of Oxygen 1s Electrons Obtained From Untreated Alpha Alumina

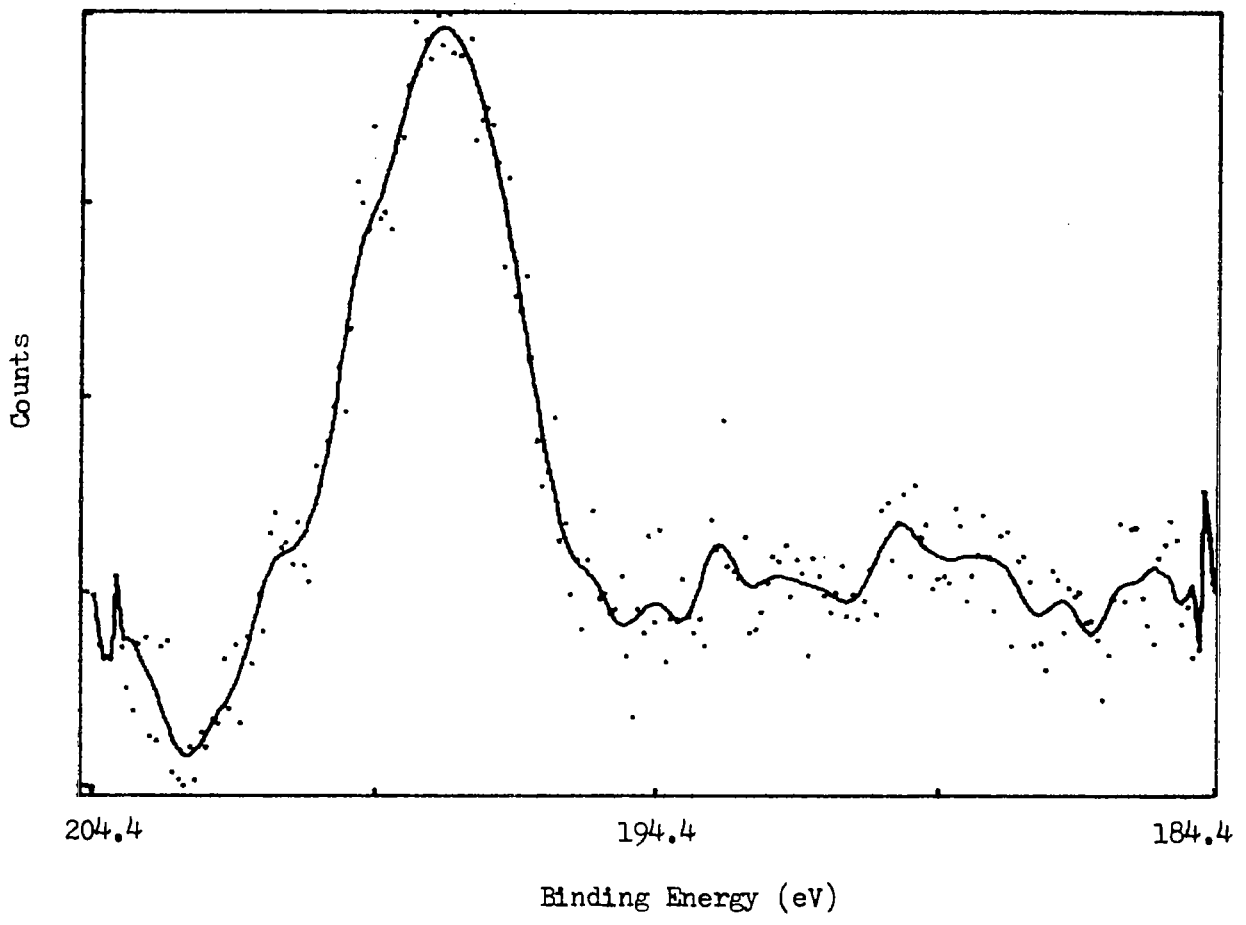

Figure 51. ESCA Spectrum of Chlorine 2p Electrons Obtained from Untreated Alpha Alumina

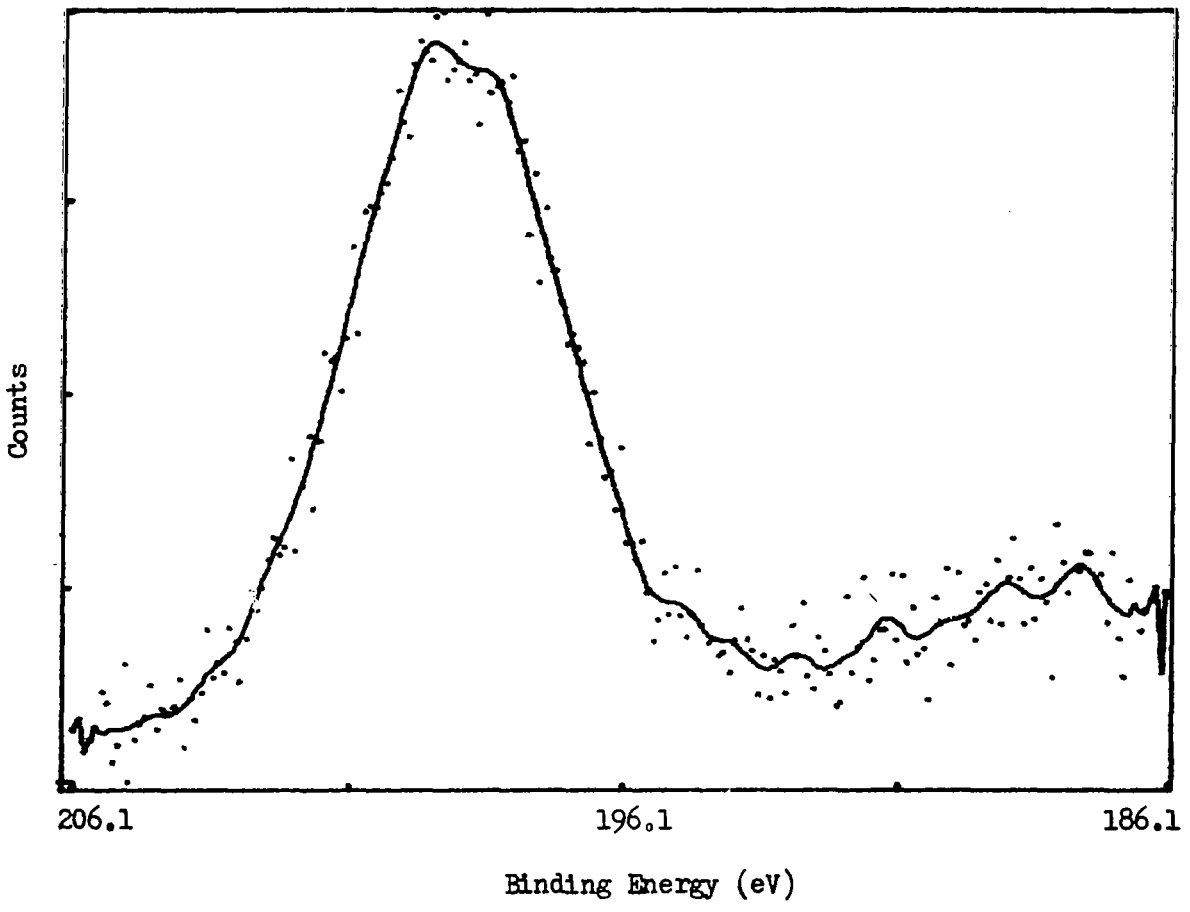

Figure 52. ESCA Spectrum of Chlorine 2p Electrons Obtained from Untreated Theta Alumina

in the binding energy or shape of the chlorine, aluminum or oxygen peaks. Tables XV and XVI show the electron binding energy, full peak width at half maximum, range of the ESCA peaks and work function (ϕ) for gamma and alpha alumina, respectively, before and after treatment with hydrogen chloride. Failure to observe changes in the ESCA spectra after exposure to hydrogen chloride indicates that the adsorbed hydrogen chloride is being lost in the spectrometer. A simple desorption under vacuum is unlikely since isotherm data showed that the hydrogen chloride adsorption is irreversible. A photodesorption process is a possible explanation for the loss of the adsorbed hydrogen chloride. Photodesorption of gases has been observed from solids such as Mo[80] CdS[81] and stainless steel.[82]

TABLE XV

ESCA BINDING ENERGY, RANGE AND FULL PEAK WIDTH AT HALF MAXIMUM FOR GAMMA ALUMINA

		Untreated			HCl Exposed		
				Ave.			Ave.
Cl 2p	B. E. (eV)	198.9	197.3	198.1	198.1	196.1	197.5
	Range 10^2	3.7	4.3		12.3	8.7	
	FWHM (eV)	3.8	4.1			3.7	
Al 2s	B. E. (eV)	118.7	118.1	118.4	119.0	120.9	119.9
	Range 10^2	12.8	13.3		10.7	9.6	
	FWHM (eV)	3.4	3.4		3.8	5.4	
Al 2p	B. E. (eV)	73.9	73.3	73.6	74.0	74.2	74.1
	Range 10^2	16.6	21.2		16.8	15.4	
	FWHM (eV)	3.0	3.0		3.4	3.2	
O 1s	B. E. (eV)	531.1	530.7	531.0	531.3	531.5	531.2
	Range 10^2	37.3	46.7		25.9	28.9	
	FWHM (eV)	3.4	3.4		3.7	3.6	
	ø (eV)	-0.2	0.6		1.8	1.2	

TABLE XVI

ESCA BINDING ENERGY, RANGE AND FULL PEAK WIDTH AT HALF MAXIMUM FOR ALPHA ALUMINA

				Untreated		
						Ave.
Cl 2p	B. E. (eV)			198.2	198.0	198.1
	Range 10^2			0.4	1.3	
	FWHM (eV)			3.3	3.3	
Al 2s	B. E. (eV)	117.8		118.1	117.9	
	Range 10^2	15.4		17.1		
	FWHM (eV)	2.6		2.6		
Al 2p	B. E. (eV)	73.1		73.3	73.2	
	Range 10^2	20.0		27.0		
	FWHM (eV)	2.1		2.3		
O 1s	B. E. (eV)	530.3		530.6	530.4	
	Range 10^2	50.0		61.1		
	FWHM (eV)	2.4		2.6		
	ø (eV)	-3.0	-2.6	-0.6		
				HCl Exposed		
						Ave.
Cl 2p	B. E. (eV)	198.9	198.3	198.4	198.5	
	Range 10^2	1.4	1.6	0.7		
	FWHM (eV)	4.1	4.0	3.8		
Al 2s	B. E. (eV)	118.2	118.0	118.0	118.1	
	Range 10^2	16.6	17.6	18.3		
	FWHM (eV)	3.1	2.9	2.7		
Al 2p	B. E. (eV)	73.4	73.2	73.2	73.3	
	Range 10^2	25.8	28.1	31.4		
	FWHM (eV)	2.6	2.3	2.3		
O 1s	B. E. (eV)	530.8	530.5	530.4	530.6	
	Range 10^2	62.3	53.2	71.8		
	FWHM (eV)	3.1	2.6	2.5		
	ø (eV)	-0.9	-0.9	-3.0		

V. SUMMARY AND CONCLUSIONS

Characterization of the two adsorbents, alpha and gamma alumina, using BET nitrogen surface area measurements, after outgassing at 100, 200 and 400°C showed that the surface area of alpha alumina was independent of outgas temperature but gamma alumina showed a loss in surface area at 400°C. The surface area of alpha alumina was 8.1 ± 1.8 m^2/g. Gamma alumina outgassed at 100 and 200°C had a surface area of 95.4 ± 3.4 m^2/g which decreased to 85.6 ± 3.9 m^2/g after outgassing at 400°C.

Adsorption and desorption isotherms of nitrogen at 77°K obtained on both aluminas showed no hysteresis. It was concluded that neither alumina contained micropores.

Scanning electron photomicrographs of alpha and gamma alumina showed the particle size and texture of the aluminas. Gamma alumina consisted of clusters of secondary particles appearing to be larger than the particles of alpha alumina. However, the primary particles of gamma alumina studied at 5000X magnification showed that they were smaller than the primary particles of alpha alumina. This conclusion was consistent with calculated particle sizes of alpha and gamma alumina based on BET nitrogen surface areas.

Adsorption of water vapor on alpha and gamma alumina at 30, 40 and 50°C showed decreasing water vapor adsorption with increasing adsorption temperature. The isosteric heat of adsorption for water vapor was larger for alpha alumina than for gamma alumina, based on a Clausius-Claperyon analysis of the temperature dependence.

Water vapor adsorption on alpha and gamma alumina showed a dependence on outgas temperature. Alumina outgassed at 80, 200 and 400°C showed increasing adsorption of water vapor. This increase was attributed to successive removal of physisorbed water from the alumina.

Readsorption experiments of water vapor adsorption on alpha and gamma alumina showed that water vapor adsorption was completely reversible. It was concluded that water vapor adsorption on both alpha and gamma alumina involved a physisorption process.

A significant difference in the water adsorption capacity of the two aluminas was found. Alpha alumina adsorbed more water vapor per unit area than gamma alumina. The difference in adsorption capacity was explained by ideal surface models of alpha and gamma alumina. Differences in adsorbate areas, determined using the BET equation, were explained on the basis of the ideal surface. On alpha alumina each adsorbed water molecule occupied an area of 12.4 $Å^2$ consistent with the calculated value of 13.5 $Å^2$ for the adsorbate area on the ideal alpha alumina surface assuming each adsorbed water molecule required two surface oxygen ions. The adsorbed area on the ideal gamma alumina surface would be 16 $Å^2$ assuming two oxygen ions as the adsorption site. The area obtained from the adsorption isotherms was 16.2 $Å^2$/molecule on gamma alumina. On the basis of this agreement, it was concluded that the site for water vapor adsorption on alumina is two oxygen ions with hydrogen bonding occurring between the adsorption site and the adsorbate.

Hydrogen chloride adsorption on alpha and gamma alumina showed a dependence on outgas temperature and adsorption temperature.

Alumina outgassed at 80, 200 and 400°C showed increasing hydrogen chloride adsorption with increasing outgas temperature. Higher outgas temperatures removed water molecules which were blocking sites on the alumina necessary for hydrogen chloride adsorption.

Readsorption experiments of hydrogen chloride on alpha and gamma alumina showed that hydrogen chloride adsorption was approximately 60% irreversible. A study of the temperature dependence of the irreversibility showed that hydrogen chloride was not completely desorbed from alpha alumina even at temperatures as high as 341°C. Because of this irreversibility, it was concluded that hydrogen chloride adsorption on alumina involved a chemisorption process.

Hydrogen chloride adsorption on alpha and gamma alumina showed a dependence on adsorption temperature. Hydrogen chloride adsorption isotherms obtained at 0, 40 and 50°C showed a decrease in the amount adsorbed with increasing temperature. Isosteric heats of adsorption obtained from this temperature dependence showed an increasing heat of adsorption with increasing outgas temperature. The isosteric heat of adsorption decreased with increasing surface coverage.

A comparison of the isosteric heats of adsorption with calorimetric heats of adsorption was made using a water layer model. Because of the agreement of the isosteric heats and the calorimetric heats of adsorption for hydrogen chloride on alpha alumina after 80 and 200°C outgassing it was concluded that the water layer model adequately described the adsorption process. Hydrogen chloride adsorption on alumina may involve an initial solution process of the gas in the

pre-adsorbed water surrounding the alumina particle followed by the adsorption on the alumina surface.

A significant difference in the amount of hydrogen chloride adsorption on alpha and gamma alumina was observed. Alpha alumina adsorbed more hydrogen chloride per unit area than gamma alumina. This difference in adsorption capacity was explained on the basis of the ideal surface models for alpha and gamma alumina. Agreement was observed between the hydrogen chloride adsorbed area on gamma alumina (33.4 Å^2/molecule) and the area calculated for the ideal gamma surface (32 Å^2/molecule) assuming that an aluminum ion is the adsorption site. For the ideal alpha alumina surface, using the same assumption, the adsorbed area was 19.5 Å^2/molecule in agreement with 17.5 Å^2/molecule from the hydrogen chloride adsorption isotherms. On the basis of the agreement between the ideal adsorbate areas and those obtained from the adsorption isotherms it was concluded that the site for hydrogen chloride adsorption on alumina is a surface aluminum ion.

LITERATURE CITED

1. A Procko, "Encyclopedia of Industrial Chemical Analysis," F.D. Snell and S.L. Ettre, Ed., Interscience, New York, N.Y., 1971, p. 389-403.

2. H. Bassow, "Air Pollution Chemistry An Experimenter's Sourcebook," Hayden Book Company, Inc., Rochelle Park, New Jersey, 1976, Chapter 3.

3. A.C. Stern, "Air Pollution," Vol. II, Academic Press, New York, N.Y., 1968, Chapter 38.

4. "Environmental Statement for the Space Shuttle Program," NASA, TM X-68541, Washington, D.C., 1972.

5. R.A. Dobbins and L.D. Strand, AIAA Jour., 8, 1544 (1970).

6. J.W. Hightower, "Catalytic Sites on Gamma Alumina," Awards Symposium on Catalytic Sites on Oxides, Division of Petroleum Chemistry Meeting, American Chemical Society, Dallas, Texas, April, 1973.

7. J.B. Peri, J. Phys. Chem., 70, 1482 (1966).

8. J.B. Peri, J. Phys. Chem., 70, 3168 (1966).

9. M. Tanaka and S. Ogasawara, J. Catal., 16, 157 (1970).

10. S. Ogasaware, M. Takagawa and K. Takahashi, J. Catal., 29, 67 (1973).

11. D.M. Young and A.D. Crowell, "Physical Adsorption of Gases," Butterworths, London, 1962.

12. S. Ross and J.P. Oliver, "On Physical Adsorption," Interscience, New York, 1964.

13. E.A. Flood, Ed., "The Solid-Gas Interface," Vol. I and II, Marcel Dekker, New York, 1967.

14. D.O. Hayward and B.M.W. Trapnell, "Chemisorption," 2nd ed., Butterworths, London, 1964.

15. G.L. Gregory and R.W. Storey, NASA, TM X-3228, Washington, D.C., August, 1975.

16. Solid Propellant Engineering Staff, NASA, TM 33-712, Jet Propulsion Laboratory, Pasadena, California, February, 1975.

17. W.C. Hulten, R.W. Storey, G.L. Gregory, D.C. Woods and F.S. Harris, Jr., NASA, TM X-2987, Washington, D.C., July, 1974.

18. R.R. Bailey, P.E. Field and J.P. Wightman, Anal. Chem., 48, 1818 (1976).

19. M.P. Nadler, AFRPL Report 5730-73-6, Edwards Air Force Base, Calif., September 1973.

20. G. C. Pellett, ERDA Symposium Series, No. 41 (CONF 741003), pp. 437-465, June, 1977.

21. R.K. Dumbald, J.R. Bjorklund and J.F. Bowers, NASA, TR 73-301-02, Washington, D.C., 1973.

22. H.R. Rooksby in "X-ray Identification and Crystal Structures of Clay Minerals," G. Brown, Ed., Mineralogical Society, London, 1961, Chapter X.

23. K. Werfers and G.M. Bell, Technical Paper No. 19, Aluminum Company of America, East St. Louis, Illinois, 1972.

24. A. Bielanski and A. Sedzimir, "4th International Symposium on the Reactivity of Solids," J.H. De Boer, Ed., Elsevier Publishing Company, New York, 1961, p. 301.

25. M.L. Hair, "Infrared Spectroscopy in Surface Chemistry," Marcel Dekker Inc., New York, 1967, Chapter 5.

26. R.J. Cvetanovic and Y. Amenomiya, Intra-Sci. Chem. Rept., 6, 161 (1972).

27. T.L. Slager and C.H. Amberg, Can. J. Chem., 50, 3416 (1972).

28. J.H. Lunsford, L.W. Zingery and M.P. Rosynek, J. Catal., 38, 179 (1975).

29. J. Koubek, J. Volf and J. Pasek, J. Catal., 38, 385 (1975).

30. S.J. Gregg and J.D.F. Ramsay, J. Phys. Chem., 73, 1243 (1969).

31. A. Stanislaus, M.J.B. Evans and R.F. Mann, J. Phys. Chem., 76, 2349 (1972).

32. C.N. Cochran, Environ. Sci. Technol., 8, 63 (1974).

33. M.M. Bhasin, C. Curran and G.S. John, J. Phys. Chem., 74, 3973 (1970).

34. J.B. Butt and L.T. Starzec, J. Catal., 32, 99 (1974).

35. A.V. Deo and I.G. Dalla Lana, J. Catal., 21, 270 (1971).

36. P.J. Hendra, I.D.M. Turner, E.J. Loader and M. Stacey, J. Phys. Chem., 78, 300 (1974).

37. J.B. Peri and R.B. Hannan, J. Phys. Chem., 64, 1526 (1960).

38. J.B. Peri, J. Phys. Chem., 69, 211 (1965).

39. J.B. Peri, J. Phys. Chem., 72, 2917 (1968).

40. J.B. Peri, J. Phys. Chem., 70, 2937 (1966).

41. J.B. Peri, J. Phys. Chem., 69, 220 (1965).

42. J.B. Peri, J. Phys. Chem., 70, 3168 (1966).

43. J.H. De Boer, J.M.H. Fortuin, B.C. Lippens and W.H. Meijs, J. Catal., 2, 1 (1963).

44. T. Morimoto, M. Nagao and J. Imai, Bull. Chem. Soc. Jap., 44, 1282 (1971).

45. M.L. Hair, "Infrared Spectroscopy in Surface Chemistry," Marcel Dekker Inc., New York, 1967, Chapter 4.

46. J.D. Carruthers, D.A. Payne, K.S.W. Sing and L.J. Stryker, J. Colloid Interfac. Sci., 36, 205 (1971).

47. D.S. MacIver, H.H. Tobin and R.J. Barth, J. Catal., 2, 485 (1963).

48. D.S. MacIver, W.H. Wilmot and J.M. Bridges, J. Catal., 3, 502 (1964).

49. R.L. Every, W.H. Wade and N. Hackerman, J. Phys. Chem., 64, 1196 (1960).

50. R.L. Every, W.H. Wade and N. Hackerman, J. Phys. Chem., 65, 937 (1961).

51. T. Morimoto, K. Shiomi and H. Tanaka, Bull. Chem. Soc. Jap., 37, 392 (1964).

52. H. Cochrane and R. Rudham, Trans. Faraday Soc., 61, 2246 (1965).

53. B.A. Hendriksen, D.R. Pearce and R. Rudham, J. Catal., 24, 82 (1972).

54. L.G. Harrinson and Y. Koga, Proc. Roy. Soc., Ser. A, 327, 122 (1972).

55. M. Primet, J. Basset, M.V. Mathiea and M. Prette, J. Phys. Chem., 74, 2868 (1970).

56. G.D. Parfitt, J. Ramsbotham and C.H. Rochester, Trans. Faraday Soc., 67, 3100 (1971).

57. Y.M. Dadiza and J.M. Saleh, Trans. Faraday Soc., 68, 269 (1972).

58. I.I. Kurlyandskaya, S.B. Grinberg, T.F. Kudryavtseva, E.B. Svellanov, R.M. Flid and R.V. Dzhagatspanyan, Russ. J. Phys. Chem., 47, 101 (1973).

59. W.S. Lassiter, Surface Sci., 47, 669 (1975).

60. D.H. Everett and J.P. Wightman, 1976 EUCHEM Conference, Collioure, France, April, 1976.

61. S.Y. Tyree, Jr., "1st Status Report NASA Grant NSG1204," NASA Langley Research Center, Hampton, Virginia, December, 1975.

62. S.Y. Tyree, Jr., "2nd Status Report NASA Grant NSG1204," NASA Langley Research Center, Hampton, Virginia, March, 1976.

63. S.Y. Tyree, Jr., "3rd Status Report NASA Grant NSG1204," NASA Langley Research Center, Hampton, Virginia, June, 1976.

64. K. Siegbahn, C. Nordling, A. Fahlman, R. Nordberg, K. Hamrin, J. Hedman, G. Johansson, T. Bergmark, S. Karlsson, I. Lindgren, and B. Lindberg, "ESCA Atomic Molecular and Solid State Structure Studies by Means of Electron Spectroscopy," Almquist and Wiksells, Uppsala, Sweden, 1967.

65. D.M. Hercules, Anal. Chem., 44, 106R (1972).

66. D.M. Hercules and J.C. Carver, Anal. Chem., 46, 133R (1974).

67. C.D. Wagner, Anal. Chem., 4, 1050 (1972).

68. P.E. Larson, Anal. Chem., 44, 1678 (1972).

69. K. Kishi and S. Ikeda, J. Phys. Chem., 72, 107 (1974).

70. J.R. Lindsay, H.J. Rose, Jr., W.E. Swartz, Jr., P.H. Watts, Jr., and K.A. Rayburn, Appl. Spec., 27, 1 (1973).

71. R. Fricke and K. Jockers, Z. Anorg. Chem., 263, 3 (1950).

72. S.J. Gregg and K.S.W. Sing, "Adsorption, Surface Area and Porosity," Academic Press, New York, 1967.

73. G.E. Hendley, S.V. O'Neal and J.P. Wightman, Final Report NAS1-13175-7, Blacksburg, Virginia, June, 1975.

74. S.J. Gregg and K.S.W. Sing, "Adsorption, Surface Area and Porosity," Academic Press, New York, 1967, Chapter 3.

75. B.W. Smith and M.L. Parsons, J. Chem. Ed., 50, 679 (1973).

76. A. Clark, V.C.F. Holm and D.B. Blackburn, J. Catal., 1, 244 (1962).

77. H.C. Stumpf, A.S. Russell, J.W. Newsome and C.M. Tucker, Ind. Eng. Chem., 42, 1398 (1950).

78. J.F. Brown, D. Clark and W.W. Elliott, J. Chem. Soc., 84 (1953).

79. W.R. Cofer, III, NASA Langley Research Center, Hampton, Virginia, private communication, 1976.

80. D. Lichtman, R.B. McQuistan and T.R. Kirst, Surface Sci., 5, 120 (1966).

81. P. Mark, RCA Rev., 26, 461 (1965).

82. G.W. Fabel, S.M. Cox and D. Lichtman, Surface Sci., 40, 571 (1973).

83. P.E. Field, Chemistry Department, Virginia Polytechnic Institute and State University, Blacksburg, Virginia.

APPENDIX 1

Preparation of Alpha and Gamma Alumina Samples for Infrared Spectroscopy

Attempts to prepare infrared transparent disks of the two aluminas were unsuccessful. Various techniques were tried without success. The main source of problems with gamma alumina was sticking to the faces of the stainless steel press. To prevent sticking the press was polished several times, heated before pressure was applied, pressing under vacuum was attempted, variation of the pressure from 1200 to 20000 psi and the amount of alumina was also varied. Gamma alumina was pressed between filter paper, polycarbonate film and Teflon film but these techniques were unsuccessful. Attempts to release the gamma alumina from the face of the press using acetone and water only cracked the disk. Finally, the gamma alumina was pressed between ashless filter paper, the paper was ashed off at 500°C and suitable transparent disks were obtained. The crystalline phase of the alumina, however, was questionable because of the thermal treatment.

Alpha alumina could be pressed into disks without encountering the sticking problem. However, attempts to press alpha alumina into disks thin enough for good transmission properties were unsuccessful.

Because of the difficulty in preparing suitable disks of the alumina samples no infrared measurements were performed.

APPENDIX 2

Sample Calculation of Isotherm from Experimental Data

Data Table:

	Weight	Pretreatment
Sample: Alon	15.8768	2 hrs 200°C
Run: 1	15.7623	2 hrs 50°C
	0.1145 g	R_o = 526.25

Helium Volume Calibration:

R_1	R_2	VI	P_1	P_2	VT	VSB
648.10	634.80	113.43	121.8	108.5	127.3	13.9

HCl Adsorption:

R_1	R_2	P_1	P_2	P_{EXP}	P_{CAL}	P	N_1 10^5	N_s 10^5
535.50	528.05	9.25		1.80	8.24	6.44	35.52	35.52
531.80	531.00	5.55	1.80	4.75	5.14	0.39	2.15	37.67
536.95	535.95	10.70	4.75	9.70	10.05	0.35	1.93	39.60
540.15	539.35	13.90	9.70	13.10	13.44	0.34	1.87	41.47
545.40	544.45	19.15	13.10	18.20	18.49	0.29	1.59	43.06

Volume Calculation:

The system volume is calculated by first finding the pressure of Helium:

$$P_1 = R_1 - R_o = 648.10 - 526.25 = 121.8 \text{ torr} \qquad (2\text{-A})$$

$$P_2 = R_2 - R_o = 634.8 - 526.25 = 108.5 \text{ torr} \qquad (2\text{-B})$$

The total volume is then:

$$VT = \frac{(VI \times P_1)}{P_2} = \frac{113.43 \text{ cc} \times 121.8 \text{ torr}}{108.25 \text{ torr}} = 127.3 \text{ cc} \qquad (2\text{-C})$$

The sample bulb volume is:

$$VSB = VT - Vi = (127.3 - 113.4)\ cc = 13.9\ cc \qquad (2\text{-}D)$$

HCl Adsorption Calculation:

The first point on the isotherm in mole HCl/gram adsorbent is calculated by the following procedure:

$$P_{CAL} = \frac{P_1 \times VI}{VT} = \frac{9.25\ torr \times 11.43\ cc}{127.3\ cc} = 8.24\ torr \qquad (2\text{-}E)$$

then:

$$P = P_{CAL} - P_{EXP} = 8.24 - 1.80 = 6.44\ torr \qquad (2\text{-}F)$$

and then using the ideal gas law:

$$N_1 = \frac{P \times VT}{R \times T \times W} = \frac{6.44\ torr \times 127.3\ cc}{6.24 \times 10^4\ \frac{cc\text{-}torr}{mole\text{-}^oK} \cdot 323^oK \cdot 0.1145g} \qquad (2\text{-}G)$$

$$= 35.52 \quad 10^{-5}\ mole\text{-}gram^{-1}$$

The second point is:

$$P_{CAL} = \frac{(P_1 \times VI + P_2 \times VSB)}{VT} = \frac{(5.55 \times 113.43) + (1.80 \times 13.9)}{127.3}$$

$$= 5.14\ torr \qquad (2\text{-}H)$$

and then:

$$P = P_{CAL} - P_{EXP} = 5.14 - 4.75 = 0.39\ torr \qquad (2\text{-}I)$$

The number of moles adsorbed by the second dose, using equation 2-G, is then:

$$N_2 = \frac{0.39 \times 127.3}{6.24 \times 10^4 \times 323 \times 0.1145} = 2.15 \times 10^{-5}\ mole\text{-}gram^{-1}$$

This procedure is continued until all the N_i's have been calculated. To find the number of moles on the surface at each pressure a summation is made of the number of moles deposited by

each dose. Thus, the last column in the table is calculated by:

$$\text{1 st point} \quad N_s = \sum_i N_i = 35.52 \times 10^{-5} \text{ mole-gram}^{-1} \qquad (2\text{-J})$$

$$\text{2 nd point} \quad N_s = \sum_i N_i = (35.52 + 2.15)\ 10^{-5} \text{ mole-gram}^{-1}$$

etc.

The isotherm is obtained by plotting N_s vs. $P_{EXP.}$

APPENDIX 3

Results of Solubility Measurements of Alpha and Gamma Alumina in Water and 0.1 N Hydrochloric Acid

Solution	Type of Alumina	Concentration of Aluminum (ppm)
HCl	Blank (no alumina)	0.0
H_2O	γ	0.9
HCl	γ	60.6
HCl	γ	52.5
HCl	γ	72.8
H_2O	α	0.3
HCl	α	3.7
HCl	α	4.1

APPENDIX 4

"FOCAL" Program to Fit Isotherm Data to Freundlich Equation

```
 W A
C-8K  MODV 11-219

01.05 T !!!!" L NP  VS. V(MOLE/M*M) FROM FREUNDLICH"!
 01.06 T " N*10↑5-CALC."!!
01.07 A !!" TEMPERATURE"TA,"      SYSTEM"SY,!
01.08 A " SURFACE AREA"SA,!
01.15 A " NUMBER OF DETERMINATIONS" N, !!
01.20 T "     P          N*10↑5",!!
01.25 S P=0; S Q=0; S R=0; S S=0; S W=0
01.30 F I=1,N;  D 2.00
01.35 D 3.00
01.40 G 7.05

02.05 A "   " X(I),"     "Y(I),!
02.07 S X(I)=FLOG(X(I)); S Y(I)=FLOG(Y(I)/SA)
02.15 S P=P+X(I); S Q=Q+Y(I)
02.20 S R=R+X(I)*X(I); S S=S+X(I)*Y(I); S W=W+Y(I)*Y(I)

03.05 S NS=(N* S-P*Q)
03.10 S D=N* R-P*P
03.15 S NI=R*Q-P*S
03.20 S SL=NS/D; S IN=NI/D
03.26 DO 6.00
03.28 S IN=IN-(5*FLOG(10))
03.30 T %, ! " INTERCEPT"IN,"      ERROR"DB,!
03.35 T " SLOPE" SL,"      ERROR" DM,!
03.40 T " ERROR IN INTERCEPT INCORRECT",!!

06.05 S RS=SL*(NS/N)
06.10 S TS=W-(Q*Q)/N
06.15 S SS=TS-RS
06.20 S SQ=SS/(N-2)
06.25 S DM=FSQT(SQ/(D/N))
06.35 S DY=FSQT(SQ)
06.45 S DB=FSQT((SQ*R)/D)
```

```
Ø7.Ø5 A " NUMBER OF POINTS"NP,!
Ø7.1Ø A " INCREMENT MOLE/M*M"IC,!
Ø7.15 A " INITIAL MOLE/M*M"NM,!!!
Ø7.2Ø F I=1,NP; D 8.ØØ
Ø7.25 G 9.Ø1

Ø8.Ø1 S AB=FLOG(NM); S LNP=(AB-IN)/SL
Ø8.Ø8 T "   NM"NM,"      LNP"LNP,!
Ø8.1Ø S NM=NM+IC

Ø9.Ø1 G 1.Ø5
*
```

Program Output:

```
LNP VS. V(MOLE/M*M) FROM FREUNDLICH
N*10↑5-CALC.


TEMPERATURE:Ø       SYSTEM:HCLG2ØØ
SURFACE AREA:95.4
NUMBER OF DETERMINATIONS:6

     P          N*1Ø↑5

  :1.85       :45.77
  :4.85       :49.99
  :9.ØØ       :53.4Ø
  :12.ØØ       :55.14
  :15.65       :56.44
  :19.25       :58.61

INTERCEPT=-Ø.123163E+Ø2      ERROR= Ø.869187E-Ø2
 SLOPE= Ø.1Ø3212 E+ØØ      ERROR= Ø.387512E-Ø2
ERROR IN INTERCEPT INCORRECT
```

NUMBER OF POINTS:20
INCREMENT MOLE/M*M: 5.0E-7
INITIAL MOLE/M*M: 5.0E-7

NM= 0.500000E-06	LNP=-0.212416E+02
NM= 0.100000E-05	LNP=-0.145258E+02
NM= 0.150000E-05	LNP=-0.105974E+02
NM= 0.200000E-05	LNP=-0.781005E+01
NM= 0.250000E-05	LNP=-0.564805E+01
NM= 0.300000E-05	LNP=-0.388157E+01
NM= 0.350000E-05	LNP=-0.238804E+01
NM= 0.400000E-05	LNP=-0.109427E+01
NM= 0.450000E-05	LNP= 0.469021E-01
NM= 0.500000E-05	LNP= 0.106774E+01
NM= 0.550000E-05	LNP= 0.199118E+01
NM= 0.600000E-05	LNP= 0.283422E+01
NM= 0.649999E-05	LNP= 0.360973E+01
NM= 0.699999E-05	LNP= 0.432775E+01
NM= 0.749999E-05	LNP= 0.499620E+01
NM= 0.799999E-05	LNP= 0.562149E+01
NM= 0.849999E-05	LNP= 0.620887E+01
NM= 0.899999E-05	LNP= 0.676266E+01
NM= 0.949999E-05	LNP= 0.728652E+01
NM= 0.999998E-05	LNP= 0.778348E+01

APPENDIX 5

"FOCAL" Program to Calculate Isosteric Heats of Adsorption Using Freundlich Parameters

```
 W A
C-8K MODV 11-219

01.05 T !!!!" HEAT FROM FREUNDLICH"!
01.06 T " L NP  VS  1/T"!!
01.07 A " NM*10E-5" NM,!
01.15 A " NUMBER OF DETERMINATIONS" N, !!
01.20 T "     T          LNP",!!
01.25 S P=0; S Q=0; S R=0; S S=0; S W=0
01.30 F I=1,N; D 2.00
01.35 D 3.00
01.40 G 1.05

02.05 A "   " X(I),"     " Y(I),!
02.07 S X(I)=1/(X(I)+273)
02.15 S P=P+X(I); S Q=Q+Y(I)
02.20 S R=R+X(I)*X(I); S S=S+X(I)*Y(I); S W=W+Y(I)*Y(I)

03.05 S  NS=(N*S-P*Q)
03.10 S  D=N*R-P*P
03.15 S  NI=R*Q-P*S
03.20 S SL=NS/D; S IN=NI/D
03.26 DO 6.00
03.27 S HT=SL*1.987/1000; S HE=DM*1.987/1000
 03.30 T " HEAT KCAL/MOLE"HT,"     ERROR"HE,!!
 03.35 T " SLOPE"SL,"     ERROR" DM,!
03.40  T " ERROR IN Y"DY,!!

06.05 S RS=SL*(NS/N)
06.10 S  TS=W-(Q*Q)/N
06.15 S SS=TS-RS
06.20 S SQ=SS/(N-2)
06.25 S DM=FSQT(SQ/(D/N))
06.35 S DY=FSQT(SQ)
06.45 S DB=FSQT((SQ*R)/D)
*
```

APPENDIX 6

Adsorption Data for Water Vapor Adsorption on Gamma Alumina

Outgas Temperature: 80°C
Adsorption Temperature: 30°C

	P_{EXP} (torr)	$N_s \times 10^5$ (mole/g)
Run 1	0.70	61.89
	3.55	97.99
	6.40	118.99
	9.35	140.31
	14.25	161.63
Run 2	1.20	62.84
	5.05	110.84
	9.45	140.69
	15.05	167.30

Outgas Temperature: 80°C
Adsorption Temperature: 40°C

	P_{EXP} (torr)	$N_s \times 10^5$ (mole/g)
Run 1	2.30	69.33
	5.50	90.85
	9.15	107.67
	15.20	127.14
Run 2	1.35	50.93
	3.30	67.84
	6.90	90.41
	11.10	107.79
	16.60	130.56

Outgas Temperature: 80°C
Adsorption Temperature: 50°C

	P_{EXP} (torr)	$N_s \times 10^5$ (mole/g)
Run 1	1.10	34.98
	1.95	42.81
	2.30	49.93
	5.25	65.47
	7.95	71.46
	10.85	80.38
	14.95	91.60
	16.50	99.47
Run 2	1.10	44.40
	3.20	63.71
	7.00	79.59
	11.20	91.81
	15.30	100.56
	17.65	104.70

Outgas Temperature: 200°C
Adsorption Temperature: 40°C

	P_{EXP} (torr)	$N_s \times 10^5$ (mole/g)
Run 1	1.10	63.71
	3.55	86.41
	5.95	104.80
Run 2	2.20	70.76
	5.05	91.67
	8.40	110.82
	13.35	126.54
	16.45	134.76
Run 3	1.75	65.39
	4.90	90.16
	8.50	107.46
	11.60	122.25
	16.05	133.48

Run 4	1.40	66.69
	3.25	84.84
	6.75	107.29
	11.25	126.96
	17.30	141.07

Outgas Temperature: 400°C
Adsorption Temperature: 27°C

	P_{EXP} (torr)	$N_s \times 10^5$ (mole/g)
Run 1	0.35	79.15
	2.10	121.95
	6.15	163.01
	10.80	194.21
	16.70	222.89

Outgas Temperature: 400°C
Adsorption Temperature: 40°C

	P_{EXP} (torr)	$N_s \times 10^5$ (mole/g)
Run 1	2.05	79.67
	5.00	105.95
	10.75	127.31
	16.45	141.75

Outgas Temperature: 400°C
Adsorption Temperature: 50°C

	P_{EXP} (torr)	$N_s \times 10^5$ (mole/g)
Run 1	3.05	94.74
	7.70	117.81
	11.70	133.69
	16.85	146.50

APPENDIX 7

Adsorption Data for Water Vapor Adsorption on Alpha Alumina

Outgas Temperature: 80°C
Adsorption Temperature: 27°C

	P_{EXP} (torr)	$N_s \times 10^5$ (mole/g)
Run 1	0.80	5.50
	1.55	7.24
	3.20	9.80
	6.65	13.18
	11.00	16.14
	15.05	18.72

Outgas Temperature: 80°C
Adsorption Temperature: 40°C

	P_{EXP} (torr)	$N_s \times 10^5$ (mole/g)
Run 1	1.65	5.49
	3.55	7.02
	5.90	8.70
	8.65	10.18
	11.40	11.42
	17.35	12.67
Run 2	2.15	5.73
	3.65	6.87
	6.20	8.64
	8.55	9.73
	11.65	11.10
	15.20	12.25
	18.20	13.09

Outgas Temperature: 80°C
Adsorption Temperature: 50°C

	P_{EXP} (torr)	$N_s \times 10^5$ (mole/g)
Run 1	3.65	4.12
	5.45	5.05
	7.65	5.65
	10.75	6.44
	13.95	7.02
	16.80	7.25
	19.05	7.22
Run 2	1.95	3.99
	5.85	5.76
	9.50	6.82
	14.95	7.43
	17.35	7.66
Run 3	3.35	4.78
	8.85	6.66
	12.50	7.62
	16.60	8.36
	20.10	8.66

Outgas Temperature: 200°C
Adsorption Temperature: 40°C

	P_{EXP} (torr)	$N_s \times 10^5$ (mole/g)
Run 1	1.35	7.73
	6.65	10.96
	11.65	12.72
	15.95	13.96
Run 2	2.70	8.30
	5.05	10.20
	8.30	11.88
	13.75	14.02
	16.70	14.94

Outgas Temperature: 400°C
Adsorption Temperature: 30°C

	P_{EXP} (torr)	$N_s \times 10^5$ (mole/g)
Run 1	0.20	9.74
	1.85	13.35
	4.95	17.13
	8.00	20.46
	12.70	24.42
	16.00	27.73

Outgas Temperature: 400°C
Adsorption Temperature: 40°C

	P_{EXP} (torr)	$N_s \times 10^5$ (mole/g)
Run 1	1.60	9.30
	7.20	13.60
	11.05	15.54
	15.80	17.21
Run 2	0.45	8.84
	3.60	13.21
	7.30	15.99
	12.45	18.61
	19.80	21.10

Outgas Temperature: 400°C
Adsorption Temperature: 50°C

	P_{EXP} (torr)	$N_s \times 10^5$ (mole/g)
Run 1	0.40	7.68
	4.15	11.44
	9.10	13.78
	14.40	15.71

APPENDIX 8

Adsorption Data for Hydrogen Chloride Adsorption on Gamma Alumina

Outgas Temperature: 80°C
Adsorption Temperature: 0°C

	P_{EXP} (torr)	$N_s \times 10^5$ (mole/g)
Run 1	1.05	38.46
	3.00	42.42
	5.35	44.92
	9.20	47.08
	13.20	49.80
	16.80	50.80
	18.50	51.70

Outgas Temperature: 80°C
Adsorption Temperature: 40°C

	P_{EXP} (torr)	$N_s \times 10^5$ (mole/g)
Run 1	0.50	24.35
	0.60	30.63
	4.85	38.90
	11.70	42.47
	17.10	43.74
	38.10	46.65
Run 2	1.50	36.98
	4.41	39.59
	7.20	41.53
	12.20	43.33
	19.05	44.78
Run 3	0.30	31.03
	5.30	37.85
	9.10	39.57
	12.80	41.25
	16.50	46.46
	23.30	45.95

Run 4	0.50	32.03
	0.85	34.70
	2.70	37.18
	3.90	38.58
	7.40	39.86
	10.05	41.41
	13.40	42.42
	19.40	43.58
Run 5	0.40	31.21
	0.90	33.80
	1.40	34.74
	2.65	39.79
	6.70	42.82
	13.20	44.74
	20.70	47.20

Outgas Temperature: 80°C
Adsorption Temperature: 50°C

	P_{EXP} (torr)	$N_s \times 10^5$ (mole/g)
Run 1	4.25	37.95
	6.00	38.47
	10.95	40.40
	15.80	41.92
	20.70	42.23
Run 2	0.10	35.58
	4.95	36.95
	9.70	37.71
	16.90	38.93
	20.95	39.83
Run 3	0.65	34.25
	2.60	35.49
	5.75	36.85
	12.65	39.25
	18.50	40.68
Run 4	0.85	31.46
	1.50	33.20
	6.80	35.75
	11.35	37.78
	17.55	39.31

Run 5	0.80	32.38
	1.90	34.17
	4.05	36.23
	9.15	38.25
	13.35	39.88
	18.85	41.24
Run 6	1.25	31.64
	3.25	33.54
	8.35	36.56
	14.20	38.15
	19.50	39.12

Outgas Temperature: 200°C
Adsorption Temperature: 0°C

	P_{EXP} (torr)	$N_s \times 10^5$ (mole/g)
Run 1	1.85	45.77
	4.85	49.99
	9.00	53.40
	12.00	55.14
	15.65	56.44
	19.25	58.61
Run 2	0.65	39.65
	5.55	50.74
	9.05	53.93
	12.90	55.74
	17.75	57.91

Outgas Temperature: 200°C
Adsorption Temperature: 40°C

	P_{EXP} (torr)	$N_s \times 10^5$ (mole/g)
Run 1	0.80	35.75
	4.25	39.69
	8.15	41.97
	12.95	42.78
	19.50	44.65

Run 2	0.95	33.51
	4.20	38.63
	9.95	41.37
	15.90	42.56
	20.70	44.07

Outgas Temperature: 200°C
Adsorption Temperature: 50°C

	P_{EXP} (torr)	$N_s \times 10^5$ (mole/g)
Run 1	1.80	35.52
	4.75	37.67
	9.70	39.60
	13.10	41.47
	18.20	43.07
Run 2	2.15	37.92
	7.55	40.27
	13.40	41.70
	19.40	43.28

Outgas Temperature: 400°C
Adsorption Temperature: 0°C

	P_{EXP} (torr)	$N_s \times 10^5$ (mole/g)
Run 1	1.95	41.57
	3.85	44.68
	7.70	46.75
	11.95	47.04
	17.10	48.77
Run 2	1.10	41.87
	4.55	45.49
	7.30	48.20
	13.60	50.06
	19.35	51.35

Outgas Temperature: 400°C
Adsorption Temperature: 40°C

	P_{EXP} (torr)	$N_s \times 10^5$ (mole/g)
Run 1	10.05	41.38
	14.10	42.08
	18.20	42.73
Run 2	5.15	40.83
	7.70	42.35
	10.70	44.08
	16.60	44.08
	21.50	44.54
Run 3	1.25	38.59
	2.60	39.24
	5.40	39.63
	7.45	40.74
	10.65	41.13
	16.95	41.14
	19.95	41.08
Run 4	1.95	36.67
	4.10	37.95
	6.80	38.80
	9.70	38.76
	13.10	38.79
	15.95	38.91
	19.90	38.79

Outgas Temperature: 400°C
Adsorption Temperature: 50°C

	P_{EXP} (torr)	$N_s \times 10^5$ (mole/g)
Run 1	0.25	26.54
	1.20	32.56
	5.85	35.83
	10.30	37.22
	15.25	38.58
	19.60	40.16

Run 2	0.50	29.72
	3.70	32.02
	7.15	34.54
	10.85	35.70
	17.70	36.80

APPENDIX 9

Adsorption Data for Hydrogen Chloride Adsorption on Alpha Alumina

Outgas Temperature: 80°C
Adsorption Temperature: 0°C

	P_{EXP} (torr)	$N_s \times 10^5$ (mole/g)
Run 1	0.55	5.80
	5.75	7.09
	9.30	7.42
	14.30	7.59
	19.85	7.81
Run 2	0.65	6.67
	4.95	7.39
	11.60	7.90
	17.60	8.10

Outgas Temperature: 80°C
Adsorption Temperature: 40°C

	P_{EXP} (torr)	$N_s \times 10^5$ (mole/g)
Run 1	1.15	4.89
	2.95	5.98
	7.30	6.44
	12.95	6.69
	19.35	6.87
Run 2	0.65	4.33
	6.60	5.71
	12.55	5.88
	17.65	6.03
	20.05	6.03

Outgas Temperature: 80°C
Adsorption Temperature: 50°C

	P_{EXP} (torr)	$N_s \times 10^5$ (mole/g)
Run 1	1.45	4.28
	2.70	5.30
	7.80	5.66
	11.60	5.74
	16.50	5.85
	19.40	6.20
Run 2	0.50	2.95
	1.15	3.59
	2.00	4.55
	5.80	5.35
	10.50	5.57
	15.35	5.72
	21.40	5.76

Outgas Temperature: 200°C
Adsorption Temperature: 0°C

	P_{EXP} (torr)	$N_s \times 10^5$ (mole/g)
Run 1	0.75	8.08
	3.40	8.34
	6.55	8.53
	11.75	8.67
	15.90	8.77
	20.55	8.85
Run 2	1.30	8.64
	4.20	8.83
	8.20	9.04
	11.55	9.27
	15.80	9.35
	19.50	9.33

Outgas Temperature: 200°C
Adsorption Temperature: 40°C

	P_{EXP} (torr)	$N_s \times 10^5$ (mole/g)
Run 1	2.25	7.31
	5.50	7.43
	8.60	7.52
	13.10	7.55
	18.45	7.61
Run 2	4.40	7.43
	7.85	7.57
	12.30	7.65
	16.60	7.70

Outgas Temperature: 200°C
Adsorption Temperature: 50°C

	P_{EXP} (torr)	$N_s \times 10^5$ (mole/g)
Run 1	0.50	6.36
	4.00	7.07
	9.20	7.33
	13.30	7.48
	18.40	7.58
Run 2	0.65	6.67
	4.90	7.21
	10.50	7.37
	16.90	7.49
	18.60	7.57

Outgas Temperature: 400°C
Adsorption Temperature: 0°C

	P_{EXP} (torr)	$N_s \times 10^5$ (mole/g)
Run 1	2.05	9.40
	6.25	9.54
	9.80	9.70
	13.55	9.93
	19.55	10.03
Run 2	1.10	8.98
	3.55	9.05
	7.15	9.25
	11.80	9.38
	17.55	9.49

Outgas Temperature: 400°C
Adsorption Temperature: 40°C

	P_{EXP} (torr)	$N_s \times 10^5$ (mole/g)
Run 1	2.30	7.73
	6.75	7.96
	12.55	8.09
	21.05	8.41
Run 2	0.15	5.60
	1.65	6.85
	3.80	7.11
	11.60	7.47
	18.75	7.65
Run 3	0.15	6.67
	0.90	7.23
	3.55	7.60
	14.00	7.95
	19.95	8.04

Run 4	0.40	7.46
	2.98	7.75
	8.50	7.98
	14.00	8.15
	19.05	8.22

Outgas Temperature: 400°C
Adsorption Temperature: 50°C

	P_{EXP} (torr)	$N_s \times 10^5$ (mole/g)
Run 1	0.10	4.57
	0.20	5.62
	0.85	6.85
	6.05	7.62
	11.70	7.87
Run 2	1.15	7.45
	8.60	7.81
	13.20	7.93
	18.05	8.04

APPENDIX 10

"FOCAL" Program to Fit Isosteric Heats of Adsorption vs. Surface Coverage to a Quadratic Equation (83)

```
   W A
C-8K  MODV 11-219

01.01 T !!!!!!!!!!
01.05 T " NON-LINEAR LEAST SQUARES FIT OF",!
01.06 T " Y = A + BX + C(X↑2) ",!!
01.07 A " X"NX,"                    Y"NY,!!
01.08 A " SURFACE AREA"SA,!
01.10 S DF=0; S YS=0; S YX=0; S Y2=0
01.15 S XS=0; S X2=0; S X3=0; S X4=0
01.20 A " NUMBER OF POINTS"N,!!
01.25 T "       X              Y",!!
01.30 F I=1,N; D 2.00
01.31 F P=0,2; F Q=0,6; S A(P+3*Q)=0
01.35 F R=0,2; F C=0,2; D 3.00
01.40 F R=0,2; S C=3; D 4.00
01.45 F K=12,20; S A(K)=0
01.46 S A(12)=1; S A(16)=1; S A(20)=1
01.47 T %,!," ORIGINAL ADJUNCT MATRIX",!; D 10
 01.50 F C=4,6; S R=C-4; S K=R+3*C; S A(K)=1
01.55 F R=0,2; D 5.00
01.56 T !!," GAUSS-JORDEN INVERTED MATRIX",!; D 10
 01.60 S AQ=A(9); T %,!!," A",AQ,!
01.61 S BQ=A(10); T " B",BQ,!
01.62 S CQ=A(11); T " C",CQ,!
01.65 T !!,"      X              Y[OBS]          Y[CALC]
   01.66 F I=1,N; D 9.00
01.67 T !!," AVERAGE % DEVIATION",DF/N,!!!!!!!!; Q

02.05 A "    " X(I),"      " Y(I),!
02.07 S X(I)=FLOG(X(I)); S Y(I)=FLOG(Y(I)/SA)
02.10 S XS=XS+X(I); S X2=X2+(X(I)↑2); S X3=X3+(X(I)↑3)
 02.15 S X4=X4+(X(I)↑4)
02.20 S YS=YS+Y(I); S YX=YX+Y(I)*X(I)
02.25 S Y2=Y2+(Y(I)*(X(I)↑2))
```

```
03.05 S RC=R+C; S K=R+3*C
03.10 I (RC-3)3.15,3.20,3.45
03.15 I (RC-1)3.30,3.35,3.40
03.20 S A(K)=X3; R
03.26 DO 6.00
03.28 S IN=IN-(5*FLOG(10))
03.30 S A(K)=N; R
03.35 S A(K)=XS; R
03.40 S A(K)=X2; R
03.45 S A(K)=X4; R

04.05 S K=R+3*C
04.10 I (R-1)4.15,4.20,4.30
04.15 S A(K)=YS; R
04.20 S A(K)=YX; R
04.30 S A(K)=Y2; R

05.05 F C=R+1,6; S A(R+3*C)=A(R+3*C)/A(R+3*R)
05.10 S A(R+3*R)=1
05.15 F I=0,2; F C=R+1,6; D 6.00
05.20 F I=0,2; D 7.00
05.25 R

06.05 I (I-R)6.10,6.15,6.10
06.10 S A(I+3*C)=A(I+3*C)-A(I+3*R)*A(R+3*C)
06.15 R
06.20 S SQ=SS/(N-2)
06.25 S DM=FSQT(SQ/(D/N))
06.35 S DY=FSQT(SQ)
06.45 S DB=FSQT((SQ*R)/D)

07.05 I (I-R)7.10,7.15,7.10
07.10 S A(I+3* R)=0
07.15 R
07.20 F I=1,NP; D 8.00
07.25 G 9.01

08.01 S AB=FLOG(NM); S LNP=(AB-IN)/SL
08.08 T "    NM"NM,"      LNP"LNP,!
08.10 S NM=NM+IC
```

```
09.01  G 1.05
09.05  S YC(I)=AQ+BQ*X(I)+CQ*(X(I)↑2)
09.07  I (Y(I))9.10,9.15,9.10
09.10  S DF(I)=100*((Y(I)-YC(I))/Y(I))
09.15  T %6.03,X(I)
09.17  T %6.03,"      ",Y(I),"        ",YC(I)
09.19  I (Y(I))9.20,9.21,9.20
09.20  T %5.02,"      ",DF(I)
09.21  T !; S DF=DF+FABS(DF(I)); R

10.05  F P=0,2; T !; F Q=0,3; T A(P+3*Q)
10.10  F P=0,2; T !,"                "; F Q=4,6; T A(P+3*Q)
 *
```

APPENDIX 11

Calculation of the Amount of Hydrogen Chloride Adsorbed on Alumina in Exhaust Cloud

Exhaust Composition:[16] 30.2% Al_2O_3, 20.9% HCl, 9.4% H_2O, 24.2% CO, 3.4% CO_2, 2.1% H_2, 8.7% N_2 and 0.6% $FeCl_3$

The Amount Adsorbed from the Exhaust is:

$$W_C = N_s \times MW \times Rev \times W_{Al_2O_3}$$

where: N_s = mole adsorbed/g alumina

MW = molecular weight of HCl

Rev = percent of HCl adsorbed that is irreversible

$W_{Al_2O_3}$ = wt. of Al_2O_3 in exhaust cloud

Assuming that all the Al_2O_3 is gamma alumina and using the data for HCl adsorption at 0°C on gamma alumina, outgassed at 400°C which were the conditions for maximum adsorption. For a 100g cloud:

$$W_{HCl/Ads} = 50 \times 10^{-5} \frac{mole}{g} \times \frac{36g}{mole} \times 0.60 \times 30.2g = 0.326g\ HCl$$

$$\text{or} \quad \frac{0.326g \times 100\%}{20.9} = 1.56\%$$

APPENDIX 12

Heats of Immersion of Aluminas in Water and Hydrochloric Acid

J.P. Wightman
Visiting Professor*

Department of Physical Chemistry, University of Bristol,
Bristol BS8 1TS, England.

INTRODUCTION

Heats of immersion have been widely reported for a number of systems (1). There have been a number of such studies reported for the water/alumina system (2-6). In particular, the effects of pre-treatment temperature (2,3,6), particle size (2) and crystalline phase (2,5) on the heat of immersion have been examined. The enhanced catalytic activity of alumina exposed to $HCl_{(g)}$ has been noted (7-9). In conjunction with recent infrared spectroscopic, electron spectroscopy for chemical analysis (ESCA) and adsorption studies of $HCl_{(g)}$ on alumina in our laboratory, a heat of immersion study was also begun. There is no heat of immersion data reported for the alumina/$HCl_{(aq)}$ system.

EXPERIMENTAL

Calorimeter. The heats of immersion were determined in a Calvet microcalorimeter (10). There has been infrequent use of this type of calorimeter in heat of immersion studies (11,12). A block diagram

* From: Department of Chemistry,
Virginia Polytechnic Institute and State University,
Blacksburg, Virginia 24061, U.S.A.

of the calorimeter is shown in Figure 1. The Calvet microcalorimeter model MS 70 was manufactured by SETARAM (Lyons, France). The calorimeter has a measurement threshold (detection limit) of $\sim$ 200 μJ and a sensitivity of $\sim$ 60 μV/mW. Other SETARAM components included the temperature regulator (D) model 3000R, the DC nanovolt amplifier (E) model NV 724 and the ITC integrator (G) with counter. A 10 mV Graphispot recorder (F) was used to obtain the thermogram for visual inspection only.

The detector (A) consisted of a pile of 124 chromel-alumel thermocouples. One detector surrounded the measuring (sample) cell and a second detector surrounded the reference cell. The pair constitutes one sample system . Two sample systems were used and are labelled "I" and "II". The measuring and reference cells in each system were electrically opposed so that any effect fluctuation in the temperature of the calorimeter on the output of the sample cell was minimized. This arrangement resulted in good base line stability over very long times necessary in this study. The output from the sample cell was amplified and simultaneously recorded and integrated.

Materials. A stock solution of 0.1 N HCl was prepared from a standard HCl solution (BDH Chemicals Ltd. - CVS). Solutions of specified concentrations were prepared volumetrically by dilution of the 0.1 N stock solution. Alon-C was obtained from Cabot Co. and used without further pretreatment. An X-ray powder diffraction pattern exhibited lines characteristic of γ-Al_2O_3. Average BET surface areas of 95.4 and 85.6 $m^2 g^{-1}$ for samples outgassed at 100-200 and 400°C, respectively, were obtained by low temperature nitrogen adsorption based on a cross-sectional area of nitrogen of 0.164 nm^2 (13). Reactive alumina A16SG was obtained from Alcoa and used without further pretreatment. An X-ray powder diffraction pattern exhibited lines characteristic of

α-Al_2O_3. An average BET surface area of 8.14 $m^2 g^{-1}$ was obtained independent of outgassing temperature in the range 100 to 400°C (13).

Procedure. Samples of γ-Al_2O_3 ($\sim$0.05 g) and of α-Al_2O_3 ($\sim$ 0.5 g) were weighed into pyrex ampoules with break-off tips. The ampoules were prepared in the University Glass Shop. The samples were then evacuated at $\leq 10^{-5}$ Torr for 1 hr at the specified temperature. The ampoules were then sealed off in vacuo. The sample ampoule was aligned carefully in the sample holder of the calorimeter and 2.5 cm^3 of either distilled water or $HCl_{(aq)}$ was added to a pyrex insert in the stainless steel vessel. The insert prevented possible reaction between $HCl_{(aq)}$ and stainless steel. The assembled cell was placed in the calorimeter and allowed to come to steady state typically in 2 hrs. The ampoule tip was then broken by depressing the plunger assembly and the area under the thermogram (proportional to the enthalpy change) was obtained via the integrator-counter. Typical thermograms are shown in Figures 2a and 2b with and without Peltier compensation, respectively. The steady state condition was re-established at times ranging from 50 to 140 minutes. The heat of empty bulb breaking in both water and 0.1 M $HCl_{(aq)}$ was determined also.

Calibration. The sensitivity, S, of the calorimeter was determined periodically by placing resistance heaters in the sample cell position of the two systems. The measured resistance (R_H) of the heaters are given in Table I. The sensitivity is the ratio of the measured electrical input to the integrated counts (C) and was calculated by the equation

$$S = \frac{E_{SR}^2}{R_{SR}^2} R_H \, t/C \qquad [1]$$

where E_{SR} is the potential in volts across a 10 Ω standard resistor

while current is passed through the resistance heater for t seconds. Values of S determined for both systems are given in Table I.

Heats of immersion were obtained with and without Peltier compensation. Since the first 14 runs were made using Peltier compensation, the calculation of the effective Peltier coefficient, P_{eff}, is described. In Peltier compensation, the exothermic wetting process is compensated by cooling the sample cell (via the Peltier effect) thus making the calorimeter more nearly isothermal. Two independent circuits were used to determine P_{eff}, namely, a Joule circuit (JC) and a Peltier circuit (PC). The idea is to achieve a steady state in which the Joule heating is in excess of the Peltier cooling. The value of P_{eff} was calculated by the equation,

$$P_{eff} = \frac{\left[\frac{E_{SR}}{R_{SR}}\right]^2_{JC} R_H t - SC}{\left[\frac{E_{SR}}{R_{SR}}\right]^2_{PC} t} \qquad [2]$$

standard resistors of 1 Ω were used in both circuits. When steady state has been established, the number of counts (C) over time (t) is noted. Values of P_{eff} determined with 3 ma flowing in the Peltier circuit are given in Table I for both systems.

There are a number of references to use of Peltier compensation in heats determined in the Calvet microcalorimeter[10,12]. Thorne used Peltier cooling in the heats of immersion of Graphon in organic liquids[12]. On the other hand, there is no discussion as to what difference it makes in the measured heat whether Peltier cooling is used or not. The operation of the calorimeter is obviously simplified if Peltier cooling is not used. A series of experiments were done to assess whether the accuracy of the measured heat is improved by the use of Peltier cooling.

The experiment here is to use the Joule heater and introduce

a measured quantity of heat (I^2Rt) into the system. The heat input can also be checked by using the integrator and the determined sensitivity. The results are shown in Table II. The agreement between the heat calculated in both ways is > 99%, for both systems. Now in a separate experiment, nearly the same quantity of heat is input into the system. But in this case, Peltier cooling is used to compensate for > 80% of the heat input. So the compensated heat $\Delta_C H$ can be calculated from the equation

$$\Delta_C H = P_{eff} \left(\frac{E_{SR}}{R_{SR}}\right)_{PC} t \qquad [3]$$

where P_{eff} is the determined Peltier coefficient, E_{SR}, is the measured potential across the standard resistor of resistance R_{SR} in the Peltier circuit during a time, t, of Peltier cooling. The non-compensated heat, $\Delta_{NC} H$ is simply the product of the integrated counts and the determined sensitivity. The sum of the compensated ($\Delta_C H$) and non-compensated ($\Delta_{NC} H$) heats should equal the heat input. The results are shown in Table II. No improvement in accuracy is gained by using Peltier cooling.

The conclusion reached here is that the use of Peltier cooling does not increase the accuracy of the measured heat (~2%) obtained directly from the sensitivity. This simplifies the operation of the calorimeter considerably in the following ways:

1. the Peltier coefficient does not have to be determined;
2. measurements of parameters in the Peltier circuit during a run are eliminated;
3. concern about stability of the Peltier circuit is removed; and
4. cumulative errors in the heat of immersion calculation via $\Delta_C H$ are reduced.

Data Reduction. The calorimetric data are collected in Appendix A in

chronological order. The run number and the system used are given in the first column. The operating temperature of the calorimeter is denoted by "T". The potential (in mV) across a 1 Ω standard resistor (E_{SR}) in the Peltier circuit is measured while current is passed for t seconds. These data are necessary for Peltier compensation which was not used after run No. 73. The net number of counts, C_{net}, were recorded at steady state after time, t_{ss}. The last column is the deviation from base line at steady state, Δ_{ss}, expressed in mm.

The calorimetric results are collected in Appendix B. The sample weight in air and the outgassing temperature are W and T_{pre}, respectively. The molar concentration of $HCl_{(aq)}$ is C_{HCl}. The compensated heat, $\Delta_C H$ (in Joules) was calculated using equation [3] The non-compensated heat, $\Delta_{NC}H$ was calculated by the equation

$$\Delta_{NC}H = S.C_{net} \qquad [4]$$

The values of S for both systems were given in Table I. The heats of wetting were calculated by equations [5] and [6] on both unit weight and unit area basis

$$(Jg^{-1}) - \Delta_W H = \frac{\Delta_C H + \Delta_{NC}H}{W} \qquad [5]$$

$$(mJm^{-2}) - \Delta_W H = \frac{\Delta_C H + \Delta_{NC}H}{\Sigma . W} \qquad [6]$$

where Σ is the specific surface area.

The weight loss on outgassing α-Al_2O_3 for 1 hr up to 400°C at $\lesssim 10^{-5}$ Torr was measured as 1.2%. Hence, the heats of immersion were not corrected for weight loss on outgassing. The average (for both systems) heat of evacuated bulb breaking determined in water and 0.1 N HCl was 0.035 ±0.035 J and 0.062 ±0.024 J, respectively. These values represent 3.0% and 3.9% in the worst cases (No.28, No. 108) for α-Al_2O_3 and γ-Al_2O_3, respectively. Therefore, the heats of immersion

were not corrected for heats of bulb breaking.

Error Analysis. The equation for calculating the sensitivity, S, was given above (see equation [1]).

Typical values of the parameters in equation [1] are given below

Parameter	Value	Δ	% Error
E_{SR}	15.093 mV	±0.002	±0.013%
R_{JH}	994.7 Ω	±0.3	±0.030%
t	480 sec	±0.2	±0.042%
C	482 counts	±2	±0.207%
R_{SR}	10 Ω		

Since the calculation of S involves only multiplication and division the percent error in S is given by a sum of the percent errors of the parameters (0.013% + 0.013% + 0.030% + 0.04% + 0.207%) or 0.306%. Thus the calculated value of S and the expected error limits would be 2.256×10^{-3}(±0.007) Joules $count^{-1}$. The average value of S was 2.258×10^{-3} which is within the expected error range.

The equation for calculating the heat of immersion ($\Delta_w H$) was given above (see equation [5]).

Typical values of the parameters in equation [5] are given below for run No. 81.

Parameter	Value	Δ	% Error
S	2.258×10^{-3} J $count^{-1}$	±0.007	0.31%
C	1886 counts	±25	1.32%
W	0.5894 g	±0.0003	0.05%

Again the percent error in $\Delta_w H$ is given by the sum of the parameters (0.31% + 1.32% + 0.05%) or 1.68%. Thus the calculated value of

$\Delta_w H$ and the expected error limits would be 7.23 ±0.12 J g^{-1}.

The largest source of error is the uncertainty in the number of counts which in turn depends upon the criteria selected for reaching steady state. That is, at what point is the thermogram to be considered complete? As can be seen from Figure 2, there is an asymptotic approach to steady state. The immersion of Graphon a graphitized carbon black, in a variety of organic liquids reaches a well defined steady state in ∿50 minutes[14]. The rationale for the longer and less well defined steady state in the alumina systems are due to diffusion, re-hydroxylation and chemical processes absent in the Graphon system. In most cases, steady state was chosen when the count rate was <2 counts min^{-1} over a 10 min period, which corresponds to a 1.5 mm deflection from the base line (see Appendix A). The effect of the ill-defined steady state is seen in the heats of immersion calculated at different times in Table III. The time figures in parenthesis were arbitrarily selected as steady state. The low count rate suggests that this is a valid assumption. Note that a significant percent error can be obtained by terminating the thermogram too soon.

A second source of error is the heat of bulb breaking which although it is small, it is non-reproducible and hence particularly in those cases of smaller heats of immersion would be expected to cause deviation.

RESULTS

$\underline{\alpha\text{-}Al_2O_3}$ The heats of immersion of α-Al_2O_3 in water at 30° as a function of outgassing temperature are given in Table IV and shown in Figure 3. The heats of immersion in Table IV are average values of the heats given in Appendix B and are expressed on both a unit weight and unit area basis. The heat measured is independent of the sample

weight as shown on comparison of run Nos.89 and 101.

There is a marked increase in the heats of immersion of α-Al_2O_3 in water as the outgassing temperature is increased from 100 to 400°C. There is no measured decrease in the surface area of α-Al_2O_3 over this temperature range[3,13]. Therefore the increase in the heat of immersion per unit area is attributed to "re-hydration" of the surface following removal of successive layers of water as the outgassing temperature is increased rather than to a decrease in the surface area. The value of $\Delta_w H$ after 100° outgassing is in the range of values reported in the literature of 370-656 mJ m^{-2}[2,3,6]. However, the value of 1467 mJ m^{-2} after 400° outgassing is outside the reported range of 503-1076 mJ m^{-2}[2,3,6]. The larger heat in the present work may be due to several factors including interaction of water with a surface coating.

The measured pH of an α-Al_2O_3 (outgassed at 100°C) slurry (1g/5cc H_2O - an equivalent loading to that used in the calorimetric studies) was 9.99 after 10 min as noted in Table V. The initial pH before α-Al_2O_3 addition was 5.70.

The kinetics of the wetting process were obtained from an analysis of the individual thermograms. Although not a part of the original proposal, these kinetic studies were a bonus since such studies are not possible with more conventional calorimeters which are usually stirred and not designed for long time stability and kinetic processes are masked. The average time required to reach steady state after immersion in water of α-Al_2O_3 outgassed at different temperatures are given in Table VI. There is a slight temperature dependence on the steady state time, the higher outgassing temperatures requiring the longer times.

The heats of immersion of α-Al_2O_3 in 0.1 N HCl as a function of

outgassing temperature are given in Table VII and shown in Figure 3. Strictly speaking the term heat of interaction rather than heat of immersion should be used in this case since there is partial dissolution of α-Al_2O_3 in 0.1 N HCl[13]. The heat of immersion of α-Al_2O_3 in 0.1 N HCl also increases with an increase in outgassing temperature. Further, the heat of immersion is significantly higher in 0.1 N HCl than in water at any given outgassing temperature. The increased heat amounts to about 400 mJ m^{-2} independent of outgassing temperature. There is no comparable literature data available. The heat of interaction should be related to the heat of adsorption as deduced from $HCl_{(g)}$ adsorption data[13].

The measured pH of an α-Al_2O_3 slurry (1g/5cc 0.1 N HCl) was 1.49 after 10 min (Table V). The initial pH before α-Al_2O_3 addition was 1.43.

The kinetic results in Table VI again suggest a slight temperature dependence on steady state time, the higher outgassing temperature requiring the longer time. Note that 65± 15 min are required to reach steady state after immersion of α-Al_2O_3 in <u>both</u> water and 0.1 N HCl.

The effect of HCl concentration on the heat of interaction of α-Al_2O_3 outgassed at 200°C is shown in Table VIII and plotted in Figure 4. The heat is fairly constant from 0.1 N to 0.032 N followed by a sharp drop to 0.01 N and again a constant value to 0.001 N. The value for the 0.001 N solution is still considerably above the heat of immersion in water, presumably related to the strong electrostatic forces of adsorption coupled with any dissolution which occurs. The initial HCl concentrations were plotted in Figure 4. A more instructive plot is obtained by combining the calorimetric data with the pH measurements (see Table V) as shown in Figure 5. Here the heats of immersion (left-hand ordinate) are plotted against equilibrium pH

while the change in pH on addition of α-Al_2O_3 is plotted in the right-hand ordinate. The same basic feature is seen, that is, a sharp decrease in the heat of immersion in the pH range 3-5 but the constant heat of immersion for the 0.01 and 0.001 N HCl solutions is presumably due to the depletion of H^+ ions in solution on interaction with alumina.

γ-Al_2O_3. The heats of immersion of γ-Al_2O_3 in water as a function of outgassing temperature is given in Table IV and shown in Figure 3. Again, as in the case of α-Al_2O_3, the heat of immersion of γ-Al_2O_3 increases as the outgassing temperature is increased. Although the surface area decreases from 95.4 at 100°C for 85.6 m^2g^{-1} at 400° the heat increases by a factor of 2. Again, the increased heat of immersion is attributed to removal of adsorbed water. Although ten times less γ-Al_2O_3 was used than α-Al_2O_3(Appendix B), the weights used correspond to equivalent surface areas. That a surface phenomena and not a bulk process is involved in wetting by water is gauged by comparison of the heats on unit weight and a unit area basis. For a 100°C outgas, the heats on a unit area basis differ by 40% but on a unit weight basis differ by a factor of 8. The heat of immersion of γ-Al_2O_3 is less than that for α-Al_2O_3 on a unit area basis which agrees with the results of Morimoto et al.[3] but not with the results of Hendriksen et al.[6] The reported values of $\Delta_w H$ for γ-Al_2O_3 outgassed at 100° range from 300 to 470 mJ m^{-2} and at 400° range from 600 to 762 mJ m^{-2}[2,3,6]. The present results fall within the reported range in both cases.

The pH measurements (see Table V) are particularly instructive here on comparing α-Al_2O_3 with γ-Al_2O_3. The pH of a γ-Al_2O_3 (100° outgas) slurry (0.1g/5 cc H_2O) was 4.46 after 10 min. In the case of α-Al_2O_3 (100° outgas) an <u>increase</u> in pH from 5.70 to 9.99 was

observed rather than a decrease from 5.82 to 4.46 for γ-Al_2O_3. These pH measurements are consistent with the significantly larger heat observed for α-Al_2O_3 immersion in water compared to γ-Al_2O_3.

The heats of immersion of γ-Al_2O_3 in 0.1 N HCl as a function of outgassing temperature are given in Table VII and are shown in Figure 3. The heat of immersion of γ-Al_2O_3 in 0.1 N HCl is significantly higher at 400°C than at 100°C as was the case for α-Al_2O_3. Again, the heat of interaction is greater in 0.1 N HCl than in water although not separated apparently by a constant amount as was observed for α-Al_2O_3.

The measured pH of a γ-Al_2O_3 (outgassed at 100°C) slurry in 0.1 N HCl was 1.42 after 10 min as noted in Table V unchanged from the initial pH. A similar invariant pH was obtained for α-Al_2O_3 in 0.1 N HCl.

The immersion in water of γ-Al_2O_3 outgassed at 100°C required 80 min to re-establish steady state whereas 125 min were required for 0.1 N HCl. For both α-Al_2O_3 and γ-Al_2O_3 (100° outgas), about the same time ($\sim$ 50 min) was required to reach steady state with water but in 0.1 N HCl the time (125 min) with γ-Al_2O_3 was considerably longer than the time (55 min) for α-Al_2O_3. The use of the Calvet microcalorimeter has allowed the kinetics of thermal processes in the alumina/$HCl_{(aq)}$ system to be probed at a level not heretofore possible.

SUMMARY

Definite differences in the immersion process of α-Al_2O_3 and γ-Al_2O_3 in both water and aqueous HCl solution were noted.

Water - The heat of wetting (per unit area) of α-Al_2O_3 in water was greater than that for γ-Al_2O_3. The heat of wetting for both aluminas increase with increasing outgas temperature. The time to reach steady state on immersion of α-Al_2O_3 was less than that for γ-Al_2O_3.

There was no marked dependence of the time to reach steady state on outgassing temperature for α-Al_2O_3. The pH of an α-Al_2O_3 slurry increased whereas a decrease was noted for a γ-Al_2O_3 slurry.

0.1 N HCl - The heat of wetting of α-Al_2O_3 in 0.1 N HCl was greater than that for γ-Al_2O_3. The heat of wetting for both aluminas increase with increasing outgas temperature. The heat of immersion of α-Al_2O_3 decreased with decreasing HCl concentration. The time to reach steady state on immersion of α-Al_2O_3 was less than that for γ-Al_2O_3. Samples of α-Al_2O_3 outgassed at higher temperatures tended to take longer to reach steady state. The time to reach steady state for α-Al_2O_3 was about the same in both water and 0.1 N HCl whereas for γ-Al_2O_3 a longer time was required in 0.1 N HCl compared to water. The pH of slurries of both α-Al_2O_3 and γ-Al_2O_3 remained unchanged compared to the initial pH of 0.1 N HCl.

The above summary is shown in abbreviated form in Table IX.

ACKNOWLEDGMENTS

I would like to thank Professor D.H. Everett for the opportunity to carry out this research in the Physical Chemistry Department at the University of Bristol. The help of R.J. Manning in keeping me on-stream is appreciated. Mr. R.E. (Rex) Garrard in the Chemistry Department Glass Shop was responsible for the preparation of the glass sample bulbs.

REFERENCES

1. A.C. Zettlemoyer and K. Naravan, in "The Solid-Gas Interface" Ed. E.A. Flood (Marcel Dekker, New York, 1967) Vol.1, pp.145-174.

2. W.H. Wade and N. Hackerman, J.Phys.Chem., 64, 1196 (1960).

3. T. Morimoto, K. Shiomi and H. Tanaka, Bull.Chem.Soc.Japan, 37, 392 (1964).

4. N. Hackerman and W.H. Wade, J.Phys.Chem., 68, 1592 (1964).

5. H. Cochrane and R. Rudham, Trans.Faraday Soc., 61, 2246 (1965).

6. B.A. Hendriksen, D.R. Pearce and R. Rudham, J.Catalysis, 24, 82 (1972).

7. J.B. Peri, J.Phys.Chem., 70, 1482 (1966).

8. M. Tanaka and S. Ogasawara, J.Catalysis, 16, 157 (1970).

9. S. Ogasawara, M. Takagava and K. Takahashi, J.Catalysis, 29, 67 (1973).

10. E. Calvet and H. Prat, "Recent Progress in Microcalorimetry", Pergamon Press (1963).

11. L. Robert, Bull.Soc.Chim., France 2309 (1967).

12. P. Thorne, Ph.D. Thesis, Bristol University, 1974.

13. R.R. Bailey, Ph.D. Thesis, V.P.I. & S.U., 1976.

14. D.H. Everett and J.P. Wightman, EUCHEM Conference, Collioure, France, April, 1976.

TABLE I

CALIBRATION PARAMETERS

System	R_H (Ω)	S (J count^{-1})	P_{eff} (V)
I	994.7	2.258×10^{-3}	4.606
II	992.0	1.916×10^{-3}	4.843

TABLE II

EFFECT OF PELTIER COMPENSATION

	System I		System II	
	no P.C.[a]	P.C.[b]	no P.C.	P.C.
ΔH_{input} (J)[c]	2.160	2.153	2.696	2.709
$\Delta_c H$ (J)[d]	-	1.832	-	2.198
$\Delta_{NC} H$ (J)[e]	-	0.301	-	0.497
ΔH_{measd} (J)[f]	2.149	2.133	2.683	2.695
Error (%)	0.51	0.93	0.48	0.52

a no Peltier compensation

b with Peltier compensation (86% for System I. 82% for System II).

c $\Delta H_{input} = I^2 R t$

d $\Delta_c H = P_{eff} \left[\frac{E_{SR}}{R_{SR}} \right]_{PC} t$

e $\Delta_{NC} H = S \times C$

f $\Delta H_{measd} = S \times C$

TABLE III

STEADY STATE CRITERIA

Run No. 73 II	t (min)	C (counts)	$-\Delta_w H$ mJ m^{-2}	%
	53	324	1296	98.3
	67	342	1304	98.9
	72	348	1307	99.1
	79	356	1310	99.3
	(102)	374	1319	100
Run No. 176 II	30	902	331	94.3
	40	922	339	96.6
	67	946	347	98.9
	81	954	350	99.7
	(90)	956	351	100

TABLE IV

HEATS OF IMMERSION OF α-Al_2O_3 AND γ-Al_2O_3 IN WATER AT 30°

T_{pre} (°C)	$-\Delta_w H$ (mJ m^{-2})	$-\Delta_w H$ (J g^{-1})
	α-Al_2O_3	
100	529 ± 25 (4.7%)	4.30 ± 0.20
200	970 ± 55 (5.7%)	7.88 ± 0.47
300	1266 ± 42 (3.3%)	10.3 ± 0.3
400	1484 ± 7 (0.5%)	12.0 ± 0.1
	γ-Al_2O_3	
100	372 ± 26 (7.0%)	35.6 ± 2.4
400	826 ± 1 (0.1%)	70.8 ± 0.1

TABLE V

pH MEASUREMENTS FOR ALUMINA SLURRIES (13)

T_{pre} (^{o}C)	C_{HCl} (moles ℓ^{-1})	pH_0	pH_{10}	pH_{60}	pH_{180}
α-Al_2O_3					
100	0	5.70	9.99	9.72	9.48
100	0.1	1.43	1.49	-	1.47
200	0	6.15	10.22	9.83	9.36
200	0.001	3.37	10.03	9.76	9.39
200	0.01	2.30	5.17	5.76	6.03
200	0.016	2.09	3.95	-	4.14
200	0.032	1.74	2.11	2.33	2.62
200	0.1	1.25	1.33	1.36	1.32
γ-Al_2O_3					
100	0	5.82	4.46	4.63	4.72
100	0.1	1.42	1.42	1.41	1.36

TABLE VI

AVERAGE TIMES TO RE-ESTABLISH STEADY STATE

T_{pre}	H_2O		$HCl_{(aq)}$	
	α-Al_2O_3	γ-Al_2O_3	α-Al_2O_3	γ-Al_2O_3
80			65	
100	50	80	55	125
200	55		65	
300	70		80	
400	60		70	120

TABLE VII

HEATS OF IMMERSION OF α-Al_2O_3 AND γ-Al_2O_3 IN 0.1 N HCl AT 30°

T_{pre} (°C)	$-\Delta_w H$ (mJ m^{-2})	$-\Delta_w H$ (J g^{-1})
	α-Al_2O_3	
80	888	7.23
100	949	7.73
200	1351 ± 17(1.2%)	11.0 ± 0.1
300	1732 ± 38(2.2%)	14.1 ± 0.3
400	1829 ± 60(3.3%)	14.9 ± 0.5
	γ-Al_2O_3	
100	727 ± 40(5.5%)	69.3 ± 3.8
400	1728	148

TABLE VIII

HEATS OF IMMERSION OF α-Al_2O_3 (200° OUTGAS) IN $HCl_{(aq)}$ SOLUTIONS

C_{HCl} (moles ℓ^{-1})	$-\Delta_w H$ (mJ m^{-2})	$-\Delta_w H$ (Jg^{-1})
0.001	1134	9.23
0.01	1188 ± 50(4.2%)	9.68 ± 0.42
0.016	1222	9.95
0.032	1329	10.8
0.05	1333	10.8
0.1	1351 ± 17(1.2%)	11.0 ± 0.1

TABLE IX

SUMMARY OF RESULTS

	α-Al_2O_3		γ-Al_2O_3
H_2O	$\Delta_w H$	>	$\Delta_w H$
	$\Delta_w H \propto T_{pre}$		$\Delta_w H \propto T_{pre}$
	t_{ss}	<	t_{ss}
	pH ↑		pH ↓
$HCl_{(aq)}$	$\Delta_w H$	>	$\Delta_w H$
	$\Delta_w H \propto T_{pre}$		$\Delta_w H \propto T_{pre}$
	$\Delta_w H \propto C_{HCl}$		
	t_{ss}	<	t_{ss}
	$t_{ss}^{H_2O} \approx t_{ss}^{HCl}$		$t_{ss}^{H_2O} < t_{ss}^{HCl}$
	pH ↔		pH ↔

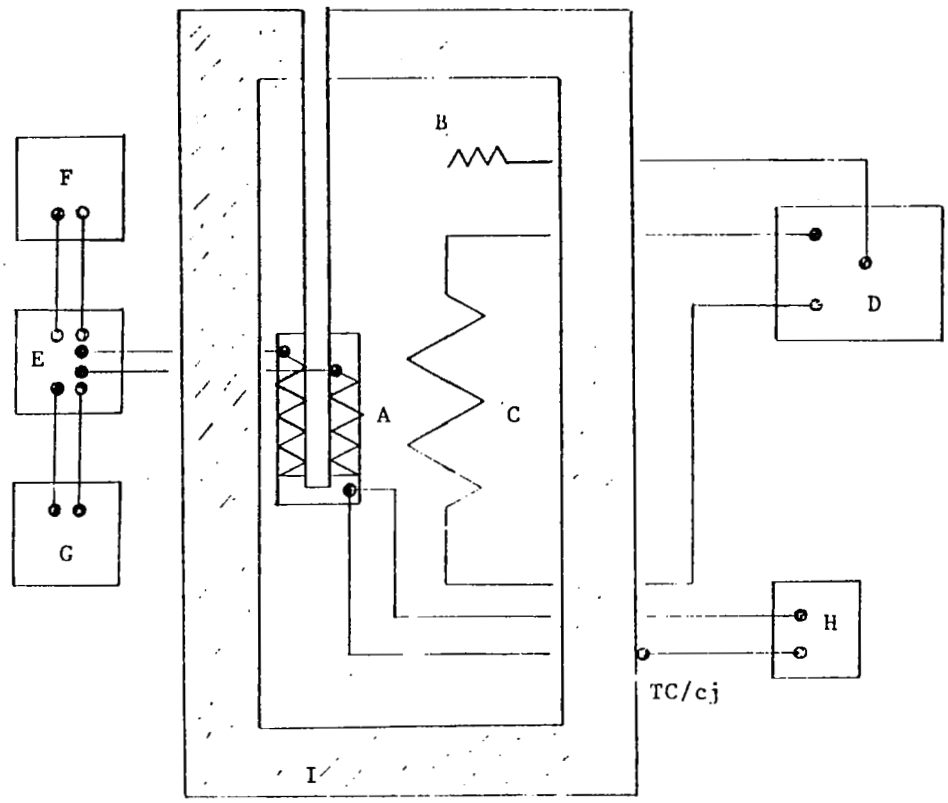

A Microcalorimetric element (detector)
B Temperature regulator probe
C Temperature regulator heater
D Temperature regulator
E Amplifier
F Recorder
G Integrator
H Potentiometer
I Insulation

Figure 1. Block diagram of Calvet microcalorimeter

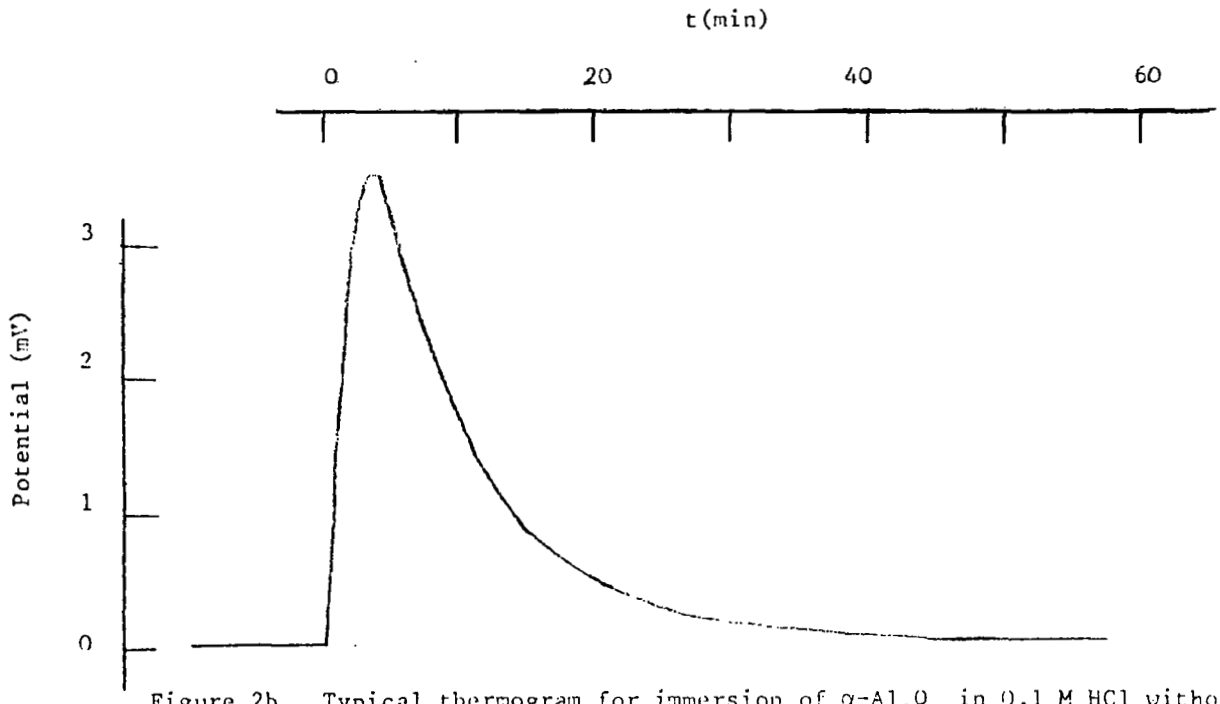

Figure 2b. Typical thermogram for immersion of α-Al_2O_3 in 0.1 M HCl without Peltier compensation (No.81).

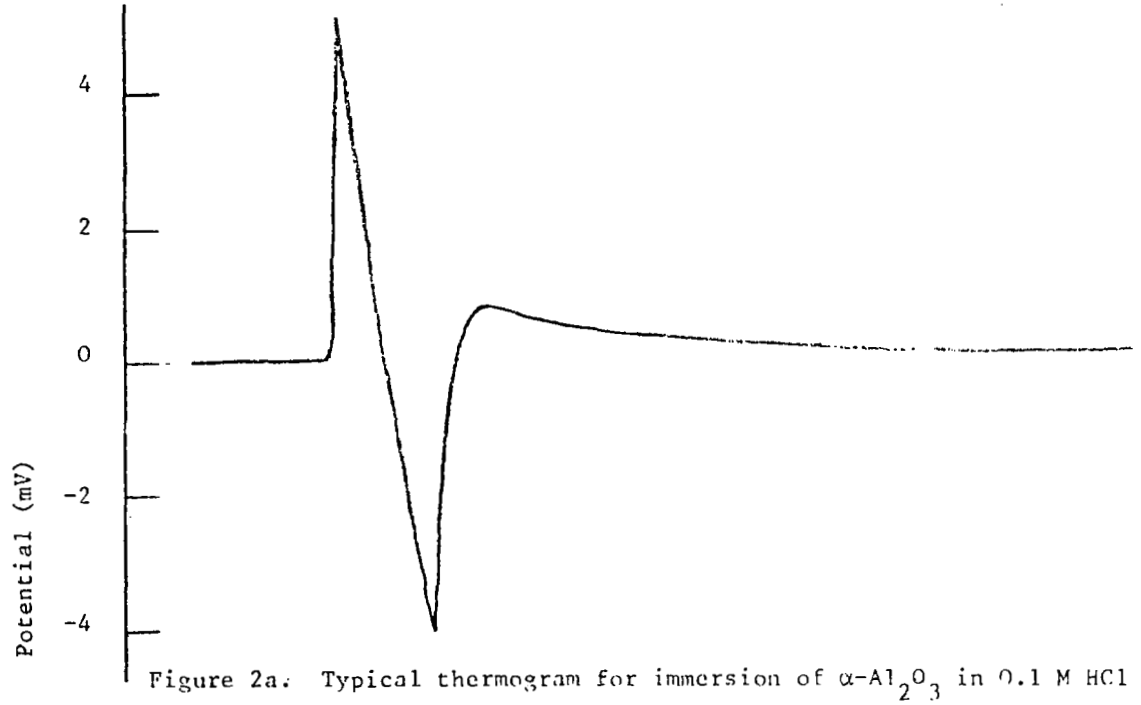

Figure 2a. Typical thermogram for immersion of α-Al_2O_3 in 0.1 M HCl with Peltier compensation (No.54).

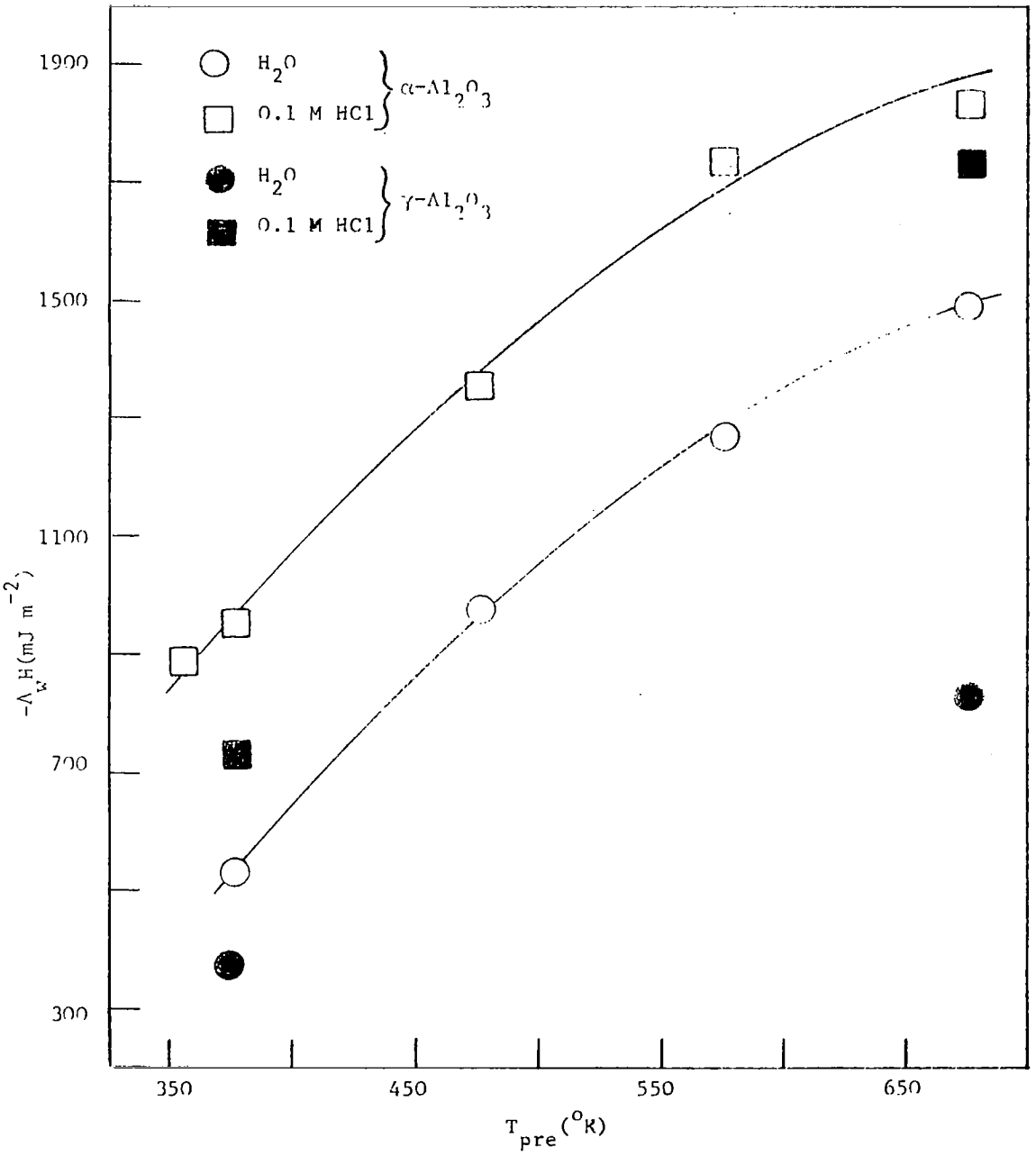

Figure 3. Heats of immersion of α-Al_2O_3 and γ-Al_2O_3 in H_2O and 0.1 M HCl as a function of outgas temperature.

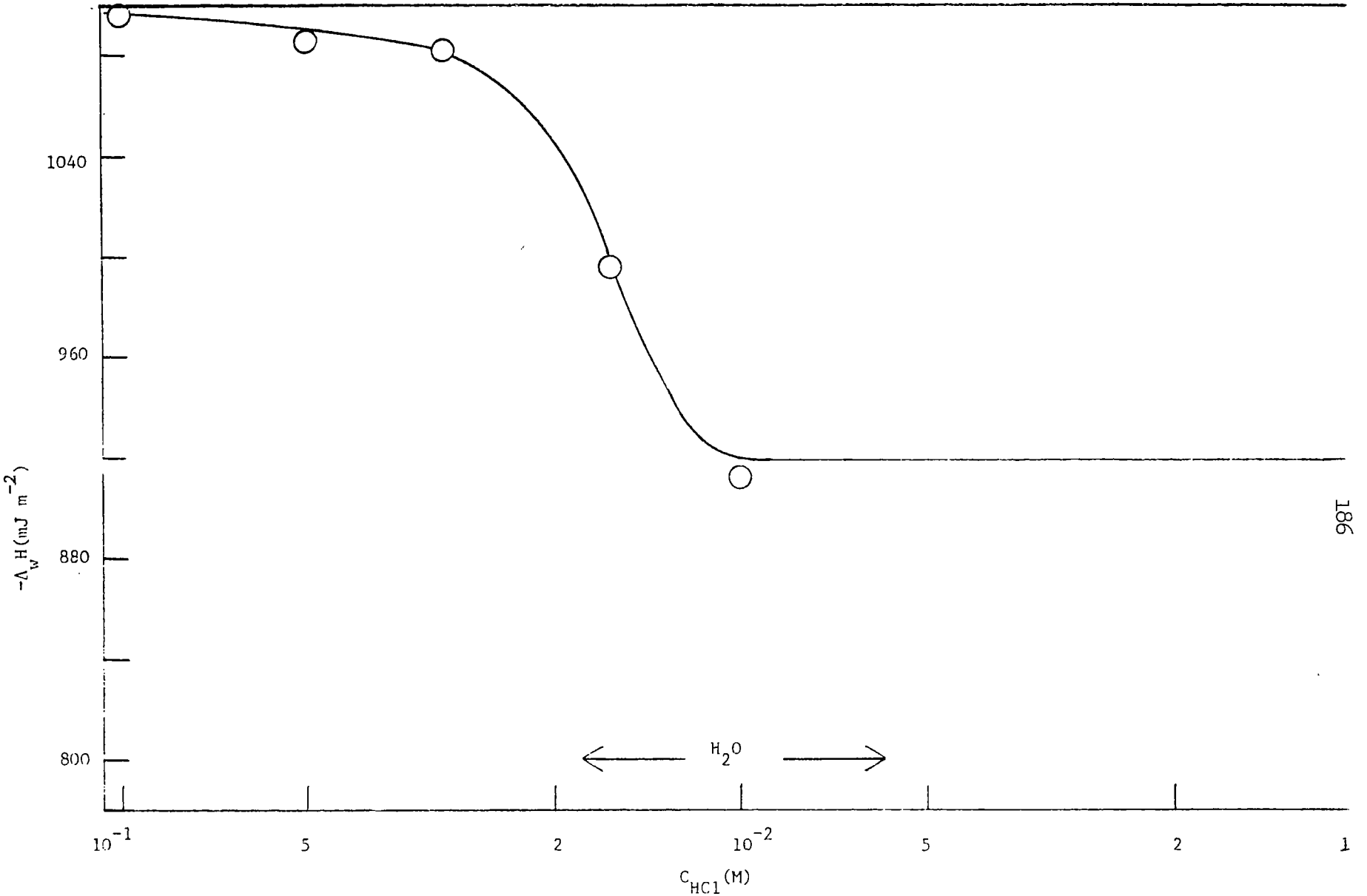

Figure 4. Heat of immersion of α-Al_2O_3 outgassed at 200°C as a function of $HCl_{(aq)}$ concentration.

APPENDIX A

CALORIMETRIC DATA

	T (^{o}C)	E_{SR} (mV)	t (sec)	C_{net} (counts)	t_{ss} (min)	Δ_{ss} (mm)
			α-Al_2O_3			
18 I	30.28	2.994	117.9	1340	55	1.5
19 II	-	2.995	179.7	925	55	1.5
24 II	30.22	2.998	179.7	1540	60	1.2
25 I	30.32	2.997	195.7	1387	65	1.2
28 II	30.20	2.994	125.3	172	50	0.8
29 I	30.25	2.993	119.3	132	50	0.6
35 I	-	2.994	180.3	540	55	0.9
48 I	30.28	2.996	240.7	1866	30	1.7
49 II	30.32	2.999	419.8	404	65	1.7
54 II	30.25	2.999	359.4	580	80	1.2
55 I	30.30	2.999	360.8	580	80	-
60 II	30.30	2.995	352.7	544	70	1.8
72 I	30.30	2.992	401.2	158	70	-
73 II	30.22	2.992	344.8	348	70	0.3
81 I	-			1886	65	1.0
88 II	30.30			2580	60	2.5
89 I	30.30			1942	85	0.4
101 I	30.30			700	70	1.0
106 I	30.60			2356	80	0.6
107 II	31.15			2324	-	-
131 I	30.32			2332	90	1.0
132 II	30.30			2588	90	0.8

APPENDIX A (continued)

	T (^{o}C)	E_{SR} (mV)	t (sec)	C_{net} (counts)	t_{ss} (min)	Δ_{ss} (mm)
			γ-Al_2O_3			
108 I	30.72			736	90	-
109 II	30.38			1008	-	-
115 II	30.28			1978	120	1.2
116 I	30.20			1410	120	
171 I	30.38			1700	-	-
172 II	30.50			2034	-	-
173 I	30.30			3100	120	2.0
175 I	30.30			784	65	0.2
176 II	30.38			954	80	0.3
177 I	30.28			1790	140	1.0
178 II	30.28			2082	120	-

APPENDIX B

CALORIMETRIC RESULTS

	W (g)	T_{pre} (^{o}C)	C_{HCl} moles ℓ^{-1}	$\Delta_{C}H$ (J)	$\Delta_{NC}H$ (J)	$-\Delta_{w}H$ (Jg^{-1})	$-\Delta_{w}H$ (mJm^{-2})
			α-Al_2O_3				
18 I	0.6279	200	0	1.626	3.026	7.41	915
19 II	0.5244	200	0	2.607	1.772	8.35	1026
24 II	0.4625	400	0	2.609	2.951	12.0	1477
25 I	0.4808	400	0	2.701	3.132	12.1	1490
28 II	0.4764	100	0	1.817	0.330	4.51	554
29 I	0.4735	100	0	1.645	0.298	4.10	504
35 I	0.4796	100	0.1	2.486	1.219	7.73	949
48 I	0.4904	400	0.1	3.322	4.213	15.4	1888
49 II	0.4772	400	0.1	6.097	0.774	14.4	1769
54 II	0.4590	300	0.1	5.220	1.111	13.8	1694
55 I	0.4371	300	0.1	4.984	1.310	14.4	1769
60 II	0.5530	200	0.1	5.116	1.042	11.1	1368
72 I	0.5907	300	0	5.529	0.357	9.96	1224
73 II	0.5323	300	0	4.996	0.667	10.6	1307
81 I	0.5894	80	0.1		4.259	7.23	888
88 II	0.4552	200	0.1		4.943	10.9	1334
89 I	0.4733	200	0.01		4.385	9.26	1138
101 I	0.1567	200	0.01		1.581	10.1	1239
106 I	0.4904	200	0.05		5.320	10.8	1333
107 II	0.4825	200	0.001		4.453	9.23	1134
131 I	0.4864	200	0.032		5.261	10.8	1329
132 II	0.4986	200	0.016		4.959	9.95	1222

APPENDIX B (continued)

	W (g)	T_{pre} (^{o}C)	C_{HCl} moles ℓ^{-1}	$\Delta_{C}H$ (J)	$\Delta_{NC}H$ (J)	$-\Delta_{w}H$ (Jg^{-1})	$-\Delta_{w}H$ (mJm^{-2})
			γ-Al_2O_3				
108 I	0.0457	100	0		1.662	36.4	381
109 II	0.0488	100	0		1.931	39.6	415
115 II	0.0493	100	0.1		3.790	76.9	806
116 I	0.0492	100	0.1		3.184	64.7	678
171 I	0.0542	400	0		3.839	70.8	827
172 II	0.0551	400	0		3.897	70.7	826
173 I	0.0473	400	0.1		7.000	148.0	1728
175 I	0.0539	100	0		1.770	32.8	344
176 II	0.0547	100	0		1.827	33.4	350
177 I	0.0603	100	0.1		4.042	67.0	703
178 II	0.0581	100	0.1		3.989	68.7	720

1. Report No.	2. Government Accession No.	3. Recipient's Catalog No.
NASA CR-2929		

4. Title and Subtitle	5. Report Date
Interaction of Hydrogen Chloride with Alumina	February 1978
	6. Performing Organization Code

7. Author(s)	8. Performing Organization Report No.
R. R. Bailey and James P. Wightman	
	10. Work Unit No.

9. Performing Organization Name and Address	11. Contract or Grant No.
Chemistry Department Virginia Polytechnic Institute & State University Blacksburg, Virginia 24061	NSG-1195
	13. Type of Report and Period Covered
12. Sponsoring Agency Name and Address	Contractor Report
National Aeronautics & Space Administration Washington, DC 20546	14. Sponsoring Agency Code

15. Supplementary Notes

Langley Technical Monitor: Gerald L. Pellett

Final Report

16. Abstract

The influence of temperature, pressure, and outgas conditions on the absorption of hydrogen chloride and water vapor on both alpha and gamma alumina has been studied. Characterization of the adsorbents was performed using x-ray powder diffraction, scanning electron microscopy (SEM), low-temperature nitrogen adsorption-desorption measurements, BET nitrogen surface area measurements and electron spectroscopy for chemical analysis (ESCA).

Water vapor adsorption isotherms at 30, 40, and 50°C were measured on alpha and gamma alumina after outgassing at 80, 200, and 400°C. Both outgas temperature and adsorption temperature influenced the adsorption of water vapor on the aluminas. The water vapor adsorption was completely reversible. Alpha alumina absorbed more water per unit area than gamma alumina. Differences in the adsorption capacity for water vapor of the two aluminas was explained on the basis of ideal surface models of alpha and gamma alumina. Isosteric heats of adsorption for water vapor on the aluminas were determined over a limited range of surface coverage.

Hydrogen chloride adsorption isotherms at 0, 40, and 50°C were measured on the two aluminas after outgassing at 80, 200, and 400°C. Alpha alumina adsorbed more hydrogen chloride per unit area than gamma alumina. Again, ideal alpha and gamma alumina surface models explained the difference in adsorption for hydrogen chloride and described the nature of the absorption site. The absorption was only partially reversible indicative of a chemisorption process.

Isosteric heats of adsorption for hydrogen chloride on the aluminas were determined for a range of surface coverages. These isosteric heats of adsorption were compared with calorimetric heats of adsorption using a water layer model which described the mechanism of hydrogen chloride adsorption as a two-step process. The first step involves a solution of the hydrogen chloride in preadsorbed water and the second is the adsorption on the alumina surface.

17. Key Words (Suggested by Author(s))	18. Distribution Statement
Adsorption, Chemisorption, Hydrogen Chloride, Water, Gamma Alumina, Alpha Alumina, Heat (Isosteric) of Adsorption, Surface Analysis, ESCA, SEM	Unclassified - Unlimited Star Category 25

19. Security Classif. (of this report)	20. Security Classif. (of this page)	21. No. of Pages	22. Price*
Unclassified	Unclassified	199	$9.00

* For sale by the National Technical Information Service, Springfield, Virginia 22161

NASA-Langley, 1978